



HAL
open science

Identification of portal mesenchymal stem cells and derived myofibroblasts in liver fibrosis

Lin Lei

► **To cite this version:**

Lin Lei. Identification of portal mesenchymal stem cells and derived myofibroblasts in liver fibrosis. Cellular Biology. Sorbonne Université, 2020. English. NNT : 2020SORUS099 . tel-03787910

HAL Id: tel-03787910

<https://theses.hal.science/tel-03787910>

Submitted on 26 Sep 2022

HAL is a multi-disciplinary open access archive for the deposit and dissemination of scientific research documents, whether they are published or not. The documents may come from teaching and research institutions in France or abroad, or from public or private research centers.

L'archive ouverte pluridisciplinaire **HAL**, est destinée au dépôt et à la diffusion de documents scientifiques de niveau recherche, publiés ou non, émanant des établissements d'enseignement et de recherche français ou étrangers, des laboratoires publics ou privés.

Sorbonne Université

Ecole doctorale 394 Physiologie et Physiopathologie

Inserm UMR_S 938, Centre de Recherche Saint-Antoine (CRSA), Equipe : Maladies fibro-inflammatoires d'origine métabolique et biliaire du foie. Pr. Chantal Housset

Présentée par

Lin LEI

Identification of portal mesenchymal stem cells and derived myofibroblasts in liver fibrosis

Présentée et soutenue publiquement le 24 septembre 2020

Devant un jury composé de :

Dr Thierry JAFFREDO	Président
Pr Pierre-Emmanuel RAUTOU	Rapporteur
Pr Selim ARACTINGI	Rapporteur
Pr Anne EICHMANN	Examineur
Pr Chantal Housset	Directeur de thèse
Dr Axelle Cadoret	Co-directeur de thèse

ACKNOWLEDGMENTS

This doctorate is the culmination of four years of hard work, commitment, and unwavering effort. I would like to express my warm thanks to all those who have contributed to this, whether by sharing their knowledge and skills, having a good time together, and, in particular, by their steadfast support.

First I would like to thank the jury members, Dr. Thierry Jaffredo, Prof. Pierre-Emmanuel RAUTOU, Prof. Selim ARACTINGI, Prof. Anne EICHMANN for having accepted to evaluate my work.

I would like to thank my supervisor, Prof. Chantal Housset, for her dedicated support and guidance. Chantal provided encouragement and was always willing and enthusiastic to assist in any way she could throughout my thesis project. I am also really grateful for her valuable time and efforts on the discussion and correction of my thesis. I admire her selfless spirit and insist on research, and she sets a good example to me not only during my PhD time but also the example for my whole research career in the future.

I would like to express my sincerest appreciation to my co-supervisor, Dr. Axelle Cadoret, who deserves my enormous esteem and gratitude. Thanks to her for paying great patience and enthusiasm, and always showing me her optimism and honesty. Her guidance, valuable suggestions, and encouragement will benefit me throughout my entire life. I appreciate all of these very much.

Haquima El Mourabit, who never stopped teaching me knowledge and skills from the first day I joined our lab, and I have learned a lot from her. Thanks for her all support she could provide, particularly the professional insights about animal experiments and cell separation. Her unremitting attitude to experiments and the endeavor to keep improving from the failure of experiments always encourage and motivate me when I met difficulties in my thesis. She helps me not only on my PhD thesis, but also helped me tremendously in my life in France, calling to deal with all sorts of problems, making doctor appointments, answering french emails, translating papers, etc., which makes words weakness, and the gratitude is deeply kept in my mind.

Special thanks to China Scholarship Council for the financial support for my PhD studies in France.

I would like to thank Dr. Thierry Jaffredo, who provided constructive suggestions and a great help for my thesis and single-cell sequencing performing. I would like to express my gratitude to Romain Morichon for the imaging experiments, Annie Meunier and Laurence Petit, for discussion and suggestions on flow cytometry experiments. I want to express my big thanks to Dr. David Ollitrault and Prof. David Sassoon for their valuable suggestions on the cell sorting experiments. Big thanks especially to Catherine Blanc and Bénédicte HOAREAU-COUDERT for their great help and support on the cell sorting experiments. Thanks to Yannick Marie for performing scRNA/RNA-sequencing and Justine Guegan for the sequencing data processing and analysis.

I want to express my warm gratitude for Dr. Sarah Mouri for her advice and strong supports in all aspects. I owe big thanks to her for helping my wife register in the hospital when my wife was pregnant, for helping my mother overcome psychological disorder when my mother was blocked in France because of the COVID-19 pandemic. I sincerely wish her significant achievements and a bright future.

I would like to thank my colleagues in our lab, Emilien, Alix, Astrid, Ester, Javier, Tounsia, Laura, Jérémie, Sara, Véronique, Patrick, Dina, Anne, Lynda, Ander, Yves, Jean-Louis, Anne-Marie, Marie, Cesar, Amine, Julie, Pierre-Antoine, Sophie and Pierre, for providing me with fantastic experimental conditions and pleasant research environment, which make me have an opportunity to access global research frontiers. I would like to thank everyone in this big warm family for your memorable accompanies and firm support. Thanks to everyone for preparing a heartwarming gift for my wedding. Especially, I would like to thank Dr. Ester Gonzalez-Sanchez, Dr. Ander Arbelaiz Cossio, and Dr. Jérémie Gautheron for providing their precious samples for my work. I would like to thank Dr. Sara Lemoine for her valuable advice for the project and correction for the paper manuscript. I would like to thank Dr. Laura Fouassier for helping on matrigel plug assays. Special thanks to Jean-Louis Delaunay for her painkiller when I had a severe toothache.

Last but not least, I would like to thank my parents and parents in law for their support and understanding in my PhD study period. Especially, I would like to express my most sincere gratitude to my wife, Ms. Wenwen Gao, for his accompanies and spiritual support. Thank her for her smile and comfort when I am sad. Thank her for her company day and night. Thank her for bringing our daughter Lexin LEI to my life.

ABBREVIATIONS

α -SMA: alpha-smooth muscle actin

aHSCs: Activated HSCs

BDL: Bile duct ligation

CaHSCs: Central vein-associated HSCs

CCl₄: Carbon tetrachloride

CFU-F: Colony forming units-fibroblast

CLDs: Chronic liver diseases

Col15A1: Collagen, type XV, alpha 1

DDC: 3,5-diethoxycarbonyl-1,4-dihydrocollidine

ECM: Extracellular matrix

ECs: Endothelial cells

EMT: Epithelial-to-mesenchymal transition

ENTPD2: Ectonucleoside triphosphate diphosphohydrolase 2

FBLN-2: Fibulin-2

Gli1: GLI family zinc finger 1

HIF: Hypoxia-inducible factor

HSC-MFs: HSC-derived myofibroblasts

HSCs: Hepatic stellate cells

iHSCs: Inactivated HSCs

LECT2: Leukocyte cell derived chemotaxin 2

LRAT: Lecithin retinol acyltransferase

LSECs: Liver sinusoidal endothelial cells

MSCs: Mesenchymal stem cells

MSLN: Mesothelin

NASH: Non-alcoholic steatohepatitis

NCD: Normal control diet

NPCs: Non-parenchymal liver cells

PaHSCs: Portal vein-associated HSCs

PBC: Primary biliary cholangitis

PFs: Portal fibroblasts

PMFs: Portal myofibroblasts

PMSC-MFs: PMSC-derived myofibroblasts

PMSCs: Portal mesenchymal stem cells

PSC: Primary sclerosing cholangitis

qHSCs: Quiescent HSCs

SBC: Secondary biliary cirrhosis

scRNA-seq: single cell RNA sequencing

TAA: Thioacetamide

TGF- β 2: Transforming growth factor beta 2

Thy-1: Thymocyte differentiation antigen-1

VEGFR2: VEGF receptor type 2

VSMCs: Vascular smooth muscle cells

TABLE OF CONTENTS

INTRODUCTION.....	1
BIBLIOGRAPHIC REVIEW.....	3
I) Liver fibrosis.....	4
A) Functional anatomy of the liver	4
B) Fibrogenesis	5
C) Major experimental models of liver fibrosis	7
1) Toxic models	7
2) Cholestatic models of liver injury	7
II) Hepatic myofibroblasts.....	9
A) General characteristics of myofibroblasts.....	9
1) Definition and functions of myofibroblasts.....	9
2) Origin of myofibroblasts	9
B) The different populations of hepatic myofibroblasts	12
1) Hepatic stellate cells (HSCs)	12
2) Portal fibroblasts (PFs)	16
2.1) Isolation and purification of PFs	17
2.2) The major markers of PFs	18
2.3) The functions of PFs/portal myofibroblasts (PMFs).....	24
III) Mesenchymal stem cells (MSCs) in liver fibrosis	26
A) General concept and characteristics of MSCs.....	26
B) MSCs in liver fibrosis	30
1) MSCs as a source of myofibroblasts	30
2) MSCs as a therapeutic approach for liver fibrosis.....	31
IV) Angiogenesis in liver fibrosis	34
A) The relationship between liver angiogenesis and fibrosis	34
B) Heterogeneity and zonation of liver ECs	36
C) The role of profibrogenic cells in liver angiogenesis.....	40

OBJECTIVES.....	44
RESULTS	46
I) Introduction.....	47
II) Article: Lei et al., Single-cell transcriptomics enable uncovering portal mesenchymal stem cells as precursors of myofibroblasts in liver fibrosis, to be submitted	48
III) Discussion	98
CONCLUSIONS AND PERSPECTIVES	105
LIST OF FIGURES AND TABLES.....	108
REFERENCES.....	109
ANNEXES	129

INTRODUCTION

Liver fibrosis results from continuous injury to the liver, including viral hepatitis, alcohol abuse, metabolic diseases, autoimmune diseases, and cholestatic liver diseases. It is characterized by extensive deposition of extracellular matrix (ECM). Excessive deposition of ECM leads to destruction of the normal architecture and the loss of hepatocytes. Thus, the fibrogenic evolution progresses to cirrhosis, which is a major global healthcare burden. Mortality rates secondary to liver cirrhosis continue to increase, with no approved antifibrotic treatments currently available, and liver transplantation only accessible to few patients.

Myofibroblasts are activated in response to tissue injury with the primary task to repair lost or damaged ECM. Enhanced collagen secretion and subsequent contraction are part of the normal wound healing response and crucial to restore tissue integrity. Dysregulation of the normal repair process can lead to persistent myofibroblast activation and pathogenic ECM deposition. Therefore, myofibroblasts have attracted considerable interest as a potential therapeutic target for tissue fibrosis. However, the precursors of myofibroblasts have yet to be identified. In most tissues, myofibroblasts are thought to originate from resident fibroblasts, but they may also be derived from other cell types, mostly of mesenchymal origin, such as pericytes, prevascular mesenchymal cells and mesenchymal stem cells (MSCs).

In the liver, as in other tissues, the origin of myofibroblasts is a matter of debate. Although different mesenchymal cell types have been proposed as the source of myofibroblasts following liver injury, the myofibroblasts presumably mainly derive from two different cell types, hepatic stellate cells (HSCs) and portal fibroblasts (PFs). HSCs phenotypic change into myofibroblasts has dominated the focus of research on liver fibrosis since their discovery. A distinct subpopulation of liver myofibroblasts referred to as portal myofibroblasts (PMFs), have been identified by our group. However, the precursors of PMFs are not yet been identified due to the lack of specific markers.

Mesenchymal stem cells (MSCs) were first isolated from the bone marrow on the basis of their self-renewal capacity and their ability to differentiate into multiple lineages. MSCs have been reported in almost all fetal and postnatal tissues and organs

and proposed as a source of myofibroblasts in response to tissue injury in the several fibrosis of organs. Recent studies addressing the role of focused on Gli1+ cells in liver showed the emerging role of MSCs in liver fibrosis.

Angiogenesis is a dynamic process leading to the formation of new vasculature from pre-existing vasculature. Evidence from both clinical and experimental conditions demonstrates that pathologic angiogenesis and sinusoidal remodeling are closely related to the progression of liver fibrosis. HSCs and portal myofibroblasts (PMFs) could act as the cellular source of angiocrine signals in the liver during fibrogenesis. However, whether intrahepatic angiogenesis represents a beneficial response for maintaining homeostasis or one that exerts pathological role leading to the progression of liver fibrosis and the mechanisms involved in angiogenesis during the progression of liver fibrosis are still poorly understood.

To better understand the role of PMFs and their precursors in liver fibrosis progression, this thesis aims to determine the cell atlas of portal mesenchymal cells, identify the precursors of PMFs, compare them with HSCs, and determine gene signatures of PMFs and their precursors.

Specific objectives were:

- 1) Reveal the atlas of portal mesenchymal cells in normal mouse liver;
- 2) Set up the method to isolate and purify the precursors of PMFs;
- 3) Characterize of the stem cell features of the precursors of PMFs;
- 4) Identify transcriptomic signatures of the precursors of PMFs and HSCs, and their derived myofibroblasts.

In the first bibliographic review part, we will report the state of scientific knowledge on liver fibrosis, hepatic myofibroblasts, mesenchymal stem cells and angiogenesis. Then in a second part we will present the results of the work. To finish, in a third part we will conclude and discuss the results and perspectives provided by this work.

PART I:
BIBLIOGRAPHIC REVIEW

I) Liver fibrosis

A) Functional anatomy of the liver

The liver is the largest solid organ in the body, constituting 2.5% of total body weight and serves as a central metabolic coordinator with a wide array of essential functions, including the regulation of glucose and lipid metabolism, protein synthesis (Juza & Pauli, 2014). The liver cellular organization is based on the building block of the hepatic acinus, which contains all the cells of the liver arranged around point(s) of the entry (portal triads (hepatic artery, portal vein, and bile duct)) and exit (central veins) of blood. Blood flows into the liver lobe via the portal vein/portal artery and drains towards the central vein through sinusoids. Sinusoids are lined with fenestrated liver sinusoidal endothelial cells (LSECs). Between the hepatocytes and the LSECs is the space of Disse, which harbors the hepatic stellate cells (HSCs), whereas Kupffer cells (KCs) protrude in the lumen of sinusoids. Bile, produced by the hepatocytes and excreted in the bile canaliculi, flows in the opposite direction of blood towards the bile ducts in the portal area (**Figure 1**). Within the acinus, parenchymal cells (hepatocytes) account for 60% of the total cell population in human liver and non-parenchymal cells (NPCs) include cholangiocytes, LSECs, vascular endothelial cells, KCs, HSCs and other mesenchymal cells, such as portal fibroblasts and vascular smooth muscle cells (VSMCs), and diverse immune cell. Recently, the emerging of sensitive single-cell RNA sequencing (scRNA-seq) methods made possible to investigate the nature of liver cells with high resolution, providing a powerful tool for unraveling the complexity of liver cells in health and disease.

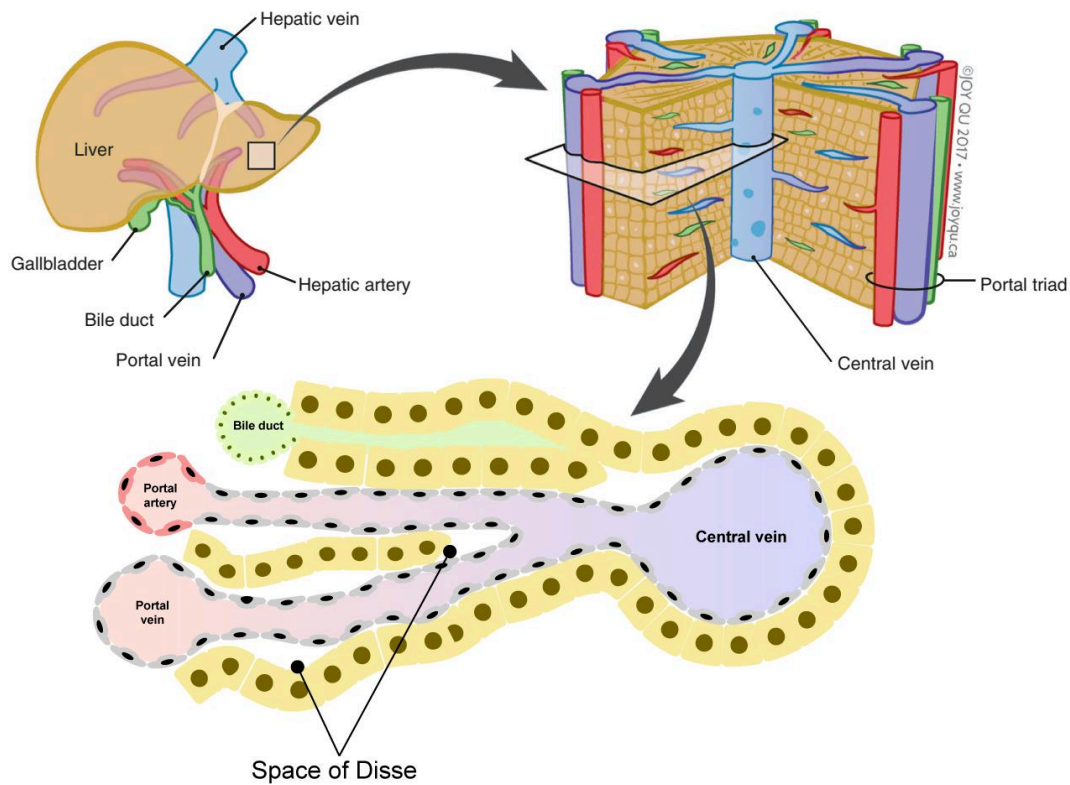


Figure 1: The hepatic lobule, a functional unit of the liver (MacParland et al., 2018).

B) Fibrogenesis

Recently, worldwide estimations suggested that over 840 million people suffer from chronic liver disease (CLDs), including cytolytic liver diseases, *i.e.* hepatitis B, hepatitis C, alcoholic liver disease (ALD), and non-alcoholic steatohepatitis (NASH), and cholestatic liver diseases, *i.e.* primary sclerosing cholangitis (PSC), primary biliary cholangitis (PBC), and secondary biliary cirrhosis (SBC) (Bataller & Brenner, 2005). CLDs are a leading cause of morbidity and mortality globally, with two million deaths annually and a rising incidence (Marcellin & Kutala, 2018). Whatever the etiology, the main mechanism for the progression of CLDs is fibrogenesis.

Liver fibrogenesis is a dynamic process including quantitative and qualitative changes of the extracellular matrix (ECM), of which the most prominent is the deposition of type I collagen. These changes progressively disrupt normal liver architecture and prevent the liver from its normal synthetic and metabolic functions.

Thus, the fibrogenesis progresses to cirrhosis, liver failure, and hepatocellular carcinoma, which can have a poor outcome and high mortality (**Figure 2**).

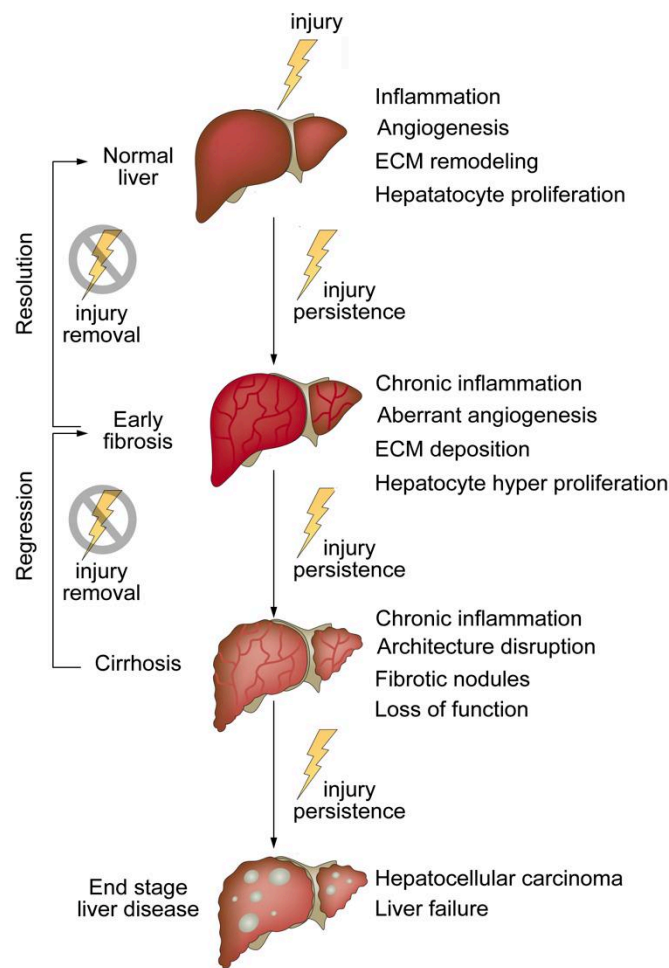


Figure 2: Natural evolution of liver fibrosis (Campana & Iredale, 2017)

During fibrogenesis, the scar tissue gradually replaces dead hepatocytes leading to the development of fibrotic septa. Fibrosis develops with different spatial patterns according to the etiology, but predominantly progress from the portal area, even if the primary targets of injury are intralobular hepatocytes (Clouston et al., 2005; Degott et al., 1999; Nobili et al., 2012; J. Xu et al., 2014). The stage of fibrosis is usually determined with the Metavir scoring system (Group & Bedossa, 1994) (**Table 1**).

Metavir scoring system	Fibrosis stage
F0	No fibrosis
F1	Mild fibrosis - Portal fibrosis without septa
F2	Moderate fibrosis - portal fibrosis and few septa
F3	Severe fibrosis - Numerous septa without cirrhosis
F4	Cirrhosis

Table 1: The Metavir scoring system and fibrosis stage (Group & Bedossa, 1994)

There is currently no specific treatment for hepatic fibrosis. The management of patients is based on the treatment of etiology (cessation of alcohol, anti-viral treatment, *ect.*) and on symptomatic treatments. At the stage of cirrhosis, the only treatment is liver transplantation, that concerns a limited number of patients.

C) Major experimental models of liver fibrosis

1) Toxic models

Carbon tetrachloride (CCl₄), is the most common toxic used to induce liver fibrosis and cirrhosis in mice and rats. Most often, 0.3-1 ml/kg body weight CCl₄ is injected intraperitoneally two to three times per week during 4-6 weeks (Constandinou et al., 2005). Similarly, Thioacetamide (TAA) administration is another well-established model of liver fibrosis in rodents. TAA administration through *i.p* results in hepatic centrilobular necrosis, elevated transaminase activity, and intense liver fibrosis within six weeks (Liedtke et al., 2013).

2) Cholestatic models of liver injury

Different animal models mimicking cholestatic liver injury have been developed. Surgical common bile duct ligation (BDL) is well known to cause cholestatic injury and periportal biliary fibrosis in both mice and rats. BDL is a rapid

and reproducible method causing to cholestatic liver injury. This model can be applied to transgenic mice easily, allowing the investigation of cholestatic injury in many different study designs (Liedtke et al., 2013). Mouse multi-drug-resistant gene 2 (*Mdr2*) or ATP binding cassette subfamily B member 4 (*Abcb4*) is the homolog of the human genes *MDR3/ABCB4*, which encodes the transporter of phosphatidylcholine into bile (Morita et al., 2013). *Mdr2*-KO mice display deficiency in the excretion of phosphatidylcholine into bile, nonpurulent inflammatory cholangitis, portal inflammation, and ductular reaction, developing a phenotype resembling human PSC, with biliary fibrosis (Mauad et al., 1994). In addition to the models mentioned above, dietary models causing cholestatic liver injury are also widely used. 3,5-diethoxycarbonyl-1,4-dihydrocollidine (DDC) feeding leads to increased biliary porphyrin secretion. A robust ductular reaction can be induced after one week of DDC feeding. DDC feeding leads to pericholangitis with infiltration of inflammatory mononuclear cells and activation of fibrogenesis around bile duct, developing biliary liver fibrosis that resembles PSC (Fickert et al., 2007).

II) Hepatic myofibroblasts

A) General characteristics of myofibroblasts

1) Definition and functions of myofibroblasts

In chronic fibro-inflammatory diseases, myofibroblasts are the main effectors of fibrosis, affecting multiple organs such as liver, lung, and kidney (S. L. Friedman et al., 2013). The myofibroblast possesses the feature of fibroblastic cells, such as the production of the ECM, with the contractile functions of the smooth muscle cells involved in tissue architecture distortion. α -SMA is the most commonly used marker of myofibroblasts, although this is not an absolute requirement for myofibroblast identification. There are other markers of myofibroblasts, such as F-actin, vinculin, and extra domain A-containing fibronectin. Myofibroblasts do not express markers of smooth muscle cells like the light chain of myosin or smoothelin and are therefore distinguished from smooth muscle cells.

Myofibroblasts are the major source of ECM proteins such as collagen type I as well as other proteins that constitute pathologic fibrous tissues (S. L. Friedman, 2008). They also secrete proteolytic enzymes, mainly matrix metallo-proteinases, that degrade the ECM. Thus, myofibroblasts are the main players of both fibrogenesis and fibrolysis, and fibrosis results from the imbalance of these two processes.

2) Origin of myofibroblasts

Myofibroblasts originate typically from mesenchymal precursor cells via transdifferentiation, often referred to as the term of “activation”. Activation of myofibroblasts is regulated by cytokines synthesized by inflammatory and parenchymal cells, including transforming growth factor- β (TGF β), the main pro-fibrotic factor.

Resident mesenchymal cells are the major source of myofibroblasts across multiple organs. Mesenchymal cells have been initially isolated based on adherence and capability to expand *in vitro*. The common feature of mesenchymal cells is the lack of endothelial (CD31) or hematopoietic (CD45) markers. Localization relative to

the vasculature, as well as positive selection using a number of markers, further allows discrimination between distinct subsets of mesenchymal cells in various organs, including fibroblasts, pericytes, mesenchymal stem/stromal cells (MSCs) and others.

At homeostasis, fibroblasts, which are tissue-resident mesenchymal cells found in the interstitial space of all organs, play a key role in structural framework by generating ECM. Fibroblasts are morphologically and functionally distinct from myofibroblasts, as they do not express α -SMA and lack the contractile microfilamentous apparatus (*i.e.*, stress fibers) observed in myofibroblasts. Increasing evidence demonstrates that the historically defined fibroblast is actually not one type of cell, but a general name to describe the heterogeneous populations of mesenchymal cells (Di Carlo & Peduto, 2018).

In the microvasculature, ECs are wrapped by a discrete subset of contractile mesenchymal cells termed pericytes. These cells are embedded within the vascular basement membrane and establish close contacts with ECs (Sims, 1986). It is still a challenge to identify pericytes. Nevertheless, it can be addressed using a combination of criteria, including localization relative to ECs and the vascular basement membrane, morphology, lack of the lineage markers CD45 and CD31, and expression of markers such as PDGFR β , CD146, RGS5, and NG2, even though none of these markers are unique to pericytes, and expression levels vary with pericyte state and vessel type (Crisan et al., 2012; Murfee et al., 2005).

A growing body of research indicates that myofibroblasts can also derive from MSCs or MSC-like cells in multiple organs. This aspect will be developed in **Section III**.

It is well-established that the diverse types of mesenchymal cells in different organs contribute to the pool of myofibroblasts (**Table 2**). However, because of the lack of specific markers that discriminating the different mesenchymal cell populations. the relative contribution of distinct mesenchymal subsets to tissue homeostasis or damaged condition remains poorly understood.

Organ	Mesenchymal cell type	Positive markers	Reference
Heart	Cardiac fibroblasts	DDR2, Vimentin	(Ubil et al., 2014)
	Cardiac fibroblasts	Thy1, DDR2, COL1A1, PDGFR α	(Ali et al., 2014)
	Cardiac fibroblasts	COL1A1, PDGFR α , Vimentin, CD90	(Moore-Morris et al., 2014)
	Coronary adventitial cells	COL1A1, Sca1, PDGFR α	(Ieronimakakis et al., 2013)
Lung	Fibroblasts	FGF10	(El Agha et al., 2014)
	Lung fibroblasts	COL1A1, PDGFR α	(Hung et al., 2013)
Kidney	Pericytes	FoxD1, CD73, PDGFR β	(Humphreys et al., 2010)
	Interstitial cells	Gli1, PDGFR β	(Fabian et al., 2012)
	Pericytes	Podocin	(Lin et al., 2008)
Skeletal muscle	Fibro/adipogenic progenitors, multipotent mesenchymal progenitor cells	Sca1, PDGFR α	(Joe et al., 2010) (Lemos et al., 2015)
	Pericytes	NG2, PDGFR β , CD146	(Birbrair et al., 2013)
	Perivascular cells	Sca1, PDGFR α	(Dulauroy et al., 2012)
Adipose tissue	Pericyte-like cells	PDGFR α , PDGFR β , NG2	(Iwayama et al., 2015)
Bladder	Mesenchymal stem cells	Gli1, Sca-1, CD34	(Lilly et al., 2015)
Heart, liver, lung, kidney, bone marrow	Mesenchymal stem cells	Gli1, PDGFR β , 3G5, Nestin, PDGFR α	(Kramann et al., 2015)
Liver	Peribiliary mesenchymal cells	Gli1	(Gupta et al., 2020) (Kramann et al., 2015)
	Hepatic stellate cells	LRAT, Desmin, PDGFR β	(Mederacke et al., 2013)

Table 2: Tissue-resident mesenchymal cells source of myofibroblasts in multiple organs

B) The different populations of hepatic myofibroblasts

Hepatic myofibroblasts are not present in the healthy liver but arise and proliferate in response to injury and inflammation. As in other tissues, hepatic myofibroblasts are a heterogeneous cell population. Presumably, they mainly derive from two different cell types, hepatic stellate cells (HSCs) and portal fibroblasts (PFs) that give rise to HSC-derived myofibroblasts (HSC-MFs) and portal myofibroblasts (PMFs) respectively. Although other cell types have been proposed as alternative sources of myofibroblasts, their relative contribution is negligible or still under debate. Thus, some studies proposed fibrocytes as an extra-hepatic source of liver myofibroblasts (Kisseleva et al., 2006; J. Xu & Kisseleva, 2015), but their contribution to the myofibroblastic pool would be small (Kisseleva, 2017) even insignificant (Higashiyama et al., 2009). Liver mesothelial cells of the Glisson's capsule might also give rise to HSCs or myofibroblasts near the liver surface, contributing to fibrosis of the liver capsule (Lua et al., 2015). Another proposed source of myofibroblasts in liver is epithelial-to-mesenchymal transition (EMT), supported by *in vitro* studies (Choi & Diehl, 2009). However, cell fate tracing experiments demonstrated that myofibroblasts induced in liver fibrosis injury models are not derived from EMT (Chu et al., 2011; Osterreicher et al., 2011; Scholten et al., 2010).

1) Hepatic stellate cells (HSCs)

In healthy adult liver, HSCs constitute approximately 5-8% of total liver cells and exhibit a quiescent phenotype, and serve as major storage of Vitamin A in lipid droplets (S. L. Friedman, 2008). Quiescent HSCs are located in the sinusoidal space of Disse, between hepatocytes and LSECs (**Figure 3**), where they also play a role as pericytes for LSECs, maintaining them in sinusoidal differentiation stage (DeLeve et al., 2004), and regulate the vascular tonus. The role of HSCs in liver fibrosis was firstly described in the 70's and the paradigm of HSC as a source of liver myofibroblast has dominated the focus of research on liver fibrosis until now. In response to chronic liver injury, HSCs are activated, which leads to the conversion of a resting vitamin A-rich cell to one that has lost vitamin A droplets. Upon activation,

HSCs turn their morphology into myofibroblasts, contributing to the excessive ECM deposition observed in the pathological conditions of fibrosis and cirrhosis. HSC activation is modulated by diverse interactions with other cells, including hepatocytes, KCs, ECs, cholangiocytes and infiltrating immune cells (Ding et al., 2014; Luedde et al., 2014; Pellicoro et al., 2014; Seki & Schwabe, 2015). Thus, fibrogenesis is viewed as a multicellular hepatic wound healing response with HSCs in its center. Xiong and colleagues reported that HSCs appear to act as a “hub” of signaling by releasing growth factors, cytokines, and chemokines. (Xiong et al., 2019).

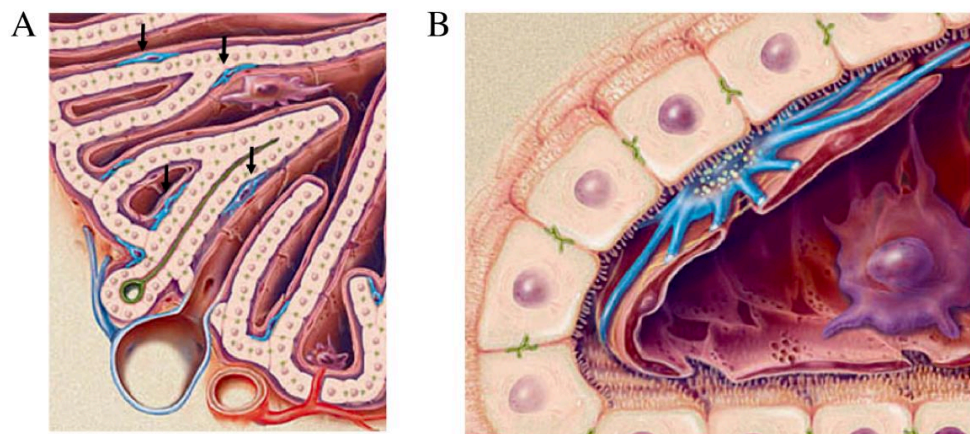


Figure 3: Localization of HSCs in the liver (S. L. Friedman, 2008)

The HSCs (in blue) are located in the space of Disse between liver sinusoidal endothelial cells (in red) and hepatocytes (in beige).

HSCs are easily isolated from normal liver and undergo spontaneous myofibroblastic differentiation when cultured on a plastic dish. A widely used experimental culture model is primary human and rodent HSCs, isolated based on retrograde pronase-collagenase perfusion of the liver and subsequent density-gradient centrifugation (Scott L Friedman & Roll, 1987). However, HSC isolation is commonly hampered by low yield and purity. An optional add-on protocol for ultrapure HSC isolation from normal and fibrotic livers via subsequent flow cytometric sorting has been described by Mederacke and colleagues (Mederacke et al., 2015).

Investigating the role of HSCs and the contribution of the different mesenchymal cell populations in normal and fibrotic liver requires specific markers. As shown in **Figure 4A**, several markers have been identified for HSCs, including

glial fibrillar acidic protein (GFAP), desmin, cytoglobin and lecithin retinol acyl-transferase (LRAT) (Bataller & Brenner, 2005; Scott L Friedman, 2008; Higashi et al., 2017; Kawada, 2015). Recently, two scRNA-seq studies focusing on HSCs have uncovered other putative markers of HSCs, such as *Ecm1*, *Vipr1*, *Colec11*, *Reln*, *Pth1r*, *Hgf*, *Fcna*, *Angptl6*, *Tmem56* and *Plvap* (Dobie et al., 2019; Krenkel et al., 2019). Besides, HSC-specific gene signatures, associated with poorer patients' prognoses, have been identified by using genome-wide transcriptome profiling (J. Ji et al., 2015; D. Y. Zhang et al., 2016). One study focusing on epigenetic alteration revealed determining transcription factors (**Figure 4C**) for HSCs at different stages of activation (Liu et al., 2020).

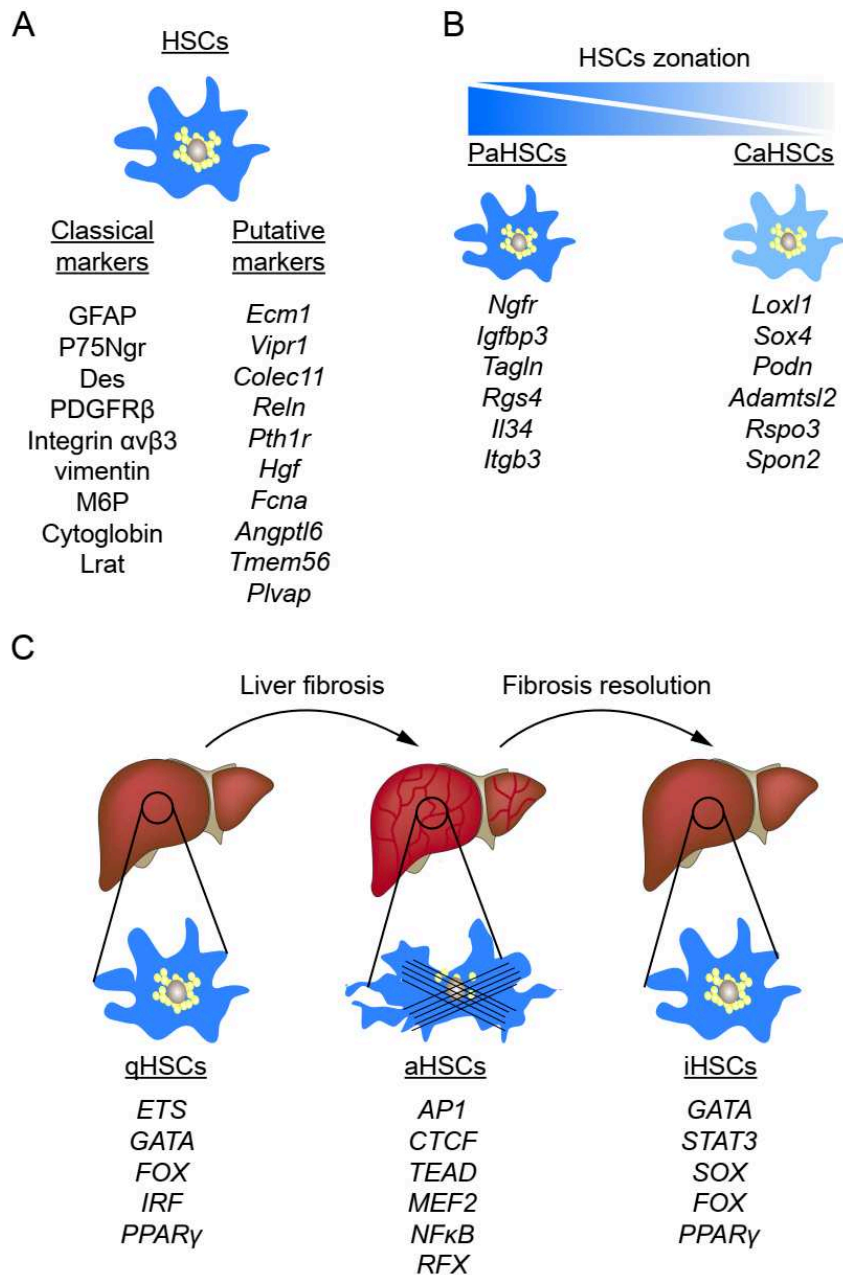


Figure 4: HSC specific markers

(A) Classical and putative markers of HSCs. (B) Zonation of HSCs across the liver sinusoid. PaHSCs, portal vein-associated HSCs; CaHSCs, central vein-associated HSCs (Dobie et al., 2019). (C) Specific transcription factors for HSC at different stages of activation. qHSCs, quiescent HSCs; aHSCs, activated HSCs; iHSCs, inactivated HSCs (Liu et al., 2020)

There is now both *in vitro* and *in vivo* evidence for the existence of more than one origin of liver myofibroblasts. HSCs are recognized by the fluorescence of their retinoid droplets under UV excitation. Culture studies have clearly demonstrated that other liver cell types, without fluorescent retinoid droplets, can give rise to

myofibroblasts (Kinnman et al., 2003; Thomas Knittel et al., 1999). A genetic cell fate study has provided strong evidence that HSCs were the major source of myofibroblasts in several mouse liver fibrosis models, including CCl₄, BDL, DDC, and Mdr2-KO mice (Mederacke et al., 2013). Another study demonstrated that myofibroblasts predominantly derived from HSCs in the CCl₄ model, and from PFs at the onset of cholestatic injury (BDL) (Iwaisako et al., 2014). Moreover, a recent study reported that the contribution of Thy1⁺ activated PFs to the myofibroblastic population increased with fibrosis progression in Mdr2-KO mice. The remaining myofibroblasts were composed of activated HSCs, suggesting that PFs and HSCs are both activated in Mdr2-KO mice (Nishio et al., 2019). Taking advantage of scRNA-seq, Dobie and colleagues recently showed HSCs subpopulation spatial zonation in healthy and fibrotic mouse liver (**Figure 4B**, **Figure 8**), designated portal vein-associated HSCs (Landmarkers: *Ngfr*, *Igfbp3*, *Tagln*, *Rgs4*, *Il34*, and *Itgb3*) and central vein-associated HSCs (Landmarkers: *Loxl1*, *Sox4*, *Podn*, *Adamtsl2*, *Rspo3*, and *Spon2*). Importantly, they provided evidence that central vein-associated HSCs were the dominant pathogenic collagen-producing cells in a mouse model of centrilobular fibrosis (CCl₄ liver injury) (Dobie et al., 2019). Collectively, these results suggested that the source of myofibroblasts may depend on the different stages of liver fibrosis progression and zonation of the liver lobule.

2) Portal fibroblasts (PFs)

The portal area contains three main structures, portal vein and artery with their wall and bile duct with its basal membrane, surrounded by fibroblasts. The term “portal fibroblast” refers to any fibroblast in the portal region, and the term “portal myofibroblasts” to any myofibroblast that originates in the portal area and is not derived from HSCs (Wells, 2014). Their roles in liver homeostasis and response to injury are undefined and controversial. In almost all types of chronic liver disease, including biliary (*i.e.*, primary biliary cholangitis, biliary atresia), viral, alcoholic, and non-alcoholic fatty liver diseases, fibrosis develops predominantly in the portal area and appears to progress from this area (Lemoine et al., 2013). However, two cell-fate tracing studies have provided conflicting results on the relative contribution of PFs in experimental conditions of biliary fibrosis, with one study suggesting that more than

70% of myofibroblasts were derived from PFs (Iwaisako et al., 2014). In contrast, another study suggested that their contribution to fibrogenesis is limited compared to that of HSCs (Mederacke et al., 2013). Along these lines, PFs may represent the “rapid responders” cell population activated following the injury to cholangiocytes (Kinnman & Housset, 2002; Lemoinne et al., 2013).

2.1) Isolation and purification of PFs

PFs were first described as “mesenchymal cells not related to sinusoids”, and since then were called “periductular fibroblasts” or “portal/periportal mesenchymal cells” (Dranoff & Wells, 2010), which comprise a small population of mesenchymal cells that surround the portal tracts (**Figure 5**).

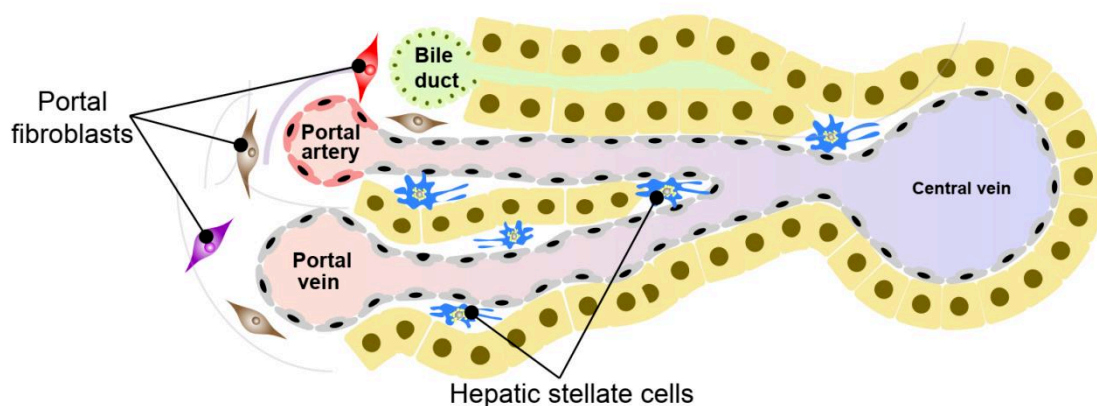


Figure 5: Localization of portal fibroblasts and hepatic stellate cells in normal liver

PFs are located around portal tracts, while HSCs are located in the space of Disse, which is between sinusoidal endothelial cells and hepatocytes trabeculae.

PFs are challenging to isolate and purify due to their embedding into the ECM and the lack of reliable markers, which is the main reason why the contribution of PFs to liver fibrosis remains undetermined. Non-HSC derived myofibroblasts were obtained in culture by different methods of cell isolation. Among them, a method described to isolate cells assumed to be PFs, is based on rat liver perfusion with enzymatic digestion, followed by size selection of cells enriched in PFs; PFs undergo

progressive myofibroblastic activation and differentiated into PMFs (Kruglov et al., 2002; Wen et al., 2012). We also have established a culture model for PMFs obtained by outgrowth from rat bilio-vascular tree preparations (El Mourabit et al., 2016). This method is highly reproducible, giving rise to PMFs with a clear phenotype and transcriptomic signature distinct from those of myofibroblasts derived from HSCs (Lemoinne et al., 2015). Similar to other protocols (Kruglov et al., 2002; Wen et al., 2012), the limitations are the abundance of contaminant bile duct epithelial cells, endothelial cells, and vascular smooth muscle cells in the initial preparation, and none of them has yet allowed to identify the progenitor cells of PMFs. A more physiological method of PFs culturing in a precision-cut liver slice is designed to maintain cell-cell and cell-matrix interactions and mimic the natural microenvironment of PFs (Clouzeau-Girard et al., 2006).

Taking advantage of reporter mice called collagen-GFP mice, and the feature of vitamin A content in HSCs, the method of PFs purification has been reported. Collagen-GFP mice were generated 20 years ago (Krempein et al., 1999), using GFP as a marker of activated myofibroblasts in the injured liver. Collagen-1 expressing myofibroblasts, which are supposed to comprise all myofibroblasts derived from diverse origins, can be identified by GFP signal in hepatic non-parenchymal cell fraction. HSCs and PFs can be purified from the pool of GFP+ myofibroblasts by detecting Vitamin A (which emits autofluorescent signal detected at 405 nm wavelength by flow cytometry) as VitA+ GFP+ (HSCs) and VitA- GFP+ (PFs), respectively (Iwaisako et al., 2014). Another study separated VitA+ HSCs, VitA-GFP+GPM6A- PFs, and VitA-GFP+GPM6A+ mesothelial cells from the same Colla1-GFP reporter mouse (Lua et al., 2016a). However, contradictory results was generated regarding the relative contribution of VitA-GFP+ PFs to liver fibrosis, and none of these methods identified or isolated PFs by positive selection.

2.2) The major markers of PFs

Determining the roles of PFs in physiological and pathophysiological conditions has been hampered by the lack of reliable markers to distinguish them from HSCs. A variety of markers have been used to identify PFs, but none of them has

been validated as both sensitive and specific (Wells, 2014). The main PF markers were summarized in **Table 3**.

Col15a1

Type 15 collagen belongs to the group of non-fibrillar collagens, characterized by extensive interruptions in their collagenous sequences and a conserved noncollagenous carboxyl-terminal structure (Kivirikko et al., 1994; Muragaki et al., 1994; Myers et al., 1992). We have shown that a marked increase in the hepatic expression of COL15A1 occurs in advanced liver fibrosis, both in animal models and in patients with chronic liver diseases (Lemoinne et al., 2015). This is the case not only in biliary-type liver fibrosis (*i.e.*, bile-duct ligated rats and patients with primary biliary cholangitis) but also in post-necrotic liver fibrosis (*i.e.*, carbon-tetrachloride-treated rats and patients with NAFLD), suggesting that PMFs or at least subpopulations of PMFs are involved in the progression of all types of liver fibrosis. Moreover, Col15a1+ PMFs secrete vascular endothelial growth factor (VEGF) A-containing microparticles, which activate VEGF receptor 2 in ECs and largely mediate vascular remodeling (Lemoinne et al., 2015).

Thy-1

Thymocyte differentiation antigen-1 (Thy-1) is a glycosphosphatidylinositol (GPI)-anchored surface protein expressed on various cell types, including neurons, thymocytes, myofibroblasts, endothelial cells, and mesangial cells (Karin et al., 2016) and is widely used as a stem cell marker that is expressed in hematopoietic stem cells and mesenchymal stem cells. It has been reported that in mouse models of chronic liver injury, periportal Thy-1 expressing mesenchymal cells appeared in close proximity to liver progenitor cells and constituted the functional niche for liver progenitor cells via paracrine signaling of fibroblast growth factor 7, which was required for stimulation of liver progenitor cells, thereby contributing to liver stem/progenitor cell-mediated regeneration (Takase et al., 2013). On the other hand, Thy-1 has been reported to be a marker of liver myofibroblasts that reside in the portal area (Dezso et al., 2007; Dudas et al., 2009b; Dudas et al., 2007). Katsumata and colleagues found that CD45- subpopulation of Thy-1 expressing cells with features of mesenchymal cells localized in the periportal area. Such CD45-Thy-1+ PFs displayed key characteristics of collagen-producing myofibroblasts *in vitro* and *in vivo* while

being distinct from HSCs (Katsumata et al., 2017). Recently, another group investigated the Thy-1+ PFs in the liver of Mdr2-KO/Col-GFP mice and showed that the proportion of Thy-1+ PFs in the GFP+ myofoboblastic pool progressively increased with the progression of fibrosis (Nishio et al., 2019).

Msln

Mesothelin (MSLN), a membrane-anchored GPI-linked 71-kDa membrane protein (MSLN precursor), is a mesothelial cell marker that is proteolitically cleaved to yield 40-kDa mature mesothelin which is attached to the cell membrane by GPI linkage and a 31-kDa shed fragment named megakaryocyte-potentiating factor (MPF) (K. Chang & Pastan, 1996; Pastan & Hassan, 2014). MSLN-expressing cells reside in the mesothelial layer lining of parenchymal organs and serosal cavities in a quiescent state and do not proliferate until injured or stressed (Bera & Pastan, 2000). Lineage tracing studies at early embryogenesis have linked the expression of mesothelin to precursors of fibroblasts and smooth muscle cells (Rinkevich et al., 2012). Iwaisako and colleagues separated VitA-GFP+ cells as PFs from the Colla1-GFP mouse model and identified MSLN as a PF marker by using the whole mouse genome microarray (Iwaisako et al., 2014). However, Lua and colleagues described that the VitA-GFP+ population also contains mesothelial cells and demonstrated that *Msln* is only expressed by the liver mesothelium, and is not a marker of PFs in mouse and human livers (Lua et al., 2016a). More recently, it has also been reported that ablation of MSLN+ PFs, deletion of *Msln* in PFs, or blocking MSLN expression with anti-MSLN antibody attenuates BDL-induced fibrosis in mice, reinforcing the concept of MSLN as a marker of PFs (Koyama et al., 2017).

ENTPD2

ENTPD2 belongs to a family of ectonucleoside triphosphate diphosphohydrolases (NTPDases) that catalyze the hydrolysis of extracellular nucleotides in the normal liver, making them unable to interact with P2Y-class receptors on cholangiocytes and stimulate cholangiocyte proliferation (Jhandier et al., 2005). ENTPD2 is first described as a PF marker in 2002 by Dranoff, who showed ENTPD2 was expressed in the periportal region surrounding intrahepatic bile ducts (Dranoff et al., 2002). Furthermore, Lua and colleagues confirmed that the VitA-GFP+ population isolated from Colla1-GFP reporter mouse highly expressed *Entpd2*

and ENTPD2⁺ PFs are negative for the mesothelial marker, MSLN (Lua et al., 2016a). Recently, it has been shown that ENTPD2 expression extends from the portal areas to fibrotic septae in CCl₄-induced and DDC-induced liver fibrosis. Besides, *Entpd2* null mice exhibit significantly more severe liver fibrosis in CCl₄-induced liver fibrosis, suggesting a protective function of ENTPD2 in CCl₄-induced liver injury (Feldbrugge et al., 2018), which might be consistent with the down-regulation of its expression during the myofibroblastic differentiation of PF (Dranoff et al., 2002; Jhandier et al., 2005).

Fibulin2

Fibulin-2 is a secreted extracellular matrix protein of the fibulin family that binds various extracellular ligands and calcium (Pan et al., 1993). Fibulin-2 is present in the basement membrane and stroma of several tissues and may play a role in organ development, particularly during the differentiation of heart, skeletal, and neuronal structures (Tsuda et al., 2001). Fibulin2-expressing fibroblasts are detectable in the portal area, the wall of portal vessels, portal vein, and hepatic artery of the normal liver (Thomas Knittel et al., 1999; Piscaglia et al., 2009; Tateaki et al., 2004). Moreover, their number is increased in the septal regions during liver fibrogenesis in rat models (Thomas Knittel et al., 1999). The whole mouse genome microarray revealed a “signature genes” list of PMFs compared with activated HSCs, in which *Fbln2* was further confirmed as a PFs marker (Iwaisako et al., 2014). More recently, Katsumata and colleagues reported that *Fbln2* was significantly enriched in Thy1-expressing mesenchymal cells of the liver (Katsumata et al., 2017). However, in human cirrhotic livers, Fibulin-2 staining exceeded that of COL15A1, suggesting that Fibulin-2 is less specific for PMFs. In accordance, Fibulin-2 expression increase in rat HSC-MFs compared to quiescent HSCs, even if it remains weaker than in PMFs (Lemoine et al., 2015).

CD34

The transmembrane phosphoglycoprotein CD34, a member of the sialomucin family, is expressed by a variety of cells, including hematopoietic and endothelial cells, as well as mesenchymal progenitors and portal myofibroblasts (Iwaisako et al., 2014). Nishio and colleagues reported that CD34 was strongly expressed in PFs upon the development of cholestatic fibrosis in Mdr2-KO mice and displayed a strong

positive correlation with an increased expression of other PF-specific markers, such as Thy-1, Msln, Fibulin-2 (Nishio et al., 2019). CD34-expressing cells accumulated predominantly in the portal area. The immunohistochemical studies showed that the majority of CD34-expressing cells co-expressed Thy-1, and exhibited a fibroblast-like spindle shape in the livers of Mdr2-KO mice. CD34-expressing PFs were also detected in the livers of BDL-injured, but not CCl₄-injured, mice (Nishio et al., 2019). Recently, CD34 was confirmed as a marker of PFs by scRNA-seq analysis of the mouse hepatic mesenchyme (Dobie et al., 2019).

Gli1

Gli1, a transcription factor involved in Hedgehog signalling, has been shown to be expressed in stromal cells with mesenchymal stem cell-like properties (capable of trilineage differentiation) in many organs (Kramann et al., 2015). Kramann and colleagues reported that Gli1⁺ cells were positioned around bile ducts of the liver and gave rise to myofibroblasts in CCl₄-induced liver fibrosis (Kramann et al., 2015). Recently, Gupta and colleagues also showed that Gli1 is expressed within mesenchymal cells around the biliary tree, without overlap with parenchymal stellate cells, and that these cells proliferated and acquired a myofibroblastic phenotype after cholestatic injury (Gupta et al., 2020). These two studies clearly showed that Gli1 is a marker of portal mesenchymal cells, suggesting that the precursors of portal myofibroblasts might be a subpopulation of portal fibroblasts which possess the stemness feature.

PFs markers/species	Histology localization in liver	Reference
COL15A1/human	Adjacent to the bile ducts and canals of Hering, around peribiliary vascular plexus	(Lemoinne et al., 2015)
Thy1/rat	Wall of portal vessels, portal vein, hepatic artery, and bile duct	(Dudas et al., 2007)
Thy1/rat	Around large bile ducts and peribiliary vascular plexus but not small bile duct, positive nerve around the hepatic artery, scattered portal cells	(Dezso et al., 2007)
Thy1/rat & human	Wall of portal vein, hepatic artery and around large bile duct	(Dudas et al., 2009b)
Thy1/mouse	Wall of the portal vein and around bile duct	(Katsumata et al., 2017)
MSLN/mouse	Not detectable in portal area in normal liver. Portal area in the BDL model	(Iwaisako et al., 2014)
MSLN/mouse & human	Not detectable in portal area neither in normal nor fibrotic liver	(Lua et al., 2016a)
ENTPD2/rat	Periductular space of portal area: Surrounding bile duct, lesser extent surrounding the portal vein, hepatic artery	(Dranoff et al., 2002)
ENTPD2/mouse	Around bile duct	(Lua et al., 2016a)
Fbln2/rat	Wall of portal vessels, mostly hepatic artery	(Thomas Knittel et al., 1999)
Fbln2/rat	Wall of portal vessels, portal vein, and hepatic artery	(Tateaki et al., 2004)
Fbln 2/rat & human	Wall of portal vessels, portal vein, and hepatic artery	(Piscaglia et al., 2009)
CD34/mouse	Wall of the portal vein and around bile duct	(Nishio et al., 2019)
Gli1/mouse	Around large Hilar duct, small Hilar duct, Peripheral duct, absent in canal of Hering	(Gupta et al., 2020)
Gli1/mouse	Wall of the portal vein, hepatic artery and around the bile duct	(Kramann et al., 2015)

Table 3: Localization of the main makers of PFs in liver

2.3) The functions of PFs/portal myofibroblasts (PMFs)

PFs would be predominantly activated in response to cholestatic liver fibrosis contributing to more than 70% of myofibroblasts at the onset of injury in the BDL model (Iwaisako et al., 2014). Along these lines, portal fibroblasts were proposed to represent the first responder activated following the injury of cholangiocytes (Kinnman & Housset, 2002; Lemoinne et al., 2013). As shown in **Figure 6**, depending on their localisation in tissue, fibroblasts deposit various and specific matrix. In the portal area of the liver, PFs are the source of elastic fibers, which are composed of a cross-linked elastin core surrounded by fibrillin-rich microfibrils (Wells, 2014). In response to injury, portal myofibroblasts contribute to strength, elasticity, and stiffness of liver structures. Once fibrosis sets in, PFs/PMFs secrete collagen in addition to elastin, such as COL15A1, which is a structural collagen that underlies blood vessels and maintains basement membrane integrity (Lemoinne et al., 2015). During liver development, there is evidence that portal mesenchymal cells express TGF- β family members as well as Hedgehog ligands which induce the differentiation of hepatoblasts to cholangiocytes (Dranoff & Wells, 2010; Fabris & Strazzabosco, 2011; Wells et al., 2004). Biliary obstruction leads to bile acid accumulation in the liver and serum, liver toxicity, and ultimately fibrosis progressing to cirrhosis. A prominent response to biliary obstruction is the ductular reaction, which occurs at the interface of the portal and parenchymal compartments and is observed in virtually all forms of human liver diseases (Gouw et al., 2011). Reactive ductules express growth factors such as platelet-derived growth factor, connective tissue growth factor, or TGF- β 2, which activate PFs and increase matrix deposition (Karin et al., 2016). In turn, myofibroblasts produce both tenascin and type IV collagen, which are vital for biliary development and activation (Lepreux & Desmouliere, 2015). Besides, PFs express ENTPD2, which hydrolyses the extracellular nucleotides in the normal liver, making them unable to interact with P2Y class receptors on cholangiocytes and stimulate cholangiocyte proliferation. Upon liver injury, activated PFs do not express ENTPD2, which leads to an increase in the concentration of extracellular nucleotides, resulting in increased activation and signaling of P2Y receptors and increased cholangiocyte proliferation (Jhandier et al., 2005). However, recently, Gupta and colleagues reported that Gli1⁺ portal mesenchymal cells were found only surrounding the main duct of a portal tract, but

not around the epithelial cells of the ductular reaction after cholestatic injury. Besides, they showed that the activation of hedgehog signaling in Gli1+ portal mesenchymal cells was associated with the strong expression of Indian hedgehog (Ihh) in cholangiocytes (Gupta et al., 2020).

In addition to the interaction with cholangiocytes, we have demonstrated that PMFs interact with endothelial cells by releasing vascular endothelial growth factor (VEGF) A containing microparticles which activated VEGF receptor2 in endothelial cells and mediated their proangiogenic activity and tubulogenesis (Lemoinne et al., 2015). Our team also demonstrated that portal myofibroblasts develop Endoplasmic reticulum (ER) stress as they expand with the progression of fibrosis, which further increases their proangiogenic activity, but also inhibits their proliferation and migration. This phenotypic switch may restrict PMF expansion while they support angiogenesis (Loeuillard et al., 2018).

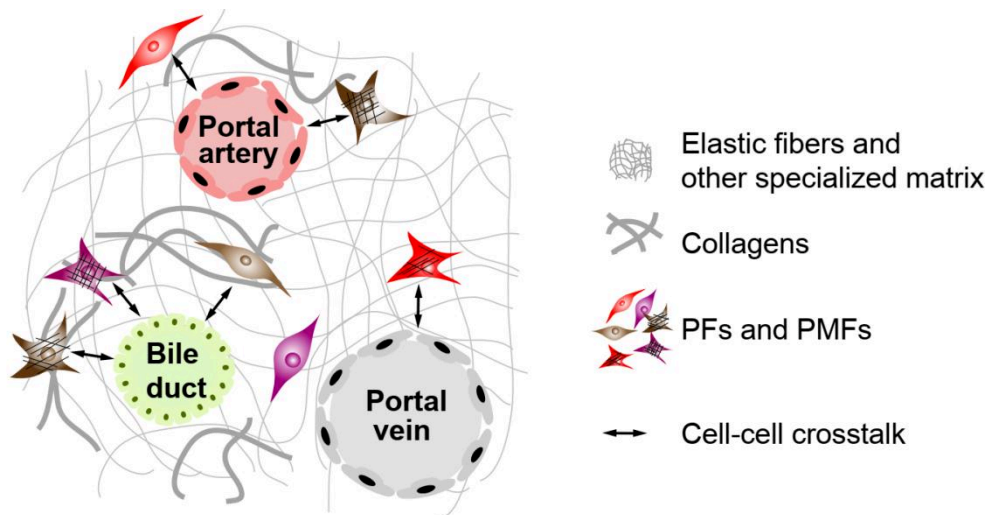


Figure 6: Potential functions of portal fibroblasts

Heterogeneous portal fibroblasts (PFs) and their myofibroblasts (PMFs) deposit elastic fibers and also collagens. PFs and PMFs also potentially interact with ductular cells and endothelial cells, to trigger profibrogenic, proangiogenic actions, depending on their microenvironment (Lemoinne et al., 2013; Wells, 2014).

III) Mesenchymal stem cells (MSCs) in liver fibrosis

A) General concept and characteristics of MSCs

Mesenchymal stem cells (MSCs) have the characteristics of self-renewal, immune regulation, and multipotency. MSCs were first described as stromal stem cells from the bone marrow that have a spindle shape in culture (Friedenstein et al., 1974). Although the main and earliest source of these cells has been the bone marrow (BM), based on the typical MSC properties of cells isolated from BM such as colony-forming (CFU-F), self-renewal and mesenchymal lineage differentiation potentials, organ-resident MSCs have been reported in almost all fetal and postnatal tissues and organs (da Silva Meirelles et al., 2006; Khuu et al., 2013). MSCs have been isolated from several organs, such as placenta, skeletal muscle, adipose tissue, lung, heart, liver, kidney, and others, and display different features in terms of surface markers, proliferation rates, and differentiation capability (Baruteau et al., 2014; El-Kehdy et al., 2016). These organ-specified MSCs are localized in the perivascular niche of small and larger blood vessels in a position compatible with pericytes and adventitial cells (Corselli et al., 2012; Crisan et al., 2009; Crisan et al., 2008). However, whether these resident MSC have a progenitor potential similar to the MSC from BM remains controversial (Bianco et al., 2013). Vasculature represents the *in vivo* niche of MSCs, helping to explain why MSCs have such a broad tissue distribution (Crisan et al., 2008). In the presence of proper growth factors and chemical stimulants, MSCs can differentiate along distinct mesodermal lineages *in vitro*, including adipocytes, osteoblasts and chondroblasts. According to the International Society for Cellular Therapy (ISCT), minimal requirements for MSC identification in humans are adherence to plastic, trilineage differentiation potential (adipocytes, osteoblasts, and chondrocytes), expression of CD105, CD90, CD73 *in vitro*, and lack of hematopoietic and endothelial markers (**Table 4**) (Dominici et al., 2006). It is generally accepted that all MSCs are devoid of the hematopoietic marker CD45 and the endothelial cell marker CD31. However, MSCs from other species do not express all the same markers as those on human MSCs; for example, although it has been confirmed that CD34 is absent from human and rat MSCs, some papers report variable expression of

CD34 in mouse MSCs (Copland et al., 2008; Peister et al., 2004). Thus, the expression of many of the MSC markers varies with the species, the tissue source and the method of isolation and expansion (Baddoo et al., 2003; Javazon et al., 2004). Moreover, the expression of MSC markers *in vitro* does not always correlate with their expression patterns *in vivo* (Gronthos et al., 2001). Although identification of MSCs in mice based on surface marker expression is less strictly defined than in humans, a panel of surface markers is commonly used to identify these cells (**Table 4**) (Boxall & Jones, 2012; Peister et al., 2004; Pelekanos et al., 2012). However, there is no real consensus or a single surface marker that specifically and exclusively defines these cells.

	Human	Mouse
Positive selection	CD105 (endoglin; ENG)	CD105
	CD73 (5'-nucleotidase; 5'-NT)	CD29 (fibronectin receptor subunit beta)
	CD90 (thymus cell antigen 1; THY1)	CD44 (hyaluronate receptor)
	n/a	SCA-1 (stem cell antigen-1)
Negative selection	Pan-leukocyte marker CD45	CD45
	Primitive hematopoietic progenitor and endothelial cell marker CD34	CD31 (Platelet endothelial cell adhesion molecule-1; PECAM-1)
	Monocyte and macrophage markers CD14 or CD11b	TER-119 (lymphocyte antigen 76; Ly76)
	B cell markers CD79 α or CD19	n/a
	Human leukocyte antigen class II HLA-DR	n/a

Table 4: Surface marker expression profile of MSCs in human and mouse (El Agha et al., 2017)

In addition to their ability to differentiate into osteoblasts, adipocytes and chondrocytes *in vitro*, it has also been reported that MSCs are able to differentiate into diverse other cell types under specific culture conditions (**Figure 7**). Caplan and Dennis presented a process that they call mesengensis, in which MSCs can give rise to myoblasts, bone marrow stromal cells and tendon-ligament fibroblasts (Caplan & Dennis, 2006). MSCs are also able to differentiate into muscle cells, including cardiomyocytes and myoblasts, with characteristics to create multinucleated myotubes and to express markers such as β -myosin heavy chain, α -actin cardiac form, and desmin in the condition of 5-azacytidine induction (W. Xu et al., 2004). Besides, MSCs originated from embryonic mesoderm can differentiate into functional hepatocyte-like cells that display a cuboidal morphology and the expression of typical hepatocyte markers (K. D. Lee et al., 2004). Other studies showed that MSCs can differentiate into the pancreatic islets of β -cells capable of producing insulin

(Govindasamy et al., 2011; Phadnis et al., 2011). Additionally, It has been shown that stimulation with appropriate factors may result in the differentiation of MSCs into cells derived ontogenetically from ectoderm, such as neurons (Arthur et al., 2008). Altogether, these studies suggest that MSC can give rise to multiple functionally mature cell populations. However, because of the lack of standardized approaches for their isolation, culture, expansion, and identification, such multipotential capabilities of MSCs are not universally accepted (Nombela-Arrieta et al., 2011).

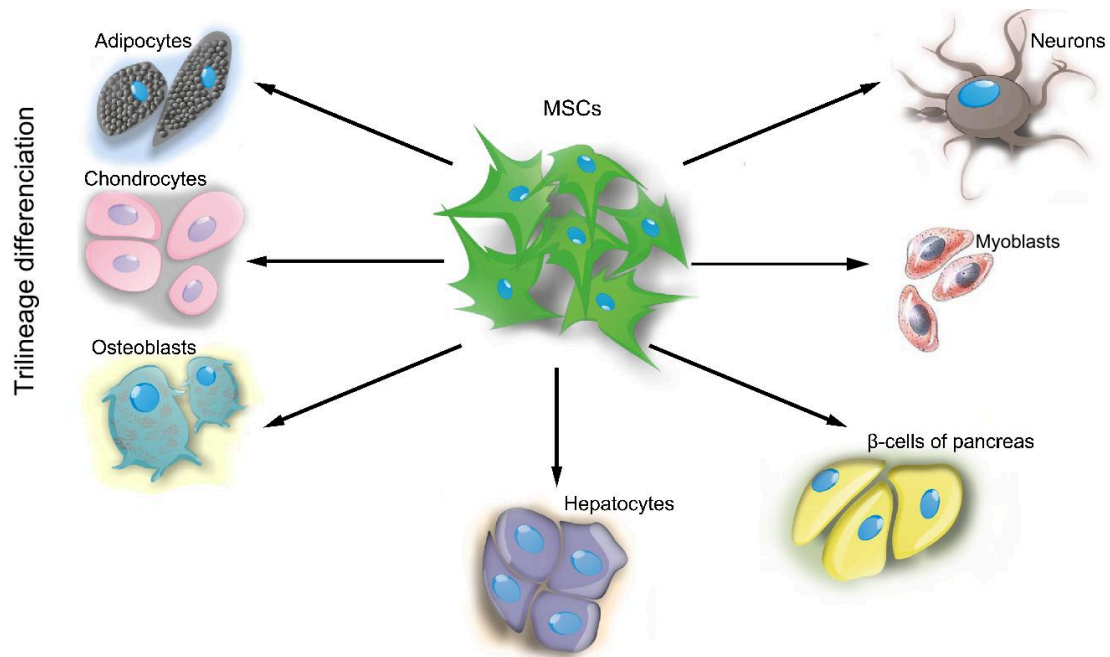


Figure 7: The differentiation potential of mesenchymal stem cells (Andrzejewska et al., 2019)

On steady state, MSCs constitutively express a low level of MHC class I surface antigens and lack of MHC class II antigen as well as of costimulatory molecules such as CD80, CD86 and CD40. With these immunological features, MSCs have been thought of as “immune-privileged” and in large outbred animals can generally be transplanted across MHC barriers without the need for immunosuppression (Devine et al., 2003; Patel et al., 2008). *In vitro*, MSCs inhibit T cell activation and dendritic cell differentiation, as well as B cell proliferation, and impair the cytolytic potential of natural killer cells (Aggarwal & Pittenger, 2005; Jiang et al., 2005). Some reports have described that direct cell-cell contact is required

for immunosuppression (Krampera et al., 2003). Immunosuppression after MSC infusion *in vivo* in diverse animal models of disease has also been shown (Meirelles Lda et al., 2009; Uccelli et al., 2008). These outcomes partially depend on the ability of MSCs to secrete a vast array of soluble factors, some of which have immunomodulatory properties, like TGF β , interleukin-10 (IL-10), nitric oxide and prostaglandin E2 (Meirelles Lda et al., 2009). Because MSC treatment appears to be encouraging for immunological disorders therapy, identification of MSC immunosuppressive properties can provide a key functional predictor for the efficacy of MSCs *in vivo*. Additionally, it is also important to bear in mind that MSCs from various sources can vary in their immunomodulation mechanisms and capacities (Mattar & Bieback, 2015).

The broad tissue distribution and multipotent differentiation of MSCs, along with the reported reparative effects of infused MSCs in many clinical and preclinical models, strongly indicate a critical role for MSCs in injury healing (Inoue et al., 2007; Parekkadan, van Poll, Suganuma, et al., 2007; Shi et al., 2010; Tzaribachev et al., 2008). It is reasonable to assume that severe tissue injury may mobilize and recruit remote MSCs to the sites of primarily inflamed or broken blood vessels (Karp & Leng Teo, 2009), although there has been no strong direct evidence of migration path of MSCs to the injured site, due to the lack of a reliable marker for MSCs. Recruited MSCs in response to chemotactic signals modulate inflammation, repair damaged tissue and facilitate tissue regeneration (Newman et al., 2009). MSCs contributes to tissue repair and regeneration by differentiating into several kinds of stromal and/or damaged cell types at the site of injury, whereas MSC paracrine signaling regulates the local cellular responses to injury, reducing inflammation, promoting angiogenesis, and inducing cell migration and proliferation (Gnecchi et al., 2008). Proteomic analyses of MSC-conditioned medium indicate that MSCs secrete many known factors of tissue repair including growth factors, cytokines, and chemokines, such as VEGF, PDGF, bFGF, EGF, keratinocyte growth factor (KGF), and TGF- β (L. Chen et al., 2008; Gnecchi et al., 2008). So far, MSCs have been widely studied and applied in regenerative medicine. Several clinical reports verify the potential efficacy of MSC-based cell therapy (Han et al., 2019). The therapeutic potential of MSC for liver fibrosis is developed in **section III-B-2.2**.

B) MSCs in liver fibrosis

1) MSCs as a source of myofibroblasts

MSCs have been proposed as a source of myofibroblasts in the fibrosis of several organs. Schepers and colleagues reported that leukemic myeloid cells stimulate MSCs to overproduce functionally altered osteoblastic lineage cells, which accumulate in the bone marrow cavity as inflammatory myelofibrotic cells to contribute to myelofibrosis (Schepers et al., 2013). In myocardial infarction, the infarct fibroblasts are generated by MSCs that respond robustly to injury by differentiating into matrix-producing fibroblasts, proliferating and accumulating in the infarct, contributing to the formation of a scar after an infarction (Carlson et al., 2011). Besides, the contribution of MSCs derived from bone marrow to the renal myofibroblast pool has also been described, showing that up to 35% of renal myofibroblasts are derived from BM-MSCs in the circulation (LeBleu et al., 2013). Together, these studies suggest that MSCs are implicated in the generation of myofibroblast during fibrosis development.

In the injured liver of patients, as well as in animal models, it has been reported that MSCs derived from bone marrow are recruited to the liver and contribute to the fibrogenic process (Baba et al., 2004; Forbes et al., 2004; Russo et al., 2006). HSCs, one of the main sources of hepatic myofibroblasts, display characteristics of stem/progenitor cells, and have thus been proposed as liver-specific MSCs. Stem cell markers CD73, CD105, CD271 and CD133 were detected in HSCs, which would have the capacity to differentiate into endothelial-like and hepatocyte-like cells (Kordes et al., 2007) and to contribute to liver regeneration (Kordes et al., 2014). However, controversy exists about the stemness of HSCs and tissue distribution analysis showed a localization of CD73 and CD90 expressing cells restricted to the periportal area (Klimczak & Kozłowska, 2016). Kramann and colleagues utilized elegant cell tracing and ablation approaches combined with *in vitro* analyses to demonstrate that perivascular Gli1+ MSC-like cells are major contributors to fibrosis in several organs, including the liver (Kramann et al., 2015).

Gli1 is a transcription factor that mediates Hedgehog signaling (Hui & Angers, 2011). Zhao and colleagues demonstrated that Gli1 marks a perivascular MSC-like

cell population in the mouse incisor (H. Zhao et al., 2014). Kramann and colleagues demonstrated that perivascular Gli1⁺ cells express several characteristic MSC markers, including 3G5, Nestin, and PDGFR α , and that they differentiate into bone, cartilage, and fat cells *in vitro*. PDGFR β ⁺/Gli1⁺ cells show increased colony-forming unit capability compared to other PDGFR β ⁺ cells, and *in vitro* experiments suggest that Gli1 may be required for their self-renewal (Kim & Braun, 2015). In the liver, Gli1⁺ cells were identified in the perivascular niche and were also positioned around bile ducts, thus displaying a similar distribution as Col15A1⁺ cells in human liver tissue sections (Lemoinne et al., 2015). Recently, Gupta and colleagues also reported that Gli1 was strictly expressed in peribiliary mesenchymal cells, wrapped around large and small bile ducts of the biliary tree. In the extrahepatic biliary tree, numerous Gli1⁺ cells were embedded within the mesenchyme containing bile ducts and the peribiliary glands. Gli1 was not expressed in HSCs, cholangiocytes, ECs or macrophages (Gupta et al., 2020). Although Gli1⁺ cells are present at low numbers under homeostatic conditions, they expand rapidly after injury and they were found to contribute to a non negligible part of myofibroblasts in CCl₄-induced fibrosis in one study (Kramann et al., 2015) but not in the other one (Gupta et al., 2020). In response to cholestatic liver injury (BDL and DDC diet-induced fibrosis), a large part of Gli1⁺ cells colocalized with α -SMA and desmin in large hilar ducts of the liver, but to a lesser extent in smaller peripheral bile ducts, suggesting distinct functions of Gli1⁺ cells with localization. These studies demonstrated that a MSCs population localized in portal area are a potential source of myofibroblasts during fibrosis progression in the liver.

2) MSCs as a therapeutic approach for liver fibrosis

Exogenously administration of MSCs modulates tissue injury and repair, which largely relies on the MSC paracrine secretion of antiapoptotic, anti-scarring, proangiogenic, and immunomodulatory factors involved in tissue regeneration (Caplan & Correa, 2011). MSCs could be derived from a patient's own tissues rather than blastocysts or embryos and be more appropriate for clinical use (Cho et al., 2009; R. Ji et al., 2012; H. Li et al., 2018). Progressive liver fibrosis is a major health issue for which no effective treatment is available, leading to cirrhosis and orthotopic liver

transplantation. However, the organ shortage is a reality. Therefore, cell-based therapy using MSCs may represent an attractive therapeutic option for cirrhosis.

Several *in vivo* studies were performed to evaluate the therapeutic potential of MSCs in the context of liver fibrosis in rats and mice (Abdel Aziz et al., 2007; Y. J. Chang et al., 2009; Jung et al., 2009; Q. Li et al., 2013; Nasir et al., 2013; Rabani et al., 2010; Tanimoto et al., 2013; Y. Wang et al., 2012; D. C. Zhao et al., 2005). Tissue-derived MSCs and BM-derived MSCs have been used and beneficial effects have been observed regardless of the origin of MSCs (Berardis et al., 2015). The mechanisms by which MSCs exert their anti-fibrotic effect still remains a controversy. Indeed, studies have proposed the differentiation of MSCs into hepatocyte-like cells, the generation of metalloproteinases by MSCs, and the modulation of inflammation (Berardis et al., 2015). Interestingly, some studies showed that pre-differentiation of MSCs into hepatocyte-like cells by incubation in the presence of HGF, results in a further significant reduction of liver fibrosis when compared to naive MSCs (Fang et al., 2004; Kuo et al., 2008). However, the improvement of liver function found in some studies seems not to be mainly mediated by MSCs differentiation and cell replacement, but by paracrine signaling improving survival of endogenous hepatocytes and proliferation of hepatocyte progenitors (Kuo et al., 2008; van Poll et al., 2008). Besides, MSCs were shown to inhibit HSC activation and proliferation, thus presenting fibrinolytic capacity (Neuss et al., 2010; Parekkadan, van Poll, Megeed, et al., 2007; D. C. Zhao et al., 2005). Furthermore, MSCs are able to modulate the immune function of HSCs and to induce HSCs apoptosis, which likely also contributes to their anti-fibrotic effects (Muhanna et al., 2008).

There is apparent discrepancy between the pro-fibrogenic capacity and the anti-fibrogenic properties of MSCs. Di Bonzo and colleagues reported that a significant proportion of transplanted MSCs were found to give rise to myofibroblasts (di Bonzo et al., 2008). Li and colleagues also showed that, indeed, many MSCs recruited to the fibrotic liver became myofibroblasts (C. Li et al., 2009). These studies suggested that MSCs are likely to differentiate into myofibroblast under a pro-fibrogenic microenvironment. Indeed, TGF- β and platelet-derived growth factor (PDGF) are known to be highly enriched in the fibrotic liver and to induce myofibroblast differentiation of MSCs (Bataller & Brenner, 2005; S. W. Chen et al., 2008). Different MSC subpopulations might have diverse multipotent and/or plastic

properties, and environmental factors might eventually determine or change their differentiation status. Therefore, this discrepancy might be explained by the coexistence of different cell populations in MSC samples. Additionally, the different stages of fibrosis generated in mice could have an effect on the behavior of transplanted MSCs favoring pro- or anti-fibrogenic effects.

IV) Angiogenesis in liver fibrosis

Angiogenesis is a dynamic process leading to the formation of a new vasculature from a pre-existing vasculature. Angiogenesis in the liver is similar to angiogenesis in other organs and tissues, which can occur in both physiological (*i.e.*, liver regeneration) and pathophysiological conditions, including ischemia, hepatocellular carcinoma, metastatic liver cancer or progressive CLDs (Elpek, 2015; Fernandez et al., 2009; J. S. Lee et al., 2007; Medina et al., 2004; Valfre di Bonzo et al., 2009). Evidence from both clinical and experimental conditions demonstrates that pathologic angiogenesis and sinusoidal remodeling are closely related to the progression of liver fibrosis (Bosch et al., 2010; Elpek, 2015; Fernandez et al., 2009; J. S. Lee et al., 2007; Medina et al., 2004; Valfre di Bonzo et al., 2009). However, it is unclear whether intrahepatic angiogenesis represents a beneficial response for maintaining homeostasis or one that exerts a pathological role leading to the progression of liver fibrosis. Previous studies showed that attenuating angiogenesis could be a promising therapeutic approach in patients with liver fibrosis as an efficient prevention of fibrosis could be achieved with antiangiogenic therapy in experimental model of CLDs. However, Patsenker and colleagues reported that promoting angiogenesis by silencing leukocyte cell derived chemotaxin 2 (LECT2) was beneficial for the improvement of liver fibrosis (M. Xu et al., 2019). These apparently conflicting conclusions indicate that the relationship between angiogenesis and fibrosis in the liver is complex and that mechanisms involved in angiogenesis during the progression of liver fibrosis are still poorly understood. In this chapter, we will address the cellular source of angiocrine signals in the liver during fibrogenesis and liver endothelial cell heterogeneity based on recently published scRNA-seq studies.

A) The relationship between liver angiogenesis and fibrosis

In any clinical condition of CLDs, angiogenesis and fibrogenesis are induced and develop in parallel (Novo et al., 2009). Similarly, angiogenesis has been reported in most experimental animal models of liver fibrosis (Corpechot et al., 2002;

Rosmorduc & Housset, 2010; Rosmorduc et al., 1999). Previous evidence supports the view that angiogenesis may contribute to the progression of liver fibrosis (Elpek, 2015) (Corpechot et al., 2002; Rosmorduc & Housset, 2010; Rosmorduc et al., 1999). In all tissues, angiogenesis is triggered by two crucial conditions, inflammation and hypoxia. During liver fibrogenesis, the accumulation of extracellular ECM in liver parenchyma (deposition of fibrillar collagen type I instead of sinusoidal collagen type IV) can contribute to the development of hypoxia, which in turn, stimulates the proangiogenic function of hypoxia-inducible factor (HIF) (Ju et al., 2016). HIF up-regulates the transcription of wound healing-related factors and mediators such as VEGF, PDGF-B, matrix metalloproteinases (MMPs), and the tissue inhibitors of metalloproteinases (TIMPs) that should facilitate liver repair and revascularization (Hamik et al., 2006; LaGory & Giaccia, 2016; Ramakrishnan et al., 2014; Shin et al., 2015). In addition, HIF-1 not only induces angiogenesis but also induces inflammation through the NF- κ B pathway (Coulon et al., 2011; Nath & Szabo, 2012). Indeed, inflammation is a biological response that activates the healing process following liver damage (Coulon et al., 2011). Inflammation, in its turn, contributes to angiogenesis and fibrotic phenomena (Seki & Schwabe, 2015). Pathologic angiogenesis can be inefficient due to the immaturity and permeability of VEGF-induced neovessels and, as a result, may be unable to correct liver hypoxia. Thereby, a vicious circle between fibrosis and pathologic angiogenesis is likely to occur (Cannito et al., 2014; Rosmorduc & Housset, 2010; Z. Zhang et al., 2015).

In conclusion, pathological angiogenesis and hypoxia drive each other and act synergistically in disrupting normal tissue repair, thereby accelerating the progression of liver fibrosis (Zadorozhna et al., 2020). Pharmacologic interventions that interrupt angiogenesis in experimental models, especially the administration of receptor tyrosine-kinase inhibitors such as sorafenib or sunitinib, attenuate liver fibrosis. However, these agents also directly target the pathways involved in fibrogenesis. Yet, drugs that specifically block angiogenesis by targeting molecules not involved in the fibrogenesis pathway, such as VEGF receptor type 2 (VEGFR2) exclusively expressed in endothelial cells, also improve liver fibrosis, strengthening the assumption that angiogenesis can accelerate the progression of liver fibrosis (Lemoinne et al., 2016; Mejias et al., 2009). Other studies indicated the dichotomous effects of anti-angiogenic interventions on liver fibrosis. The pharmacological inhibition targeting

the vitronectin receptor integrin alpha v beta 3 ($\alpha v\beta 3$) that promotes angiogenesis by mediating the migration and proliferation of ECs aggravates liver fibrosis despite its suppressive effect on angiogenesis (Patsenker et al., 2009). Kantari-Mimoun and colleagues reported that the neutralization or genetic ablation of vascular VEGF in myeloid cells resulted in delaying liver tissue repair and blocking liver fibrosis resolution through interruption of sinusoidal angiogenesis (Kantari-Mimoun et al., 2015). These findings implied that LSECs play dual roles in hepatic fibrogenesis and fibrosis resolution (Park et al., 2015).

Recently, a study showed that LECT2 inhibited the migration and tube formation of ECs through binding to tyrosine kinase with immunoglobulin like and EGF like domains 1 (Tie1) (M. Xu et al., 2019). Overexpression of LECT2 inhibited portal angiogenesis, promoted sinusoidal capillarization, and worsened liver fibrosis while silencing LECT2 was able to reverse these changes. This study suggested that portal angiogenesis and sinusoid capillarization played different roles during liver fibrogenesis: portal angiogenesis would attenuate fibrogenesis, whereas sinusoidal capillarization would promote fibrogenesis. In this study, a separate evaluation of portal angiogenesis and sinusoidal capillarization was proposed despite the lack of specific ECs markers (M. Xu et al., 2019). We would, therefore, conclude that today, the relationship between liver fibrosis and angiogenesis (portal)/capillarization (sinusoidal) remains unclear. The question deserves to be addressed in different types and stages of liver disease to develop appropriate strategies that balance efficient inhibition of fibrosis and the protection of normal angiogenic responses.

B) Heterogeneity and zonation of liver ECs

ECs are thought to be diverse between veins and arteries, large and small vessels, and different microvascular beds in various organs (Aird, 2007a, 2007b; Chi et al., 2003; Nolan et al., 2013). In the liver, there are two different types of microvascular structures: large vessels that are lined by continuous vascular endothelial cells lying on a basement membrane (such as portal vein, hepatic arteries) and liver sinusoids that are lined by highly specialized endothelial cells, LSECs, which are characterized by fenestrated and discontinuous features, and are devoid of a

basement membrane. Vascular ECs and LSECs provide a dynamic barrier between blood and the liver microenvironment. Blood dually supplied by the portal vein and hepatic artery, flows towards the central vein from portal tracts, creating gradients of nutrients, hormones, and oxygen that shape the molecular and functional heterogeneity of liver cells, a phenomenon termed liver zonation (**Figure 8**).

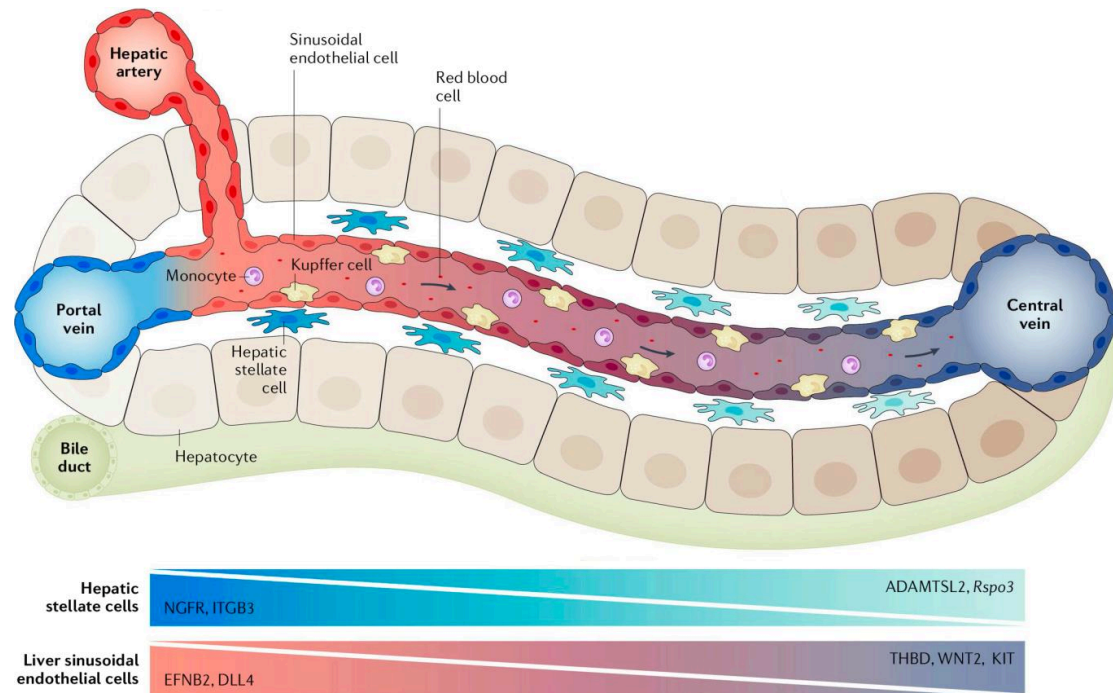


Figure 8: Zonation of HSCs and LSECs across the liver sinusoid (Ramachandran et al., 2020)

Blood oxygen and nutrients are depleted along the sinusoid creating a gradient. Concentric layers of hepatocytes (brown) are positioned between the portal triad and central vein. Non-parenchymal cells associated with the sinusoid include LSECs, Kupffer cells and HSCs which reside in the space of Disse. ScRNA-seq has revealed zonation of LSECs and HSCs.

Although vascular ECs and LSECs are drivers of angiogenesis and sinusoidal remodeling during liver fibrosis progression, their heterogeneity and regulation in both normal and damaged liver have not been fully elucidated. Strauss and colleagues first described the zonation of human LSECs by immunofluorescent labeling. One population of CD36^{hi}CD32⁻CD14⁻LYVE1⁻LSECs is located in Zone 1 of the lobule (periportal area), whereas another one, LYVE-1⁺CD32^{hi}CD14⁺CD54⁺CD36^{mid-low} LSEC population is located in Zones 2 and 3 (midzonal and perivenular areas)

(Strauss et al., 2017). Recently, with the development of scRNA-seq technology, the understanding of liver ECs heterogeneity has been rapidly advancing. Liver ECs zonation and their landmark genes have been described by several scRNA-seq studies and are summarized in **Table 5**. Based on prior histological examinations of LSECs zonation, three liver EC populations corresponding to periportal LSECs (Zone 1), midzonal and perivenular LSECs (Zone 2/3), and non-LSECs (Vascular ECs) were clustered by scRNA-seq technology. The top differentially expressed genes (DEGs) for each EC cluster were listed in the literature that might provide more landmark genes for liver ECs zonation (MacParland et al., 2018). Although the proposed LSEC zonation genes were generated by unbiased scRNA-seq, the reference of LSECs zonation was based on the immunohistological study, which was limited by protein expression levels and antibodies. To overcome this shortage, Halpern and colleagues, developed an approach termed paired-cell sequencing (pcRNA-seq) to probe heterogeneity of liver ECs and bioinformatically inferred liver ECs spatial information by using the spatial information from hepatocytes, delineating a detailed and precise mouse liver ECs landmark gene signature (Halpern et al., 2018). Another scRNA-seq study of mouse non-parenchymal liver cells (NPCs) from healthy and NASH liver proposed a similar LSEC zonation molecular signature (Xiong et al., 2019). More recently, Su and colleagues performed scRNA-seq analysis of mouse liver ECs exclusively and further confirmed the previous findings of LSECs zonation (Su et al., 2020). In the human liver, a more recent study illustrated human liver ECs zonation and revealed the limited evolutionary conservation of gene expression zonation between mouse and human liver ECs (Aizarani et al., 2019). Future work is needed to dissect the signaling mechanisms underlying liver ECs zonation and its involvement in liver physiology and disease.

Selected Zonation landmark genes of liver ECs					Method	Species	Ref
Vascular ECs	LSECs			Lymphatic EC			
	Peri-portal (Zone 1)	Mid (Zone 2)	Peri-central (Zone 3)				
CD31CD34 vWF	CD36high CD32- CD14- LYVE1-	LYVE1+ CD32B+ CD14+ CD54+ CD36 mid-low		--	IF	Human	(Strauss et al., 2017)
<i>ENG, PECAM1, RAMP3, INMT, DNASEIL3, LIFR, PTGD5, C7, CTGF, TIMP3, RNASE1, ID3, MGP, PCAT19, HSPG2, GPM6A, PTRB, vWF, SRPX</i>	<i>F8, PECAM1, MGP, SARCL1, TM4SF1, CLECL4A, ID1, IGFBP7n, ADIRF</i>	<i>CD32B, LYVE1, STAB2, CCL14, CLEC1B, FLN2, S100A13, FCN3, CRHBP, STAB1, GNG11, CLEC4G, CLDN5, CCL23, OIT3, RAMP3</i>		--	scRNA-seq (10X Genomics)	Human	(MacParland et al., 2018)
<i>Dll4, Cldn5, Efnb2, Ltbp4, Pear1, Lama4, Chst2</i>		<i>Ecml, Lyve1, Ccnd1, Pcdhgc5, Ctsl, Kcnb1, Sema6a</i>	<i>Rspo3, Wnt2, Wnt9b, Thbd, Cdh13, Fabp4, Kit, Lgals1</i>	--	pcRNA-seq (MARS-Seq)	Mouse	(Halpern et al., 2018)
<i>Ednrb, Jag1, Lrg1, Efnb1, Ltbp4, Adgrg6,</i>		<i>Fcgr2b, Gpr182</i>	<i>Wnt9b, Rspo3, Cdh13, Wnt2</i>	--	scRNA-seq (10X Genomics)	Mouse	(Xiong et al., 2019)
<i>Cd32b, Flt4, Stab2, Pecam1</i>	<i>Dll4, Msr1, Efnb2, Ltbp4, Ntn4, Adam23</i>	<i>Lyve1, Ctsl</i>	<i>Rspo3, Wnt2, Wnt9b, Kit, Cdh13, Thbd, Fabp4</i>	<i>Lyve1, Flt4, Pdpn, Prox1</i>	scRNA-seq, (10X Genomics)	Mouse	(Su et al., 2020)
<i>BTNL9, ANPEP, Defined by CD34 PECAM high</i>	--	<i>LYVE1, FCN3, Defined by CLEG4G</i>	<i>ICAM1, ENG, Defined by CLEG4G</i>	--	scRNA-seq (mCEL-Seq2)	Human	(Aizarani et al., 2019)

Table 5: Liver endothelial cell zonation and landmark genes

C) The role of profibrogenic cells in liver angiogenesis

HSC-derived myofibroblasts (HSC-MFs) and PMFs have been reported to comprise more than 90% of the collagen expressing cells, suggesting that they are the major origin of collagen expressing cells in fibrotic liver (Iwaisako et al., 2014; Kisseleva & Brenner, 2006). Under physiological conditions, PFs normally comprise a small population of the fibroblastic cells that surround the portal tract to maintain the integrity of portal tract. Moreover, HSCs in their quiescent state act as pericytes that regulate the functions of LSECs, maintaining sinusoidal homeostasis. In pathophysiological conditions, HSC-MFs and PMFs acquire a proangiogenic phenotype and secrete proangiogenic factors (Semela et al., 2008; Thabut et al., 2011). Therefore, the cellular and molecular relations between liver fibrosis and angiogenesis involve the role of PMFs and HSC-MFs (Kukla, 2013; Lemoinne et al., 2016).

Our team reported that ECs proliferation is correlated with the expansion of PMFs at late stages of fibrosis, indicating a role for PMFs in liver angiogenesis (Lemoinne et al., 2015). Col15A1, the specific marker we identified for PMFs and the precursors of PMFs belongs to the group of non-fibrillar collagens, characterized by extensive interruptions in their collagenous sequences and a conserved noncollagenous carboxyl-terminal structure (Kivirikko et al., 1994; Muragaki et al., 1994). The immunostaining of COL15A1 in human cirrhotic livers showed that PMFs display a perivascular distribution and outline vascular capillaries within large fibrotic septa (Lemoinne et al., 2015). We have demonstrated that PMFs are able to promote vascular remodeling in vitro and in vivo by various mechanisms, including the formation of direct intercellular junctions with ECs and the release of VEGF-A containing microparticles (Lemoinne et al., 2015) (**Figure 9A**). Besides, our team also found that PMFs from BDL rats liver displayed endoplasmic reticulum stress and higher proangiogenic properties, whereas their proliferative and migratory capacities were lower compared with standard PMF obtained from normal rat liver. These phenotypic switches could be reversed by PKR-like ER kinase (PERK) inhibitor treatment, indicating that the PERK arm of ER stress may play an essential role in PMFs expansion and angiogenesis during liver fibrosis. However, the contribution of PMFs to liver angiogenesis is not well understood. Therefore, further studies focusing on the interactions between PMFs and ECs in different stages of pathophysiological

conditions may dramatically increase our understanding of the relationship between liver fibrogenesis and angiogenesis (Loeuillard et al., 2018).

In physiological conditions, shear stress activates the transcription factor kruppel-like factor 2 (KLF2) in LSECs, leading to the release of vasodilating agents, including nitric oxide (NO) and to the inhibition of vasoconstrictive molecules including endothelin-1 (ET-1) (Marrone et al., 2013). HSCs are maintained quiescence through LSEC NO-dependent pathway. In the liver injury, as shown in **Figure 9B**, LSECs dedifferentiate into capillarized LSECs, which disturb the balance of vasodilation and vasoconstriction. Capillarization of LSECs cause HSCs to undergo a dramatic phenotype transformation (activation) and thus significantly alters the signaling between HSCs/HSC-MFs and LSECs, leading to a vicious cycle between LSEC capillarization and HSC activation, which contributes to fibrogenesis and abnormal sinusoids (Hammoutene & Rautou, 2019). At the early stage of liver injury, the mural coverage of sinusoidal vessels is enhanced by HSCs (Novo et al., 2007), and the contractile nature of HSCs/HSC-MFs will be remarkably enhanced because of the overproduction of ET-1 by HSCs/HSC-MFs or LSECs and a significant reduction in NO release by LSECs (Geerts, 2001; Iwakiri et al., 2008; Iwakiri et al., 2014). This process of “pathological sinusoidal remodeling” further contributes to a high-resistance, constricted sinusoidal vessel. HSCs/HSC-MFs in liver injury are likely to represent a hypoxia-sensitive condition in a HIF-1 α related pathway through the up-regulating transcription and synthesis of VEGF, Ang-1, the molecules that promote angiogenesis and also their receptors VEGFR-2 and Tie-2 (Aleffi et al., 2005; Ankoma-Sey et al., 2000; Novo et al., 2007; Y. Q. Wang et al., 2004). Meanwhile, HSCs/HSCs-MFs represent a cellular target for the action of VEGF and Ang-1 (Paternostro et al., 2010). VEGF is not only a key regulator of differentiated LSEC phenotype maintenance as it leads to the formation and maintenance of fenestrae (DeLeve, 2015; Iwakiri et al., 2014) but also a leading regulator of ECs/LSECs activity during all steps of angiogenesis (Walter et al., 2014). Furthermore, VEGF has been reported to be able to trigger HSC/HSC-MF proliferation, increase deposition of ECM components, as well as increasing migration and chemotaxis (Novo et al., 2007; Olaso et al., 2003; Yoshiji et al., 2003). Besides VEGF signaling, PDGF and TGF- β , two profibrotic growth factors, are key players in LSEC and HSC crosstalk. Capillarized LSECs, HSCs/HSC-MFs, and

Kupffer cells release PDGF and TGF- β , thereby stimulating HSC transformation, proliferation, migration, and extracellular matrix production and deposition (S. L. Friedman, 2003; J. S. Lee et al., 2007). PDGF released by capillarized LSEC can also bind its PDGFR- β receptor and promote an angiogenic phenotype of HSC, which further facilitates angiogenesis (Semela et al., 2008). Akin to PMFs that can release microparticles (MPs) containing VEGF-A, one study provided evidence that activated HSCs (PDGF-treated HSC) can produce and then release MPs containing Hedgehog (Hh) ligands. Hh ligands activate Hh signaling in LSECs, causing significant changes in LSECs with the upregulation of several genes leading to an angiogenic phenotype (Witek et al., 2009).

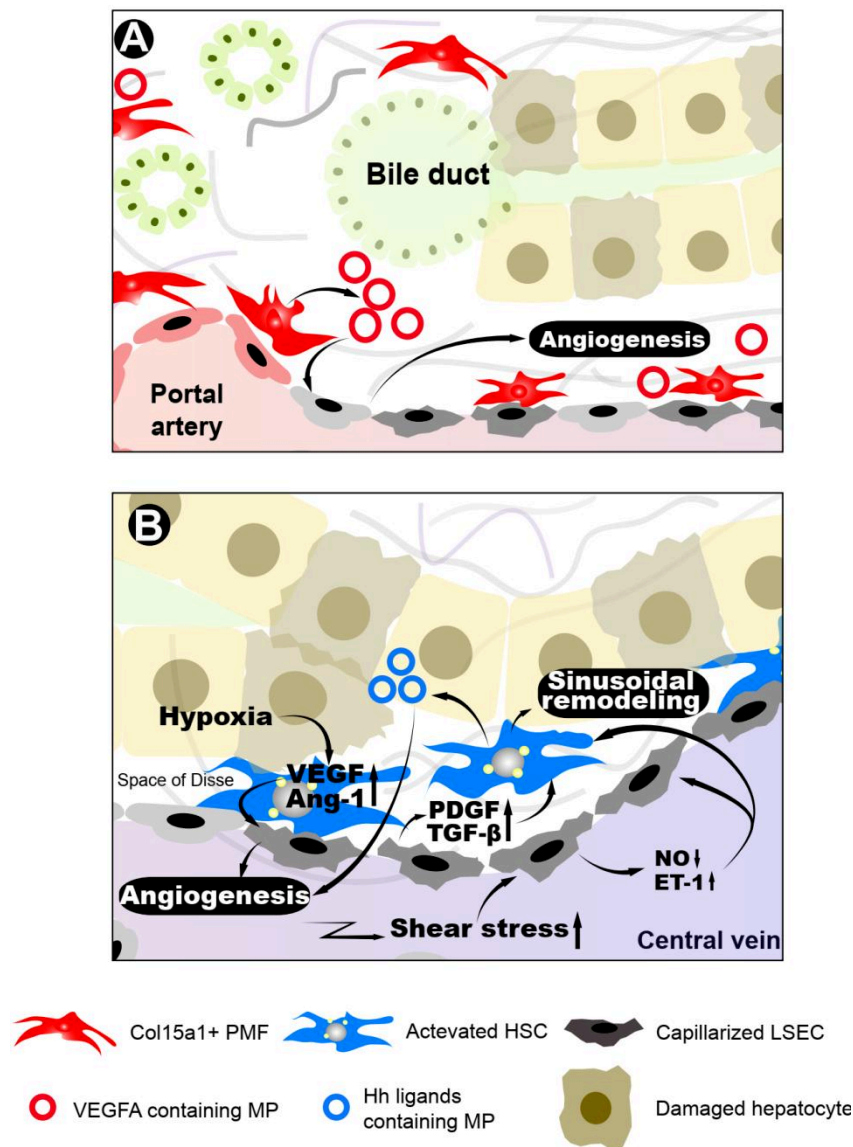


Figure 9: The role of profibrogenic cells in liver angiogenesis in a cirrhotic liver

(A) Col15A1+ PMFs proliferate and promote angiogenesis through releasing vascular endothelial growth factor (VEGF) A containing microparticles (MPs). (B) Increasing shear stress will decrease nitric oxide (NO) synthesis and increase ET-release. This process promotes sinusoidal remodeling, leading to LSECs capillarization. Capillarized LSECs permit HSC activation through increasing PDGF and TGF- β synthesis, resulting in the production and deposition of extracellular matrix (ECM). Activated HSCs could increase the production of VEGF and Ang-1 in response to hypoxia, and thus induce angiogenesis.

The literature has established an unequivocal mechanistic link between liver angiogenesis and fibrogenesis. The current challenge is to address the role of angiogenesis (portal and sinusoidal) in different types and stages of liver fibrosis. In deep, to explore the function of profibrogenic cells in liver angiogenesis and the interactions between profibrogenic cells and LSECs, new tools, such as PMF, HSC, LSEC specific transgenic and knockout and cell fate tracing animal models should be generated. Recently, scRNA-seq already showed the power to unravel cell heterogeneity in human and mouse liver including of liver mesenchymal cells and LSECs, which will allow us to define more precise markers for each cell type, and develop the new tools mentioned above, also to uncover the nature of intercellular interactions and disease-associated cellular reprogramming with high resolution.

OBJECTIVES

As a consequence of organ injury, mesenchymal cells differentiate into myofibroblasts, the key effectors of fibrosis, that also make a major contribution to other aspects of the wound healing response, including regeneration and angiogenesis. Identification of the cellular sources of myofibroblasts and the contribution of different sources to the myofibroblast pool remains a major goal in the field. In liver fibrosis, myofibroblasts are derived from two major sources: hepatic stellate cells (HSCs) and portal fibroblasts (PFs). The paradigm of HSC phenotypic change into myofibroblasts has dominated the focus of research on liver fibrosis over the past 30 years. A distinct subpopulation of liver myofibroblasts, now referred to as portal myofibroblasts (PMFs), has been identified by our group (Lemoinne et al., 2015), who suggested that PMFs are derived from portal mesenchymal cells and characterized by a high proliferative and proangiogenic activity.

Of note, as described above, PMFs are derived from the cell populations of portal mesenchymal cells, which reside in the portal area and maintain the integrity of the portal triad in the liver under physiological conditions. However, little information is available regarding the identity, spatial distribution, or functions of portal mesenchymal cells. Therefore, the first objective of this work is to elucidate the landscape of portal mesenchymal cells by using scRNA-seq. To better define the contribution of PMFs to liver fibrosis, an important issue to settle is to identify and isolate the precursors of PMFs. Because of the lack of cell-specific markers, the progenitors of PMFs, present in very small amount in the liver, were never isolated as a pure cell population. In this work, taking advantage of the scRNA-seq approach, we were able to identify and isolate PMF progenitors as a pure cell population that we designated portal mesenchymal stem cells (PMSCs). Although recent studies have provided additional evidence that PMFs may play an important role in liver fibrosis progression (Gupta et al., 2020; Nishio et al., 2019), the contribution of PMFs to liver fibrosis progression seems to be underestimated due to the low abundance of their precursors in normal liver and the lack of reliable markers to distinguish them from HSCs and their derived myofibroblast. Therefore, we were committed to defining the specific and reliable gene signatures or markers for PMSCs and HSCs and their derived myofibroblasts. The discovery of the novel gene signatures and markers

prompted us to further evaluate the behaviour of PMSCs and HSCs in mouse models of liver fibrosis and human fibrotic liver diseases. Furthermore, the correlation between the gene signature of PMSCs and those of angiogenesis and fibrosis was also evaluated in this work.

Collectively, this thesis aims to elucidate the cell atlas of portal mesenchymal cells, with a particular focus on a portal mesenchymal stem cell niche.

PART II:
RESULTS

I) Introduction

HSCs have been regarded as the major collagen-producing cells in the liver since their discovery 35 years ago. Yet, the other liver mesenchymal cells, notably portal mesenchymal cells, have gained increasing interest recently as evidence has accumulated to indicate that they contribute to myofibroblasts and interact with endothelial cells and cholangiocytes during liver fibrosis progression (Gupta et al., 2020; Nishio et al., 2019). However, it is unclear how many types of mesenchymal cell subtypes exist and how they differ from one another, and their biology is poorly defined. PMFs derived from portal mesenchymal cells distinct from HSCs that are still unknown, and the potential role of PMFs and their precursors in liver are still not clear. A major limitation to address this question has been the lack of markers that would allow us to isolate or precisely trace them *in vivo*.

Single cell RNA-sequencing (scRNA-seq) enables genomewide profiling of individual cells (Islam et al., 2011; Tang et al., 2009) and therefore it is an ideal methodology to detect cellular heterogeneity in an unbiased manner. This work was initially designed to 1) delineate portal mesenchymal cells heterogeneity in normal mouse liver and provide global insight into the nature of distinct cell subsets and 2) identify and characterize the precursors of PMFs and determine the role of these cells in liver fibrosis.

II) Article: Lei et al., Single-cell transcriptomics enable uncovering portal mesenchymal stem cells as precursors of myofibroblasts in liver fibrosis, to be submitted

Single-cell transcriptomics enable uncovering portal mesenchymal stem cells as precursors of myofibroblasts in liver fibrosis

Lin Lei¹, Haquima El Mourabit¹, Justine Guégan², Trine Folseraas,³ Sara Lemoine,^{1,4} Tom H. Karlsen,³ Bénédicte Hoareau,⁵ Ester Gonzalez-Sanchez,¹ Vlad Ratziu,⁶ Pierre Charbord,⁷ Jérémie Gautheron¹, Thierry Jaffredo⁷, Axelle Cadoret^{1*}, Chantal Housset^{1,4*}

¹Sorbonne Université, INSERM, Centre de Recherche Saint-Antoine (CRSA) and Institute of Cardiometabolism and Nutrition (ICAN), Paris, France;

²Sorbonne Université, INSERM, Institut de Cerveau et de la Moelle épinière (ICM), Bioinformatics/Biostatistics Facility, Paris, France;

³Norwegian PSC Research Center, Research Institute of Internal Medicine, Division of Surgery, Inflammatory Medicine and Transplantation, Oslo University Hospital Rikshospitalet, Oslo, Norway;

⁴Assistance Publique-Hôpitaux de Paris, Reference Center for Inflammatory Biliary Diseases and Autoimmune Hepatitis (CRMR, MIVB-H), Department of Hepatology, Saint-Antoine Hospital, Paris, France;

⁵Sorbonne Université, INSERM, Unité Mixte de Service (UMS) Production et Analyse de Données en Sciences de la Vie et en Santé (PASS), Plateforme Cytométrie Pitié-Salpêtrière (CyPS), Paris, France ;

⁶Sorbonne Université, Assistance Publique-Hôpitaux de Paris, Institute of Cardiometabolism and Nutrition (ICAN), Pitié-Salpêtrière Hospital, Paris, France ;

⁷Sorbonne Université, CNRS, INSERM, Institut de Biologie Paris Seine (IBPS), Laboratoire de Biologie du Développement, Paris, France.

*These authors share senior authorship

Corresponding authors:

Chantal Housset, M.D., Ph.D.

Sorbonne Université, Faculté de Médecine, Site Saint-Antoine,
27 rue Chaligny, 75571 Paris cedex 12, France.

E-mail: chantal.housset@inserm.fr

Phone: (33) 1-40-01-13-59

Axelle Cadoret, Ph.D.

Sorbonne Université, Faculté de Médecine, Site Saint-Antoine,

27 rue Chaligny, 75571 Paris cedex 12, France.

E-mail: axelle.cadoret@inserm.fr

Phone: (33) 1-40-01-13-53

Abstract (156/150)

Myofibroblasts are key effectors of fibrosis. In liver fibrosis, myofibroblasts derive from hepatic stellate cells (HSCs) and as yet undefined mesenchymal cells. We uncovered the landscape of portal mesenchymal cells in mouse liver, using single-cell RNA-sequencing. Trajectory analysis enabled inferring a small cell population further defined by a minimal set of surface markers used to isolate it. This population consisted of portal mesenchymal stem cells (PMSCs) according to their mesenchymal stem cell attributes, able to generate myofibroblasts in culture. We identified a transcriptomic signature, including *Slit2*, characterizing PMSCs and derived myofibroblasts. Using this signature, we showed that PMSC expansion was correlated with fibrogenesis and angiogenesis in cases of pan-etiology murine and human liver disorders. We also unraveled a transcriptomic signature of HSCs that did not vary in these disorders. In conclusion, we have uncovered PMSCs as a small population of myofibroblast precursors that largely expand with the progression of liver fibrosis, to target in antifibrotic strategies.

Mesenchymal cells are key players in organ development, tissue homeostasis and wound healing response. Their phenotype varies widely across different organs and between different compartments within the same organ. In the liver, mesenchymal cells comprise hepatic stellate cells (HSCs), that reside in sinusoids, and perivascular cells including smooth muscle cells and fibroblasts, that reside around central veins and in the portal tracts. Genetic-based lineage-tracing analyses have demonstrated that HSCs and perivascular mesenchymal cells as well as mesothelial cells all derive from the septum transversum during liver development (1). By contrast, the septum transversum did not contribute to the lineage of liver sinusoidal endothelial cells (LSECs), Kupffer cells or hepatoblasts (1). Over the past 30 years, HSCs have been extensively investigated for their capacity to undergo myofibroblastic differentiation, and as yet the paradigm of HSC phenotypic change into myofibroblasts has been the focus of research on liver fibrosis (2). However, the other liver mesenchymal cells, particularly portal mesenchymal cells have gained increasing interest as evidence has accumulated that indicate they could also generate myofibroblasts (3-10). The portal tracts contain three main structures referred to as the portal triad, *i.e.*, the portal vein, hepatic artery and bile duct, surrounded by a mesenchyme, which has remained poorly defined so far. Little is known regarding the identity, spatial distribution or functions of portal mesenchymal cells and how they contribute to fibrosis. A major limitation to address these issues has been the lack of markers, especially surface markers that would allow to isolate portal mesenchymal cells or track them *in vivo*. Using a model of outgrowth from fragments of the bilio-vascular tree isolated from rat liver, we previously showed that portal cells distinct from HSCs could generate myofibroblasts, that were referred to as portal myofibroblasts (PMFs) and characterized by type 15 collagen alpha 1 (COL15A1) expression, a high proliferation rate and pro-angiogenic properties (8, 11). However, contrarily to the

PMFs themselves the PMF precursor cells have not been identified. In the present study, we isolated portal mesenchymal cells from mouse liver as a single-cell preparation and analyzed their diversity using single-cell RNA-sequencing (scRNAseq). A minimal set of surface markers enabled us to isolate a subset of cells that we designated portal mesenchymal stem cells (PMSCs) according to their mesenchymal stem cell properties with the ability to generate myofibroblasts. Markers of PMSCs were identified and used to show the expansion of these cells in murine and human liver fibrosis.

Results

Landscape of the portal mesenchyme revealed by scRNAseq

Portal mesenchymal cells represent a very small amount of cells. They are tightly bound to the bile duct and portal vascular structures, relying on basement membranes. This makes them far more difficult to isolate than hepatocytes or sinusoidal cells, which reside in a loose, basement membrane-free, extracellular matrix (ECM) microenvironment. In the present study, we set up a specific procedure to isolate portal mesenchymal cells, for scRNAseq analysis (Fig. 1A). First, we adapted a method we previously established for the culture of rat PMFs (12), to isolate fragments of the bilio-vascular tree from mouse liver. Next, bilio-vascular fragments were submitted to enzymatic digestion, resulting in a single-cell suspension. The cell suspension was depleted in cells expressing the lineage (Lin) markers of cholangiocytes (EpCAM), endothelial cells (CD31), and hematopoietic cells (CD45 and CD11b) by means of cell sorting. Lin-negative single-cell suspension was processed to generate a scRNAseq cDNA library using the 10x Genomics technology. We captured 4,976 sequenced cells that met quality control metrics. Unsupervised clustering using the Seurat package (13) identified 16 distinct cell clusters (Fig. 1B, left). Clusters were assigned to putative identities

by matching their gene profiles with those previously attributed to specific cell types (Fig. 1B, right). The 16 cell clusters were identified as fibroblasts (5 clusters), vascular smooth muscle cells (VSCMs, 5 clusters), endothelial cells (4 clusters), HSCs (1 cluster) and mesothelial cells (1 cluster). The hierarchical clustering of gene expression profiles supported this identification, Fib, VSMC and EC each belonging to the same cluster classification, except for the smallest cluster of VSMC-5 that was far apart from the other VSCM samples (Fig. 1C). The segregation of the cell clusters according to the most selective expressed genes is illustrated by heatmap and *t*-distributed stochastic neighbor embedding (*t*-SNE) representations (Fig. 1, D and E; Suppl. Table S1). Cell cycle-related genes, *e.g.*, *Mki67*, were not upregulated in any of the clusters (Suppl. Fig. S1).

The non-mesenchymal components: mesothelial and endothelial cells.

Mesothelial cells display an intermediate phenotype between epithelial and mesenchymal cells and form a single layer that covers the liver surface (14). Here, we found such cells in the cell suspension, consistent with their migration inward from the surface during liver development (1), and for the first time, we describe their transcriptional profile at a single-cell resolution in mouse liver (Suppl. Table S1). Genes expressed in these cells included known mesothelial markers, such as *Msln*, *Pdpn*, *Wt1*, *Upk1b* and *Gpm6a*, as well as epithelial markers, such as *Krt8*, *Krt19* and *Ezr*, and mesenchymal markers, such as *Vim*. Several additional putative markers of mesothelial cells restricted to this cluster, were found, including *Sipi*, *Myl7* and *Fxyd3* (Suppl. Table S1).

We identified 4 clusters of endothelial cells, enriched in markers such as *Pecam1*, *Cdh5*, *Kdr* and *Egfl7* (Suppl. Table S1). The PECAM1 protein (alias CD31) has been reported to be intracellular in liver sinusoidal endothelial cells (LSECs) (15, 16), which explains, at least

partly, why endothelial cells escaped our negative selection according to the membrane antigen CD31. The recovery of sinusoidal cells, *i.e.* LSECs and HSCs, from the bilio-vascular preparations is consistent with the anatomical connection between the perisinusoidal and portal spaces (17). Moreover, even though cells from the bilio-vascular tree were preferentially retrieved by our method, LSECs which are basement membrane-free, adhere to other cell types and are prone to be collected during isolation procedures, as pointed out in recent scRNAseq studies of liver cells (18). Cluster EC-1 displayed enriched expression of *Rspo3*, *Wnt9b*, *Thbd*, *Fabp4*, *Wnt2*, *Cdh13* previously reported as markers of peri-central LSECs (18-20). Cluster EC-2 displayed an enriched expression of *Adam23*, *Msr1*, *Btnl9*, *Ntn4*, *Adgrg6*, *Efnb2*, previously reported as markers of peri-portal LSECs and/or portal vascular endothelial cells (18, 19, 21). Cluster EC-3 highly expressed established markers of lymphatic endothelial cells, *i.e.*, *Lyve1*, *Flt4*, *Pdpm*, *Prox1*, *Mmrn1* and *Reln* (22). EC-4 was enriched in *Cldn5*, *Pecam1* and *Tm4sf1*, previously reported in hepatic arterial endothelial cells (22). Thus, we recovered previously reported markers of endothelial cell zonation in the liver (Suppl. Fig. S2).

The mesenchymal components: fibroblasts, HSCs and VSMCs

Our single-cell analysis revealed 5 clusters of fibroblasts (Fig. 1, B-E) all enriched in common mesenchymal or fibroblast markers (*e.g.*, *Vim*, *Pdgfra* & b, *serpinh1*) and all with high expression of collagens (Suppl. Table S1). All clusters showed an enrichment for the ontology terms “ECM organization” and “Wound healing” (Suppl. Table S2). The most abundant population of fibroblasts, Fib-1 was enriched in genes involved in cell chemotaxis and leucocyte migration (Suppl., Table S2 and Fig. S3) suggesting that these cells participate in the immune surveillance of the liver. The cluster Fib-2 displayed an up-regulation of genes

involved in epithelial cell proliferation and migration, suggesting an interaction with cholangiocytes. The population Fib-3 was particularly enriched in ontology terms related to tissue development and morphogenesis (Suppl., Table S2 and Fig. S3). Notably, Fib-3 highly expressed *Runx1*, a transcription factor essential for mesenchymal stem cell proliferation and myofibroblast differentiation (23). The top differentially expressed gene in Fib-3 was Pleiotrophin (*Ptn*), which is a pericyte-derived trophic factor in particular for endothelial cells (24). Of all Fibroblast clusters, Fib-3 expressed the highest level of *Vegfa* expression, consistent with a major interaction with endothelial cells, and also an enriched expression in the head-to-head *Col4a5/Col4a6* genes that contribute to basement membranes notably of blood vessels (25) and *Col7a1*, an anchoring fibril protein with unique adhesive properties (26). Like Fib-3, Fib-4 showed enrichment in the expression of genes involved in tissue development, including *Sox9*, a marker of progenitor cells. Additionally, this cluster was the most enriched in ECM components and regulators, indicating a key role in matrix organization (Suppl., Table S2 and Fig. S3). Fib-5 cells were enriched in HSC markers, such as lecithin retinol acyltransferase (*Lrat*) (27) and reelin (*Reln*) (9), suggesting that this population may represent an intermediary population between fibroblasts and HSCs (1).

Cells of cluster 8 were recognized as HSCs on the basis of their transcriptional profile (9, 27-29). Classical markers of HSCs such as *Lrat* or *Reln* (9, 27) proved not to be fully specific, being expressed in other clusters, notably Fib-2 and Fib-5. Cytoglobin (*Cygb*) (5, 30) previously reported as an anti-oxidant in HSCs, was expressed in all mesenchymal cells. Like others (27, 28), we found virtually no expression of glial fibrillary acidic protein (*Gfap*), another classical marker of HSCs, whereas desmin (*Des*) that has also been proposed as a marker of HSCs, and vimentin (*Vim*), a marker of mesenchymal cells, were expressed at variable levels in all clusters. Among HSC markers newly identified by scRNAseq (28, 29) or

bulk RNAseq (31), our analysis highlighted genes that indeed were restricted to HSCs, such as *Tmem56*, *Colec10*, *Mapt* or *Bco1*. Other genes such as *Ngfr*, *Vipr1*, *Pth1r*, *Fcna* or *Angptl6* were largely overexpressed in HSCs, but expressed at lower levels in other mesenchymal cells, notably Fib-2 and Fib-5, whereas another subset of genes such as *Colec11*, *Ecm1* or *Rgs5* were expressed at relatively high levels in several other mesenchymal cells, in addition to HSCs (Suppl., Table S1 and Fig. S4).

We identified 5 clusters as VSMCs. With the exception of VSMC-3, these sub-populations expressed the typical markers of mature VSMCs at high levels, including alpha 2 smooth muscle actin (*Acta2*), trangelin (*Tagln*), calponin 1 (*Cnn1*), smoothelin (*Smtn*) and myosin heavy chain 11 (*Myh11*). VSMC-3 showed little or no expression of these markers (Suppl. Table S1), consistent with an immature phenotype. VSMC-1 and VSMC-5 expressed the VSMC gene signature previously identified in mouse liver (*Acta2*⁺ *Tagln*⁺ *Cnn1*⁺ *Myh11*⁺ *Tpm2*⁺ *Pln*⁺) (28), and expressed almost all VSMC genes as reported for the human liver (22). In terms of GO analysis (Suppl. Fig. S3), VSMC-2 distinguished themselves by an enrichment for the processes of “Extracellular matrix organization” and “Inflammatory response”, and VSMC-3 by an enrichment for the functions “Response to molecule of bacterial origin” and “Smooth muscle cell proliferation”, consistent with their immature phenotype.

Identification of portal mesenchymal stem cells (PMSCs)

To investigate the potential differentiation pathway from the mesenchymal progenitor cells in the adult liver to their differentiated progenies described above, we analyzed all cells after exclusion of mesothelial and endothelial cells, using Monocle (32). This analysis showed a common trajectory of portal mesenchymal cells with one bifurcation and three branches defining states (Fig. 2A). According to pseudotime the branch on the left was defined as root

state, contrasting with the two branches on the right containing cells with high pseudotime value. The root state was mainly populated by Fib-3 and Fib-4 cells, which were consequently assumed to be identical with or close relatives of progenitor cells, contrasting with the two other states populated by VSMCs and HSCs (Fig. 2A). Consistent with this assumption, GO analysis showed that Fib-3 and Fib-4 clusters were enriched in development-related pathways suggestive of multilineage potential (Fig. 2B). Genes previously reported as markers of portal (myo)fibroblasts as opposed to HSCs (8, 10, 33-36), were mainly expressed in cells from these two clusters, *e.g.*, *Thy1* alias CD90 (10, 35, 36) in Fib-3, fibulin-2 (*Fbln2*) (33) and ectonucleoside triphosphate diphosphohydrolase 2 (*Entpd2*) (34) in Fib-4 (Fig. 2C), *Col15a1* (8), *Clec3b* (28) and *Cd34* (10, 28) in both clusters. This suggested that cells of clusters Fib-3 and Fib-4 could be PMF precursors. As shown in Fig. 3A, a high expression of PDGFR α , CD34 and CD9 combined with a low expression of CD200 appeared to discriminate Fib-3 and Fib-4 from other Lin-negative cells. We FACS-sorted Lin (CD31/CD45/Epcam/CD11b)-negative, PDGFR α /CD34/CD9-positive, and CD200-low cells (Gate 4 in Fig. 3B) and examined this population for cell stem features. The percentage of cells recovered was estimated to account for approximately 0.03 % of total liver cells (data not shown). The cells of this population were highly clonogenic (80 CFU-f per 2,000 cells) (Fig. 3C) irrespective of their *Thy1* expression (Suppl. Fig. S5). They also displayed the expression of classical mesenchymal stem cell markers, *i.e.*, CD105, Sca-1, CD29 (Fig. 3D), and the ability to undergo trilineage differentiation (chondrogenic, osteogenic and adipogenic) in culture (Fig. 3E). Taken together, the cells isolated by our gating strategy qualified as mesenchymal stem cells (MSCs) and were designated as portal mesenchymal stem cells (PMSCs). When cultured on a stiff substratum (Fig. 3F, bottom panels), PMSCs proliferated and gave rise to cells phenotypically similar to myofibroblasts expressing COL15A1, here referred to as PMSC-

derived myofibroblasts (PMSC-MFs). This phenotypic change was accompanied by the expected up-regulation of *Acta2*, the gene encoding alpha-smooth muscle actin (α -SMA), no change in *Col1a1* expression, and a down-regulation of *Col15a1* (Fig. 3G). This confirmed that *Col15a1* is a marker of PMF precursors (8), and further indicated that its expression decreased in PMSC-MFs, but remained high enough in these cells to mark them as well, as suggested by our previous work (8) and illustrated later (Fig. 5D). It was possible to maintain PMSCs in quiescence by culturing them in spheroids, on ultra-low attachment plates, in which case the expression of α -SMA was not induced and that of *Col15a1* was not significantly reduced (Fig. 3, F and G). Taken together, these data indicate that our screening strategy and isolation procedure has enabled identifying PMSCs as portal mesenchymal cells characterized by high collagen expression, stem cell properties and the potential to differentiate into PMFs.

Specific molecular profiles of PMSCs, HSCs and derived myofibroblasts

The isolation of phenotypically defined PMSCs as individual cells, provided a unique opportunity to uncover specific markers of these cells compared to HSCs, to analyze their quiescent *versus* myofibroblastic states and to compare the functional pathways characterizing these states. We performed a second set of transcriptomic studies comparing phenotypically defined PMSCs (PDGFR α /CD34/CD9^{high}:CD200^{low}) to HSCs (Vitamin-A fluorescent) of high purity (37), and using bulk RNAseq. We identified 3273 genes expressed at higher levels in PMSCs, and 3122, in HSCs (Fig. 4A). We overlaid subsets of the most discriminant genes expressed by PMSCs or HSCs onto the scRNAseq data. This analysis showed that isolated PMSCs and HSCs were largely similar to the cells of Fib-3/Fib-4 and HSC clusters, respectively (Fig. 4, A and B). Consistent with the functional analyses of scRNAseq

data (Suppl. Table S2 and Fig. S3), bulk RNAseq data showed enrichment in pathways related to “Extracellular matrix organization” and “Angiogenesis” in PMSCs, and pathways related to “Immunity” and “Metabolism of fat-soluble vitamins” in HSCs (Fig. 4C).

When placed in culture on a stiff substratum, both PMSCs as shown here, and HSCs as shown in previous studies (2), undergo phenotypic changes into myofibroblasts. To determine if the two cell types maintain specificities at the stage of myofibroblasts, we extended bulk RNAseq analyses of the two cell populations to myofibroblasts derived from both cell types in culture, including an early and late stage of differentiation for PMSC-MFs. PCA indicated a clear discrimination of PMSCs and HSCs from myofibroblasts according to PC1, while PMSC-derived myofibroblasts were discriminated from HSC-derived ones according to PC2. Moreover, myofibroblast clusters were not far apart as compared to PMSCs and HSCs. These data showed that the molecular profiles of PMSCs and HSCs became more similar as they differentiated into myofibroblasts (Fig. 5A). Yet, they retained specificities at the stage of myofibroblasts as confirmed by the GO analysis (Fig. 5B). When fully differentiated in myofibroblasts, *i.e.*, after 7 days of culture, HSC-MFs were enriched in themes related to muscle contraction, whereas PMSC-MFs were enriched in those related to angiogenesis and extracellular matrix organization. At an early stage of myofibroblastic differentiation, *i.e.*, after 3 days of culture, PMSC transcriptome was highly enriched in pathways related to cell proliferation (Fig. 5B). At a later stage of myofibroblastic differentiation, *i.e.*, after 7 days of culture, PMSC-MFs compared to HSC-MFs still markedly overexpressed genes involved in cell proliferation (Suppl. Fig. S6). Taken together, comparative analyses of gene expression indicated that 100 genes in PMSCs and 112 genes in HSCs, i) were overexpressed according to both scRNAseq and bulk RNAseq analyses, and ii) remained differentially expressed in these cells throughout their myofibroblastic

differentiation (Figure 5C). We selected the most differentially expressed of these genes, to build a multigene expression signature of PMSCs/PMSC-MFs (8 genes) and of HSCs/HSC-MFs (9 genes) (Fig. 5D). One of PMSC signature genes, *Slit2*, appeared to be of particular interest as its expression was remarkably stable in PMSCs across their myofibroblastic differentiation and virtually absent in HSCs/HSC-MFs as well as in other major liver cell types (Fig. 5E, Suppl. Fig. S7).

Contribution of PMSCs to liver fibrosis

First, we analyzed *Slit2* expression in mouse and human livers at different stages of fibrosis. As previously shown in the thioacetamide mouse model of post-necrotic liver fibrosis (38), *Slit2* expression was increased in the liver of mice fed a 3,5-diethoxycarbonyl-1,4-dihydrocollidine (DDC) diet, a model of biliary fibrosis (Fig. 6A) or a choline deficient, defined amino acid (CDAA) diet, a model of NASH (Suppl. Fig. S8). Likewise, *SLIT2* was overexpressed in the liver of patients with non-alcoholic steatohepatitis (NASH), primary sclerosing cholangitis (PSC) and other chronic liver diseases (Fig. 6B). In a cohort of patients with NAFLD, we could show that the expression of *SLIT2* increased with advanced fibrosis, as assessed by the SAF score (39) (Fig. 6 C). Both in experimental and human liver fibrosis, the expression levels of *SLIT2* correlated with those of *ACTA2*, *COL1A1* and von Willebrand Factor (*vWF*). We also examined the microarray data of human liver tissue samples for the multigene expression signatures and found that in the different types of liver diseases, the gene signature of PMSCs/PMSC-MFs was increased compared to normal liver, and correlated with the expression of *ACTA2*, *COL1A1* and *vWF* (Fig. 7, A and C). We inferred from these results that PMSCs/PMSC-MFs accumulated with the progression of liver fibrosis and angiogenesis in the injured liver. By contrast, the gene signature of HSCs/HSC-MFs was not significantly

different between diseased and normal livers (Fig. 7B), consistent with little proliferation of these cells compared to PMSCs/PMSC-MFs.

Discussion

In the present study, we provide a detailed atlas of portal mesenchymal cells. Our approach was different from the one used in previous scRNAseq analyses of the liver (19, 22, 28, 29). First, the bilio-vascular tree, which contains the portal mesenchymal cells, was separated from the liver parenchyma. A specific digestion protocol was then developed to isolate individual cells that are tightly bound to this structure. Our scRNAseq analysis revealed three populations of liver mesenchymal cells *i.e.*, fibroblasts, VSMCs and HSCs, with distinct marker genes, consistent with those previously reported in a *Pdgfrb*-GFP knockin reporter mouse that was used to label mesenchymal cells in the mouse liver (28). Our analysis also went further and individualized several sub-populations of fibroblasts and VSCMs. It should be noted that the Fib-3 and Fib-4 cell populations that we subsequently authenticated as PMSCs, displayed the lowest levels of *Pdgfrb* expression (Suppl. Fig. S9), and may have been overlooked, in the study of PDGFR β ⁺ cells (28).

Mesenchymal stem cells (MSCs) were first identified in the post-natal bone marrow as clonogenic, multipotent cells, with the capacity to generate skeletal tissues and to organize the hematopoietic stem cell niche (40, 41). MSCs from the bone marrow are perivascular cells and they are able to differentiate into lineages of mesenchymal tissues including osteoblasts, chondrocytes and adipocytes in culture (40, 41). Subsequently, cells with similar properties have been identified in multiple organs and have also been referred to as MSCs (42). It was shown that MSCs from different tissues did not have identical differentiation

capacities (43), which has fueled a controversy over the “MSC” terminology. However, MSCs from different tissues also share a number of common features including clonogenicity, the ability to differentiate into the mesenchymal lineages cited above *in vitro* and they often exhibit a perivascular distribution (42, 43). On this basis, we herein uncovered a small population of portal mesenchymal cell that displayed clonogenicity as well as osteogenic, chondrogenic and adipogenic potentials, and designated this population PMSCs. Using trajectory analysis, we inferred that these progenitors were contained within the Fib-3 and Fib-4 fibroblastic populations and designed a set of surface markers that enabled us to isolate them and define their final phenotype. In normal liver, Thy1 (35, 36, 44) that marks Fib-3, fibulin-2 (45, 46) and ENTPD2 (34) that mark Fib-4, were previously immunodetected in portal tracts. Both Thy1 cells and fibulin-2 expressions were found in the wall of the portal vein and hepatic artery. Thy1 expression (35, 36, 44) was also found in the surrounding of bile ducts like ENTPD2 (34), and around the peribiliary vascular plexus. We showed that the sub-populations of Thy1⁺ and Thy1⁻ PMSCs were equally clonogenic, implying that Fib-3 and Fib-4 both contribute to the MSC repository in the liver (Suppl. Fig. S6). As previously proposed for other MSCs, *e.g.* of the skeletal muscle, we suggest that these cells represent subsets of the same original population, recruited to distinct anatomical niches based on local cell-cell interactions, that direct individual progenitors either to the surface of nascent portal blood vessels or to the surface of developing bile ducts. Another possibility is that the perivascular subsets are more primitive than the periductal subsets, in as much as the formation of blood vessels precedes that of bile ducts, during liver development (47).

Gli1, a transcription factor of the Hedgehog pathway, marks a network of perivascular mesenchymal stem cells that contribute to fibrosis across different tissues (48). Studies

based on genetic lineage tracing showed that resident Gli1⁺ cells proliferated in injured organs including the kidney, heart, lung and liver to generate myofibroblasts (48). In the liver, Gli1 demarcates a population of portal mesenchymal cells that display a periductal and to a lesser extent perivascular distribution (31, 48). Our data show that Gli1 is expressed at low level in PMSCs and no longer detected in PMSC-MFs (Suppl. Fig. S10). Using a model of genetic lineage tracing, Gupta *et al.* reported that Gli1⁺ myofibroblasts accumulated in biliary fibrosis but not in post-necrotic model of CCL4-induced fibrosis (31). However, Kramann *et al.* using exactly the same model, did find the accumulation of Gli1⁺ cells in the fibrotic septa of CCL4-treated mice (48), a discrepancy that remains to be solved. The former study supports the view that portal fibroblasts play a substantial role in fibrosis of biliary type only (7, 9), whereas the latter is in keeping with our previous study showing that COL15A1⁺ portal myofibroblasts expand in the lobule in all types of liver fibrosis (8). We herein found that *Col15a1*, a marker of perivascular fibroblast-like cells in the lung and brain (49, 50), was mainly expressed in PMSCs suggesting that PMFs as we originally described them (8, 51), were largely PMSC-derived.

The lack of markers that would enable to differentiate HSC- from non-HSC-derived myofibroblasts has been a major hurdle so far, to gain insight into the origins of the different types of liver myofibroblasts and their contributions to liver fibrosis. The isolation of PMSCs that are myofibroblast precursors distinct from HSCs, allowed us to seek such markers. The comparison of transcriptional profiles showed that in their quiescent state, PMSCs primarily ensure extracellular matrix organization and vasculature development whereas HSCs are mainly involved in immunity and the metabolism of vitamin A. As they transform into myofibroblasts, the expression of α -SMA is induced in both cell types but only PMSCs

become highly proliferative, and the expression of extracellular matrix proteins, *e.g.*, *Col1a1*, is up-regulated in HSCs but not in PMSCs, so that they both converge towards similar phenotypes. As a result, most of the genes that could be potentially used as markers of PMSCs, are modulated with myofibroblastic differentiation. Thus, *Gli1* and *Entpd2* expressions are totally suppressed, *Col15a1* is down-regulated and *Thy1*, up-regulated in PMSC-derived myofibroblasts. *Fbln2* expression is not only up-regulated in PMSC-derived myofibroblasts but also, it is induced in HSC-MFs. Therefore, our first strategy was to build multigene expression signatures that were subsequently used to determine the relative contribution of PMSCs/PMSC-MFs and HSCs/HSC-MFs in liver fibrosis. Only genes that maintained high differential expression throughout myofibroblastic differentiation were included in these signatures. The PMSC/PMSC-MF multigene signature was overexpressed in human fibrotic liver irrespective of the etiology, indicating that this cell population contributes to all types of liver fibrosis including of biliary and non-biliary type. In a previous study, a 122-gene expression HSC signature was shown to be increased in experimental and human fibrosis (52). However, this latter signature was designed in comparison with other liver cell types that did not include other liver mesenchymal cells, and likely comprised genes that were herein found to be expressed not only in HSCs/HSC-MFs but also PMSCs/PMSC-MFs, such as *Pcdh7* (Suppl. Fig. S11). Our HSC/HSC-MF gene expression signature did not increase in human fibrosis. Although apparently surprising, this finding is consistent with the low proliferation rate of highly pure HSC, as previously reported (53) and herein attested by the low expression of cell proliferation genes in HSC-MFs. Our PMSC/PMSC-MF gene expression signature included *Slit2* that was previously thought to be expressed in HSCs (38). *Slit2* expression was absent from all other liver cell types including HSCs, and did not change with myofibroblastic differentiation. Akin to *COL15A1* (8), *SLIT2* expression increased in

injured liver at the stage of advanced fibrosis. This was previously shown in a thioacetamide model of post-necrotic liver fibrosis (38), and here in the DDC and CDAA models of biliary fibrosis and NASH, respectively, as well as in the liver of patients with NASH, PSC and other types of liver diseases. Both in experimental and human liver fibrosis the expression of *SLIT2* was correlated with that of vWF and COL1A1, consistent with a contribution of PMSCs to angiogenesis as a driving force for fibrosis progression. Although PMSCs are by far fewer than HSCs in normal liver, they proliferate much more than HSCs, whereby both cell types may ultimately contribute to fibrosis in the injured liver.

Methods

Animal experiments. Animal experiments were conducted in the CRSA animal facility (DPP agreement No. C 75-12-01), in compliance with the European Directive 2010/63/UE and were approved under No. #15358-2018060418401070 v2 and 2018102211507258 by the Ethics Committee of Animal Experiments, Charles Darwin, Ile-de-France, Paris No. 5. C57BL/6J mice were purchased from Janvier Europe, Saint-Berthevin, France, and housed in a temperature-controlled, specific pathogen-free environment, on a 12-hour light-dark cycle, with free access to chow and water. Experiments were performed in 8-12-week-old male mice.

Cell isolation

Cell collection from the bilio-vascular tree. The bilio-vascular tree was isolated from mouse liver, by adapting a procedure we previously described in rat (12). *In situ* retrograde perfusion of the liver was performed through the inferior vena cava with Ca^{2+} , Mg^{2+} -free HBSS (Gibco, 14170-088)/1% EDTA (Sigma, 03690) for 5 minutes at 37°C, and then with HBSS containing Ca^{2+} , Mg^{2+} (Gibco, 24020117)/0.15 mg/mL collagenase P (Sigma, 11213873001)

for 20 minutes at 37°C. Next, the liver was collected and placed in L15 Leibovitz medium (Sigma, L5520) at 4°C. The liver capsule was peeled off and the liver parenchyma was mechanically detached and discarded. The remaining bilio-vascular tree was minced and incubated in MEM (Gibco, 21090-022) containing 0.075 mg/mL collagenase P, 0.02 mg/mL DNase (Sigma, DN25), 3% fetal bovine serum (FBS; Gibco, 10270-098), 1 mg/mL bovine serum albumin (Sigma, A7030), 1% HEPES (Gibco, 15630) and 1% Penicillin-Streptomycin (Gibco, 15140-122), under agitation for 15 minutes at 37°C. The bilio-vascular segments were collected on top of a 40-µm cell strainer and centrifuged at 1,500 rpm, 4°C for 5 minutes. The cell pellet was resuspended in 0.05% Trypsin-EDTA (Invitrogen, 25300-054) with 0.02mg/mL DNase and incubated under agitation for 15 minutes at 37°C, and the dissociated cells were filtered three times through a 20-µm cell strainer. Following red blood cell lysis with ACK lysis buffer, the cell suspension was centrifuged at 1,500 rpm, 4°C for 5 minutes, and the cell pellet was resuspended in a FACS buffer composed of PBS with 2% FBS, 1% HEPES and 1% Penicillin-Streptomycin, at a concentration of 1×10^8 cells/mL for cell sorting. For cholangiocyte isolation, cells were incubated with anti-Epcam-FITC (BioLegend, Clone: G8.8) for 30 minutes at 4°C and cells were sorted using a FACSAria II cell sorter (BD Biosciences).

Hepatocyte, KC, LSEC and HSC collection. Hepatocytes were isolated as previously described (54) with modifications. Briefly, the liver was perfused *in situ* with HBSS containing 0.15 mg/mL collagenase P for 20 minutes at 37°C. The cell suspension was filtered through a 70-µm strainer and centrifuged twice at 400 rpm, 4°C, for 5 minutes, to eliminate non-parenchymal cells. LSEC and KC isolation was performed as previously described (54) by *ex situ* dissociation of the liver using a gentleMACs dissociator (Miltenyi, Bergisch Gladbach, Germany) and magnetic selection using CD146 microbeads (Miltenyi, 130-092-007) and anti-

F4/80 microbeads (Miltenyi, 130-110-443) antibody, respectively. For HSC isolation, the liver was perfused *in situ*, with HBSS containing 0.4 mg/mL pronase (Sigma, 10165921001) for 5 minutes at 37°C, and then 0.05 mg/mL collagenase P for 15 min at 37°C. The liver was collected, minced and further digested in HBSS containing 0.044 mg/mL collagenase P, 0.5 mg/mL pronase and 0.02 mg/mL DNase, under agitation for 15 minutes at 37°C. The resulting cell suspension was submitted to density gradient-centrifugation at 1,380 g for 17 minutes, in Gey's Balanced Salt Solution (GBSS, Gibco)/Histodenz (Sigma, D2158) at 4°C. HSCs were collected from the interface and resuspended in FACS buffer for further purification by cell sorting based on retinoid autofluorescence, as previously described (37).

Cell sorting and flow cytometry analysis. Cells isolated from the bilio-vascular tree were incubated with 1% anti-mouse CD16/CD32 antibody (BD Pharmingen, 553141) for 10 minutes on ice, to block Fc receptors before incubation with anti-CD31-FITC (BD Biosciences, 563089, Clone: MEC 13.3), anti-CD45-FITC (BioLegend, 103137, Clone: 30-F11), anti-Epcam-FITC (BioLegend, 118207, Clone: G8.8), and anti-CD11b-FITC (BioLegend, 101245, Clone M1/70), all at concentrations of 1:100, for 30 minutes at 4°C. Dead cells were stained with 7-aminoactinomycin D (7-AAD; BD Biosciences, 559925) immediately before cell sorting was performed, using a FACS Aria II cell sorter (BD Biosciences). Lin-negative cells, gated as CD31⁻CD45⁻Epcam⁻CD11b⁻ cells, were collected and subjected to scRNAseq analysis. To isolate PMSCs from the bilio-vascular tree, cells were labeled with anti-CD31-FITC, anti-CD45-FITC, anti-Epcam-FITC and anti-CD11b-FITC antibodies as above, and anti-PDGFR α -PE (eBioscience, 12-1401-81, Clone: APA5), anti-CD34-APC (BioLegend, 119310, Clone: MEC14.7), anti-CD9-BV421 (BD Biosciences, 564235, Clone: KMC8) and anti-CD200-APC-R700 (BD Biosciences, 565546, Clone: OX-90), all at concentrations of 1:100 except for anti-PDGFR α -PE (1:50). PMSCs were gated as Lin-PDGFR α ⁺CD34⁺CD9⁺CD200^{low} cells. To sort Thy1⁻, Thy1^{low} and

Thy1^{high} PMSCs, cells from the bilio-vascular tree were labeled with anti-CD31-FITC, anti-CD45-FITC, anti-Epcam-FITC, anti-CD11b-FITC, anti-PDGFR α -PE, anti-CD34-APC, anti-CD9-BV421, anti-CD200-APC-R700 antibodies as above, and anti-Thy1-PE/Cy7 antibodies (eBioscience, 25-0902-81, Clone: 53-2.1) at a concentration of 1:100. For flow cytometry analysis, freshly isolated PMSCs were labeled either with anti-Sca1-BV510 (BD Biosciences, 565507, Clone: D7), anti-CD105-BV510 (BD Biosciences, 740188, Clone: MJ7/18) or anti-CD29-PE/Cy7 (BioLegend, 102222, Clone: HM β 1-1), all at concentrations of 1:100. Analyses were performed using BD FACSDiVa™ and FlowJo (Tree Star) software.

Cell culture. PMSCs and HSCs were seeded into 6-well plates at a density of 20,000 cells/cm² and cultured in DMEM containing 20% FBS, 1% HEPES and 1% Penicillin-Streptomycin to obtain PMSC-MFs and HSC-MFs, respectively. To maintain PMSCs in a quiescent stage, cells were seeded into 96-well Ultra-Low Attachment (ULA) round-bottomed plates.

Single-cell RNA-sequencing. ScRNAseq analysis of the bilio-vascular Lin-negative cells was performed using the 10X Genomics 3' v3 kit (10x Genomics, Pleasanton, CA, USA). Cells were loaded onto a GemCode instrument (10x Genomics) to generate single-cell barcoded droplets, *i.e.*, gel beads in emulsion (GEMs). Sequencing libraries were constructed using the Chromium Single-cell 3' Library Kit (10x Genomics) according to the manufacturer's protocol and sequenced using NextSeq500 (Illumina) platform. Average read depth of the sample was 79,199 reads/cell. Reads were then aligned to the mouse genome mm10/Grcm38 using the Cell Ranger 3.0.2 software. Subsequent analysis was performed in R using the filtered barcode and count matrices produced by Cell Ranger. The data were analyzed using Seurat 3.6.1 (55). Genes expressed in less than 6 cells, as well as cells with less than 500 or more than 25,000 unique molecular identifiers (UMIs), were filtered out. Any single-cell with more than 10% UMIs mapped to mitochondrial genes was also removed. Seurat SCTransform

function was used to normalize and scale the data (56). Dimensionality reduction was performed through Principal Component Analysis (PCA) on the gene expression matrix and using the first 30 PCs for clustering and visualization. Unsupervised shared nearest neighbor clustering was performed using Seurat FindClusters function at the resolution of 0.6 and visualization was achieved using spectral *t*-SNE of the principal components as implemented in Seurat. Cluster dendrogram was constructed using BuildClustertree built-in function of the R package Seurat which used cluster averaged PCs for calculating a PC distance matrix. The cell clusters identified were evaluated for differential genes expression, using Seurat FindAllMarkers function. All genes considered for cell-type classification were determined with p value < 0.01 and $\log(\text{fold-change}) > 0.25$ as cutoff by performing differential gene expression analysis between the clusters using Wilcoxon rank sum test and Benjamini and Hochberg procedure for p -values adjustment. We used the Monocle version 2.14.0 R package (32) to organize cells in pseudotime and infer cell trajectories from the Seurat dataset. The top 1,000 differentially expressed genes were then used in Monocle for clustering and ordering cells using the DDRTree method and reverse graph embedding.

Bulk RNA-sequencing. RNA was extracted using Rneasy Micro Kit (Qiagen). Libraries were generated from total RNA and paired-end sequencing was performed on a NextSeq 500 device, using ILLUMINA technology. Raw sequencing data were quality-controlled with the FastQC program. Paired reads were aligned to the mouse reference genome (mm10 build) with the STAR software (option for no multihits). Mapping results were quality-checked using RNASeQC. Gene counts were obtained by using RSEM tools (rsem-calculate-expression, option for paired-end and stranded). Gene counts represented as counts per million (CPM) were first nominalized using TMM method in the edgeR R package and genes with a CPM < 1 in 20% of samples, were removed.

Gene ontology enrichment and gene set enrichment analysis. Symbol gene IDs were first converted to Entrez gene IDs using the clusterProfiler R package (57). Functional enrichment in GO biological processes of differential expressed genes was performed using EnrichGO built-in function of the clusterProfiler version 3.14 with default parameters. The comparison of enriched functional enrichment among mesenchymal cell populations was performed using clusterProfiler CompareCluster function (57). Heatmap of enriched term was generated in R. GSEA was implemented using the R package ReactomePA with default parameters (58).

Cell clonogenicity and differentiation assays. Cell clonogenicity was examined by colony forming unit-fibroblast (CFU-F) assay, as follows: 2,000 sorted cells were plated onto a 10-cm plastic dish and maintained in DMEM/20% FBS medium. The presence of more than 50 cells in a cluster after 14 days in culture, was counted as a colony. The capacity of PMSCs to differentiate towards adipogenic, osteogenic and chondrogenic lineages was analyzed using specific protocols. For adipogenic and osteogenic differentiation, sorted PMSCs were plated into 48-well plates coated with matrigel (Corning, 356231) at a density of 5,000 cells/cm² in the DMEM/20% FBS medium until subconfluence. Then, the culture medium was changed for adipogenic (R&D Systems, CCM011) or osteogenic (R&D Systems, CCM009) differentiation medium, respectively. After 21 days, cells were fixed with 4% paraformaldehyde and stained using Oil Red O (Sigma) or Alizarin Red solution (Sigma), respectively. For chondrogenic differentiation, 50,000 sorted PMSCs were plated into ULA plate in chondrogenic differentiation medium (R&D Systems, CCM006) to form spheroids. After 21 days, the spheroids were fixed in 4% paraformaldehyde, embedded in OCT (Sakura Finetek) and cryosections (8 µm) were stained with Alcian blue (Santa Cruz Biotechnology) and counterstained with nuclear fast red (VECTOR).

Immunofluorescence. Cell preparations were fixed in 4% paraformaldehyde and incubated with primary antibodies against COL15A1(1:200, ab58717, abcam) or α -SMA (1:100, 1A4, Dako). Nuclear staining was performed using Draq5 (Ozyme, Saint-Quentin-en-Yvelines, France). Cells were examined with a SP2 confocal microscope (Leica, Bannockburn, IL, USA).

Human liver tissue samples. Frozen samples of liver biopsy from subjects with a suspicion of non-alcoholic fatty liver disease were provided by the Biological Resource Center, BIO-ICAN, Paris, France, with ethical approval from the Persons Protection Committee (CPP Ile de France VI) for RT-qPCR analyses. The RNA used for the microarray experiments was extracted from fresh frozen tissue obtained from explanted livers or diagnostic liver biopsies from i) normal human liver tissue (tumor-free tissue from livers with colorectal cancer metastasis) (n=5) and ii) liver tissue from patients with chronic liver diseases, including PSC (n=6), NASH (n=7) and other liver diseases (*i.e.*, primary biliary cholangitis, autoimmune hepatitis, alcoholic liver disease and haemochromatosis) (n=8). The liver specimens were provided by the Norwegian biobank for primary sclerosing cholangitis, Oslo, Norway with ethical approval from the Regional Committee for Medical and Health Research ethics of South East Norway. All subjects gave written informed consent before to allow the use of the samples.

RT-qPCR and microarray analyses. Total RNA was extracted from frozen liver tissue samples or harvested cells using the RNeasy Mini Kit or Micro Kit (Qiagen), respectively. The cDNA was synthesized using the MMLV-RT (Invitrogen, 28025013) or SuperScript™ II (Invitrogen, 18064014) and real-time PCR was performed using the LightCycler 480 SYBR Green I Master Kit on an LC480 device (Roche Diagnostics). The primers (Suppl. Table S3) were designed using the primer software from Roche Diagnostics. Pangenomic analysis of frozen liver tissue samples were performed using the Affymetrix human gene 1.0 st microarray. Analysis was

conducted using R. *oligo* bioconductor package to import raw data CEL files in an ExpressionSet object and *rma* function to normalize the data. After normalization, summarization was performed because transcripts are represented by multiple probes, on the Affymetrix platform. For each gene, the background-adjusted and normalized intensities of all probes were summarized into one estimated amount proportional to the amount of RNA transcripts. Summarized data have been annotated with hugene10sttranscriptcluster.db bioconductor package. Statistical analysis was performed using non-parametric wilcoxon test.

Statistical analyses. Unless otherwise stated, statistical analyses were performed using Graphpad Prism v6.0 and R. Unpaired two-sided Student *t* test and ANOVA with a Bonferroni post-test were used to compare differences between two groups, and more than two groups, respectively. A significant difference was defined as $p < 0.05$.

Acknowledgements: This work was supported by funding from the ANRS (ECTZ35217) and the Microbiome Foundation. Lin Lei received a fellowship from the China Scholarship Council (CSC). The authors acknowledge Tatiana Ledent (CRSA Animal Facility), Yannick Marie and Delphine Bouteiller (ICM Sequencing Facility).

Contributors: L.L., T.J., A.C., C.H. designed the study; L.L., H.E.M., T.F., B.H., E.G-S., J.Ga., T.J., conducted experiments; L.L., J.Gu., S.L., T.J., C.H., A.C. analyzed and interpreted the data; L.L., S.L., A.C., C.H. prepared the manuscript, with critical revision from all authors.

Competing interests: The authors declare no competing interests.

References

1. Asahina K, Zhou B, Pu WT, Tsukamoto H. Septum transversum-derived mesothelium gives rise to hepatic stellate cells and perivascular mesenchymal cells in developing mouse liver. *Hepatology*. 2011;53(3):983-95.
2. Tsuchida T, Friedman SL. Mechanisms of hepatic stellate cell activation. *Nat Rev Gastroenterol Hepatol*. 2017;14(7):397-411.
3. Beaussier M, Wendum D, Schiffer E, Dumont S, Rey C, Lienhart A, Housset C. Prominent contribution of portal mesenchymal cells to liver fibrosis in ischemic and obstructive cholestatic injuries. *Laboratory investigation; a journal of technical methods and pathology*. 2007;87(3):292-303.
4. Dranoff JA, Wells RG. Portal fibroblasts: Underappreciated mediators of biliary fibrosis. *Hepatology*. 2010;51(4):1438-44.
5. Bosselut N, Housset C, Marcelo P, Rey C, Burmester T, Vinh J, Vaubourdolle M, Cadoret A, Baudin B. Distinct proteomic features of two fibrogenic liver cell populations: hepatic stellate cells and portal myofibroblasts. *Proteomics*. 2010;10(5):1017-28.
6. Lemoine S, Cadoret A, El Mourabit H, Thabut D, Housset C. Origins and functions of liver myofibroblasts. *Biochimica et biophysica acta*. 2013;1832(7):948-54.
7. Iwaisako K, Jiang C, Zhang M, Cong M, Moore-Morris TJ, Park TJ, Liu X, Xu J, Wang P, Paik YH, Meng F, Asagiri M, Murray LA, Hofmann AF, Iida T, Glass CK, Brenner DA, Kisseleva T. Origin of myofibroblasts in the fibrotic liver in mice. *Proceedings of the National Academy of Sciences of the United States of America*. 2014;111(32):E3297-305.
8. Lemoine S, Cadoret A, Rautou PE, El Mourabit H, Ratzu V, Corpechot C, Rey C, Bosselut N, Barbu V, Wendum D, Feldmann G, Boulanger C, Henegar C, Housset C, Thabut D. Portal myofibroblasts promote vascular remodeling underlying cirrhosis formation through the release of microparticles. *Hepatology*. 2015;61(3):1041-55.
9. Lua I, Li Y, Zagory JA, Wang KS, French SW, Sevigny J, Asahina K. Characterization of hepatic stellate cells, portal fibroblasts, and mesothelial cells in normal and fibrotic livers. *Journal of hepatology*. 2016;64(5):1137-46.
10. Nishio T, Hu R, Koyama Y, Liang S, Rosenthal SB, Yamamoto G, Karin D, Baglieri J, Ma HY, Xu J, Liu X, Dhar D, Iwaisako K, Taura K, Brenner DA, Kisseleva T. Activated hepatic stellate cells and portal fibroblasts contribute to cholestatic liver fibrosis in MDR2 knockout mice. *Journal of hepatology*. 2019;71(3):573-85.
11. Loeuillard E, El Mourabit H, Lei L, Lemoine S, Housset C, Cadoret A. Endoplasmic reticulum stress induces inverse regulations of major functions in portal myofibroblasts during liver fibrosis progression. *Biochim Biophys Acta Mol Basis Dis*. 2018;1864(12):3688-96.
12. El Mourabit H, Loeuillard E, Lemoine S, Cadoret A, Housset C. Culture Model of Rat Portal Myofibroblasts. *Front Physiol*. 2016;7:120.
13. Satija R, Farrell JA, Gennert D, Schier AF, Regev A. Spatial reconstruction of single-cell gene expression data. *Nat Biotechnol*. 2015;33(5):495-502.
14. Lua I, Asahina K. The Role of Mesothelial Cells in Liver Development, Injury, and Regeneration. *Gut Liver*. 2016;10(2):166-76.
15. DeLeve LD, Wang X, Hu L, McCuskey MK, McCuskey RS. Rat liver sinusoidal endothelial cell phenotype is maintained by paracrine and autocrine regulation. *American journal of physiology Gastrointestinal and liver physiology*. 2004;287(4):G757-63.

16. Poisson J, Lemoine S, Boulanger C, Durand F, Moreau R, Valla D, Rautou PE. Liver sinusoidal endothelial cells: Physiology and role in liver diseases. *Journal of hepatology*. 2017;66(1):212-27.
17. Hardonk MJ, Atmosoerodjo-Briggs J. Evidence for the anatomical connection between the space of Disse and the portal tract in human and rat liver. Knook DL and Wisse E, editors *Cells of the hepatic sinusoid: Proceedings of the Sixth International Kupffer Cell Symposium Antwerp: The Kupffer Cell Foundation*. 1992:182-4.
18. Halpern KB, Shenhav R, Massalha H, Toth B, Egozi A, Massasa EE, Medgalia C, David E, Giladi A, Moor AE, Porat Z, Amit I, Itzkovitz S. Paired-cell sequencing enables spatial gene expression mapping of liver endothelial cells. *Nat Biotechnol*. 2018;36(10):962-70.
19. Xiong X, Kuang H, Ansari S, Liu T, Gong J, Wang S, Zhao XY, Ji Y, Li C, Guo L, Zhou L, Chen Z, Leon-Mimila P, Chung MT, Kurabayashi K, Opp J, Campos-Perez F, Villamil-Ramirez H, Canizales-Quinteros S, Lyons R, Lumeng CN, Zhou B, Qi L, Huertas-Vazquez A, Lusic AJ, Xu XZS, Li S, Yu Y, Li JZ, Lin JD. Landscape of Intercellular Crosstalk in Healthy and NASH Liver Revealed by Single-Cell Secretome Gene Analysis. *Mol Cell*. 2019;75(3):644-60 e5.
20. Rocha AS, Vidal V, Mertz M, Kendall TJ, Charlet A, Okamoto H, Schedl A. The Angiocrine Factor Rspodin3 Is a Key Determinant of Liver Zonation. *Cell Rep*. 2015;13(9):1757-64.
21. Aizarani N, Saviano A, Sagar, Mailly L, Durand S, Herman JS, Pessaux P, Baumert TF, Grun D. A human liver cell atlas reveals heterogeneity and epithelial progenitors. *Nature*. 2019;572(7768):199-204.
22. Ramachandran P, Dobie R, Wilson-Kanamori JR, Dora EF, Henderson BEP, Luu NT, Portman JR, Matchett KP, Brice M, Marwick JA, Taylor RS, Efremova M, Vento-Tormo R, Carragher NO, Kendall TJ, Fallowfield JA, Harrison EM, Mole DJ, Wigmore SJ, Newsome PN, Weston CJ, Iredale JP, Tacke F, Pollard JW, Ponting CP, Marioni JC, Teichmann SA, Henderson NC. Resolving the fibrotic niche of human liver cirrhosis at single-cell level. *Nature*. 2019;575(7783):512-8.
23. Kim W, Barron DA, San Martin R, Chan KS, Tran LL, Yang F, Ressler SJ, Rowley DR. RUNX1 is essential for mesenchymal stem cell proliferation and myofibroblast differentiation. *Proceedings of the National Academy of Sciences of the United States of America*. 2014;111(46):16389-94.
24. Copes F, Ramella M, Fusaro L, Mantovani D, Cannas M, Boccafoschi F. Pleiotrophin: Analysis of the endothelialisation potential. *Adv Med Sci*. 2019;64(1):144-51.
25. Sado Y, Kagawa M, Naito I, Ueki Y, Seki T, Momota R, Oohashi T, Ninomiya Y. Organization and expression of basement membrane collagen IV genes and their roles in human disorders. *J Biochem*. 1998;123(5):767-76.
26. Chung HJ, Uitto J. Type VII collagen: the anchoring fibril protein at fault in dystrophic epidermolysis bullosa. *Dermatol Clin*. 2010;28(1):93-105.
27. Mederacke I, Hsu CC, Troeger JS, Huebener P, Mu X, Dapito DH, Pradere JP, Schwabe RF. Fate tracing reveals hepatic stellate cells as dominant contributors to liver fibrosis independent of its aetiology. *Nat Commun*. 2013;4:2823.
28. Dobie R, Wilson-Kanamori JR, Henderson BEP, Smith JR, Matchett KP, Portman JR, Wallenborg K, Picelli S, Zagorska A, Pendem SV, Hudson TE, Wu MM, Budas GR, Breckenridge DG, Harrison EM, Mole DJ, Wigmore SJ, Ramachandran P, Ponting CP, Teichmann SA, Marioni JC, Henderson NC. Single-Cell Transcriptomics Uncovers Zonation of Function in the Mesenchyme during Liver Fibrosis. *Cell Rep*. 2019;29(7):1832-47 e8.

29. Krenkel O, Hundertmark J, Ritz TP, Weiskirchen R, Tacke F. Single Cell RNA Sequencing Identifies Subsets of Hepatic Stellate Cells and Myofibroblasts in Liver Fibrosis. *Cells*. 2019;8(5).
30. Okina Y, Sato-Matsubara M, Matsubara T, Daikoku A, Longato L, Rombouts K, Thanh Thuy LT, Ichikawa H, Minamiyama Y, Kadota M, Fujii H, Enomoto M, Ikeda K, Yoshizato K, Pinzani M, Kawada N. TGF-beta-driven reduction of cytoglobin leads to oxidative DNA damage in stellate cells during non-alcoholic steatohepatitis. *Journal of hepatology*. 2020.
31. Gupta V, Gupta I, Park J, Bram Y, Schwartz RE. Hedgehog Signaling Demarcates a Niche of Fibrogenic Peribiliary Mesenchymal Cells. *Gastroenterology*. 2020.
32. Trapnell C, Cacchiarelli D, Grimsby J, Pokharel P, Li S, Morse M, Lennon NJ, Livak KJ, Mikkelsen TS, Rinn JL. The dynamics and regulators of cell fate decisions are revealed by pseudotemporal ordering of single cells. *Nat Biotechnol*. 2014;32(4):381-6.
33. Knittel T, Kobold D, Saile B, Grundmann A, Neubauer K, Piscaglia F, Ramadori G. Rat liver myofibroblasts and hepatic stellate cells: different cell populations of the fibroblast lineage with fibrogenic potential. *Gastroenterology*. 1999;117(5):1205-21.
34. Dranoff JA, Kruglov EA, Robson SC, Braun N, Zimmermann H, Sevigny J. The ecto-nucleoside triphosphate diphosphohydrolase NTPDase2/CD39L1 is expressed in a novel functional compartment within the liver. *Hepatology*. 2002;36(5):1135-44.
35. Dudas J, Mansuroglu T, Batusic D, Ramadori G. Thy-1 is expressed in myofibroblasts but not found in hepatic stellate cells following liver injury. *Histochemistry and cell biology*. 2009;131(1):115-27.
36. Katsumata LW, Miyajima A, Itoh T. Portal fibroblasts marked by the surface antigen Thy1 contribute to fibrosis in mouse models of cholestatic liver injury. *Hepatol Commun*. 2017;1(3):198-214.
37. Mederacke I, Dapito DH, Affo S, Uchinami H, Schwabe RF. High-yield and high-purity isolation of hepatic stellate cells from normal and fibrotic mouse livers. *Nat Protoc*. 2015;10(2):305-15.
38. Zeng Z, Wu Y, Cao Y, Yuan Z, Zhang Y, Zhang DY, Hasegawa D, Friedman SL, Guo J. Slit2-Robo2 signaling modulates the fibrogenic activity and migration of hepatic stellate cells. *Life Sci*. 2018;203:39-47.
39. Bedossa P, Consortium FP. Utility and appropriateness of the fatty liver inhibition of progression (FLIP) algorithm and steatosis, activity, and fibrosis (SAF) score in the evaluation of biopsies of nonalcoholic fatty liver disease. *Hepatology*. 2014;60(2):565-75.
40. Pittenger MF, Mackay AM, Beck SC, Jaiswal RK, Douglas R, Mosca JD, Moorman MA, Simonetti DW, Craig S, Marshak DR. Multilineage potential of adult human mesenchymal stem cells. *Science*. 1999;284(5411):143-7.
41. Sacchetti B, Funari A, Michienzi S, Di Cesare S, Piersanti S, Saggio I, Tagliafico E, Ferrari S, Robey PG, Riminucci M, Bianco P. Self-renewing osteoprogenitors in bone marrow sinusoids can organize a hematopoietic microenvironment. *Cell*. 2007;131(2):324-36.
42. Crisan M, Yap S, Casteilla L, Chen CW, Corselli M, Park TS, Andriolo G, Sun B, Zheng B, Zhang L, Norotte C, Teng PN, Traas J, Schugar R, Deasy BM, Badylak S, Buhring HJ, Jacobino JP, Lazzari L, Huard J, Peault B. A perivascular origin for mesenchymal stem cells in multiple human organs. *Cell Stem Cell*. 2008;3(3):301-13.
43. Sacchetti B, Funari A, Remoli C, Giannicola G, Kogler G, Liedtke S, Cossu G, Serafini M, Sampaolesi M, Tagliafico E, Tenedini E, Saggio I, Robey PG, Riminucci M, Bianco P. No Identical "Mesenchymal Stem Cells" at Different Times and Sites: Human Committed

Progenitors of Distinct Origin and Differentiation Potential Are Incorporated as Adventitial Cells in Microvessels. *Stem Cell Reports*. 2016;6(6):897-913.

44. Dezsó K, Jelnes P, Laszlo V, Baghy K, Bodor C, Páku S, Tygstrup N, Bisgaard HC, Nagy P. Thy-1 is expressed in hepatic myofibroblasts and not oval cells in stem cell-mediated liver regeneration. *Am J Pathol*. 2007;171(5):1529-37.

45. Knittel T, Kobold D, Piscaglia F, Saile B, Neubauer K, Mehde M, Timpl R, Ramadori G. Localization of liver myofibroblasts and hepatic stellate cells in normal and diseased rat livers: distinct roles of (myo-)fibroblast subpopulations in hepatic tissue repair. *Histochemistry and cell biology*. 1999;112(5):387-401.

46. Tateaki Y, Ogawa T, Kawada N, Kohashi T, Arihiro K, Tateno C, Obara M, Yoshizato K. Typing of hepatic nonparenchymal cells using fibulin-2 and cytoglobin/STAP as liver fibrogenesis-related markers. *Histochemistry and cell biology*. 2004;122(1):41-9.

47. Ober EA, Lemaigre FP. Development of the liver: Insights into organ and tissue morphogenesis. *Journal of hepatology*. 2018;68(5):1049-62.

48. Kramann R, Schneider RK, DiRocco DP, Machado F, Fleig S, Bondzie PA, Henderson JM, Ebert BL, Humphreys BD. Perivascular Gli1+ progenitors are key contributors to injury-induced organ fibrosis. *Cell Stem Cell*. 2015;16(1):51-66.

49. Vanlandewijck M, He L, Mae MA, Andrae J, Ando K, Del Gaudio F, Nahar K, Lebouvier T, Lavina B, Gouveia L, Sun Y, Raschperger E, Rasanen M, Zarb Y, Mochizuki N, Keller A, Lendahl U, Betsholtz C. A molecular atlas of cell types and zonation in the brain vasculature. *Nature*. 2018;554(7693):475-80.

50. He L, Vanlandewijck M, Mae MA, Andrae J, Ando K, Del Gaudio F, Nahar K, Lebouvier T, Lavina B, Gouveia L, Sun Y, Raschperger E, Segerstolpe A, Liu J, Gustafsson S, Rasanen M, Zarb Y, Mochizuki N, Keller A, Lendahl U, Betsholtz C. Single-cell RNA sequencing of mouse brain and lung vascular and vessel-associated cell types. *Sci Data*. 2018;5:180160.

51. Lemoine S, Thabut D, Housset C. Portal myofibroblasts connect angiogenesis and fibrosis in liver. *Cell and tissue research*. 2016;365(3):583-9.

52. Zhang DY, Goossens N, Guo J, Tsai MC, Chou HI, Altunkaynak C, Sangiovanni A, Iavarone M, Colombo M, Kobayashi M, Kumada H, Villanueva A, Llovet JM, Hoshida Y, Friedman SL. A hepatic stellate cell gene expression signature associated with outcomes in hepatitis C cirrhosis and hepatocellular carcinoma after curative resection. *Gut*. 2016;65(10):1754-64.

53. Bartneck M, Warzecha KT, Tag CG, Sauer-Lehnen S, Heymann F, Trautwein C, Weiskirchen R, Tacke F. Isolation and time lapse microscopy of highly pure hepatic stellate cells. *Anal Cell Pathol (Amst)*. 2015;2015:417023.

54. Gonzalez-Sanchez E, Firrincieli D, Housset C, Chignard N. Expression patterns of nuclear receptors in parenchymal and non-parenchymal mouse liver cells and their modulation in cholestasis. *Biochim Biophys Acta Mol Basis Dis*. 2017;1863(7):1699-708.

55. Stuart T, Butler A, Hoffman P, Hafemeister C, Papalexi E, Mauck WM, 3rd, Hao Y, Stoeckius M, Smibert P, Satija R. Comprehensive Integration of Single-Cell Data. *Cell*. 2019;177(7):1888-902 e21.

56. Hafemeister C, Satija R. Normalization and variance stabilization of single-cell RNA-seq data using regularized negative binomial regression. *Genome Biol*. 2019;20(1):296.

57. Yu G, Wang LG, Han Y, He QY. clusterProfiler: an R package for comparing biological themes among gene clusters. *OMICS*. 2012;16(5):284-7.

58. Yu G, He QY. ReactomePA: an R/Bioconductor package for reactome pathway analysis and visualization. *Mol Biosyst*. 2016;12(2):477-9.

Figure legends

Fig. 1 ScRNAseq profiling of mesenchymal cells from the bilio-vascular tree. (A) Outline of the experimental procedure for preparation of Lin (EpCam,CD31,CD45,CD11b)-negative cells from the mouse liver bilio-vascular tree for single-cell RNAseq analysis. (B) *t*-distributed stochastic neighbor embedding (*t*-SNE) projection of 4,976 single cells, revealed 16 distinct clusters (C, color-coded). Clusters were identified by matching their expression profiles with those previously assigned to distinct cell types, and ordered according to the number of cells they comprise. (C) Dendrogram showing the relationships of cell clusters (D) Heatmap of differentially expressed genes. For each cluster the top 10 genes and their relative expression levels in all sequenced cells are shown (color-coded, ordered as in (B)). (E) *t*-SNE visualization of top differentially expressed genes in each cluster (encircled). Each cell is colored according to the scaled expression of the indicated marker.

Fig. 2 Analysis of progenitor features among mesenchymal cell clusters. (A) Inference of all sequenced cells excluding mesothelial and endothelial cells by Monocle 2 reverse graph embedding. Color code is the same as in Fig. 1B, showing bifurcation of cells into two primary lineages. Inset shows pseudotime picturing using a white-to-gray gradient along the differentiation trajectory (B) Heatmap of Gene Ontology (GO) enrichment related to development. Heatmap colors correspond to the $-\log_{10}$ of *p* values. (C) Dot plot showing the expression of portal (myo)fibroblast markers across the mesenchymal cell clusters. Individual dot size and color reflect the percentage of cells expressing the marker gene (% Exp) and its average expression (Avg exp) across all cells. Fib3/Fib4 (framed) combine multilineage potential and PMF markers expression.

Fig. 3 Isolation of portal mesenchymal cells qualifying for MSCs and PMF progenitors.

(A) Dot plot showing the average expression of genes encoding surface markers *Pdgfra/Cd34/Cd9* and *Cd200* in all clusters. (B) FACS plot showing the gating strategy for Fib-3/Fib-4 cell sorting from the bilio-vascular tree cell suspension. (C) CFU-F formed by sorted cells from gates-3, 4, 5 and 6, as defined in (B). Cells from gate 4 (Fib-3/Fib-4) form more colonies than other sorted cells. Data represent means \pm SEM (n=3-9). (D) Flow cytometry analysis of typical MSC surface markers in cells from gate 4 (n=4-10). (E) Trilineage differentiation capacity of cells from gate 4 (*i.e.*, PMSCs), towards adipocytes (Oil red O staining), osteoblasts (Alizarin red S), and chondrocytes (Alcian blue); scale bars=50 μ m. (F) Immunofluorescence of Col15A1 and α -SMA in PMSC spheroids (upper panels) or PMSCs growing on stiff substratum (lower panels). (G) Expression of *Col15a*, *Acta2* and *Col1a1* in freshly isolated PMSCs, PMSC spheroids or in PMSC-derived myofibroblasts grown on stiff substratum (PMSC-MFs). Data represent means \pm SEM (n=3). Statistical significance was evaluated by one-way ANOVA. ** $p < 0.01$; *** $p < 0.001$; **** $p < 0.0001$; ns, non-significant.

Fig. 4 Transcriptomic features of PMSCs compared to HSCs.

Freshly isolated PMSCs and HSCs were analyzed by bulk RNAseq. (A) Volcano plot showing 3273 and 3122 differentially expressed genes ($p \leq 0.01$, FDR ≤ 0.05 , fold-difference ≥ 2) in PMSCs and HSCs, respectively. Selected PMSC and HSC markers are labeled. (B) Average expression of selected PMSC and HSC markers labeled in (A) was projected on the *t*-SNE plot of scRNAseq. (C) Gene Set Enrichment Analysis (GSEA), among all genes overexpressed in PMSCs and HSCs (n=6,395 genes).

Fig. 5 Identification of PMSC and HSC gene signatures. (A) Overview of the cell preparations, *i.e.*, PMSCs and HSCs, freshly isolated or myofibroblastic after 3 days (-MFs-3d) or 7 days (-MFs-7d) in culture, analyzed by bulk RNAseq (upper panel) and principal component analysis of variance (lower panel) of read counts for whole transcriptomes; ellipses indicate 95% confidence interval of group membership. Axis percentages indicate variance contribution. (B) K-means clustering of 5000 genes with highest variance in bulk RNAseq analysis; scale bar, expression Z score of differentially expressed genes (DEGs). Enriched GO terms in each cell preparation are shown on the right. (C) Venn diagram showing 100 DEGs in PMSCs and 112 DEGs in HSCs, both in scRNAseq of Fib-3/Fib-4 vs. HSCs ($p \leq 0.01$, fold-difference ≥ 2) and bulk RNAseq of PMSCs vs. HSCs and maintaining high differential expression after myofibroblastic differentiation (PMSC-MFs-7d vs. HSC-MFs-7d) (D) Heatmaps of PMSC and HSC signature genes expression in the different samples (1-4) of cell preparations. (E) *Slit2* expression assessed by RT-qPCR in freshly isolated PMSCs, HSCs, their derived myofibroblasts (-MFs-7d), hepatocytes, cholangiocytes, liver sinusoidal endothelial cells (LSECs) and Kupffer cells (KCs) from mouse liver. Data represent means \pm SEM (n=3). Statistical significance was evaluated by one-way ANOVA. **** $p < 0.0001$; ns, non-significant.

Fig. 6 Expression of *Slit2* in mouse and human liver fibrosis. (A) Hepatic expression of *Slit2*, *Acta2*, *Col1a1* and *vWF* was measured by RT-qPCR in liver tissue from normal control diet (NCD, n= 12) and 3,5-diethoxycarbonyl-1,4-dihydrocollidine (DDC, n= 8) diet-fed mice (upper panels). Correlations between *Slit2* and *Acta2*, *Col1a1* or *vWF* mRNA levels are shown in lower panels. (B) Hepatic expression of *SLIT2*, *ACTA2*, *COL1A1* and *vWF* mRNA, was assessed by Affymetrix microarray analysis of normal human liver (n=5) and of liver tissue samples from patients with non-alcoholic steatohepatitis (NASH, n=7), primary sclerosing cholangitis

(PSC, n=6) or other liver diseases (n=8) (left panel). Correlations between *SLIT2* and *ACTA2*, *COL1A1* or *vWF* mRNA levels in all samples are shown in right panels. (C) Expression of *SLIT2* was assessed by RT-qPCR in liver biopsy specimens from patients with non-alcoholic fatty liver diseases (NAFLD), at different stages of fibrosis, as defined by SAF score (n=7-26). Correlations between *SLIT2* and *ACTA2*, *COL1A1* or *vWF* mRNA levels are shown. Data represent means \pm SEM. * $p < 0.05$; ** $p < 0.01$; *** $p < 0.001$; **** $p < 0.0001$; ns, non-significant; Statistical significance was evaluated by Student *t* test and one-way ANOVA; *r* values are Pearson correlation coefficients.

Fig.7 Expression of PMSC and HSC multigene signature in human liver fibrosis. Hepatic expression of PMSC (A) and HSC (B) multigene signature was assessed by Affymetrix microarray analysis of normal human liver (n=5) and of liver tissue samples from patients with non-alcoholic steatohepatitis (NASH, n=7), primary sclerosing cholangitis (PSC, n=6) or other liver diseases (n=8). (C) Correlations between PMSC multigene signature and *ACTA2*, *COL1A1*, and *vWF* mRNA levels in all liver groups. Data represent means \pm SEM. ** $p < 0.01$; **** $p < 0.0001$; ns, non-significant; Statistical significance was evaluated by non-parametric Wilcoxon test; *r* values are Pearson correlation coefficients.

Figure 1

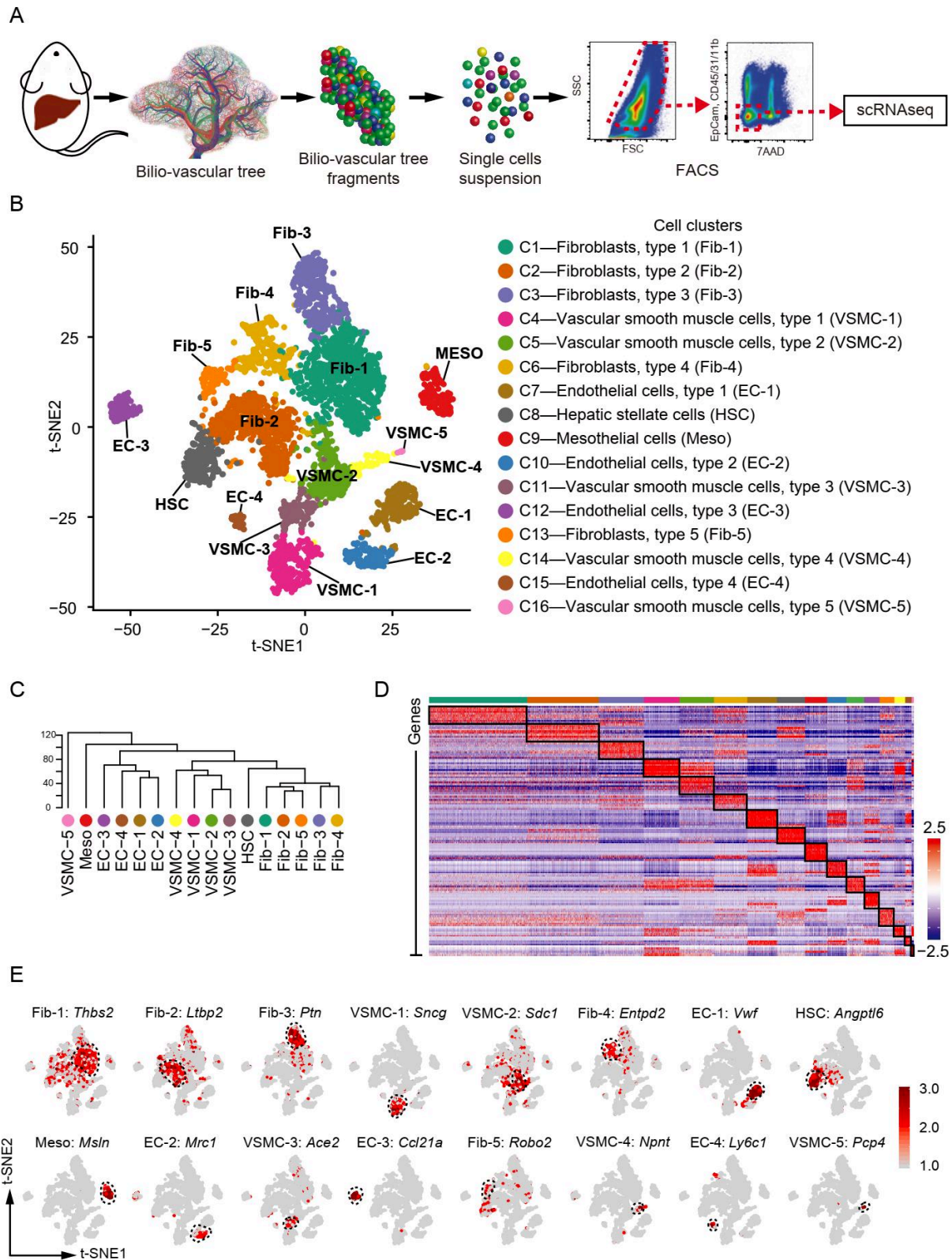


Figure 2

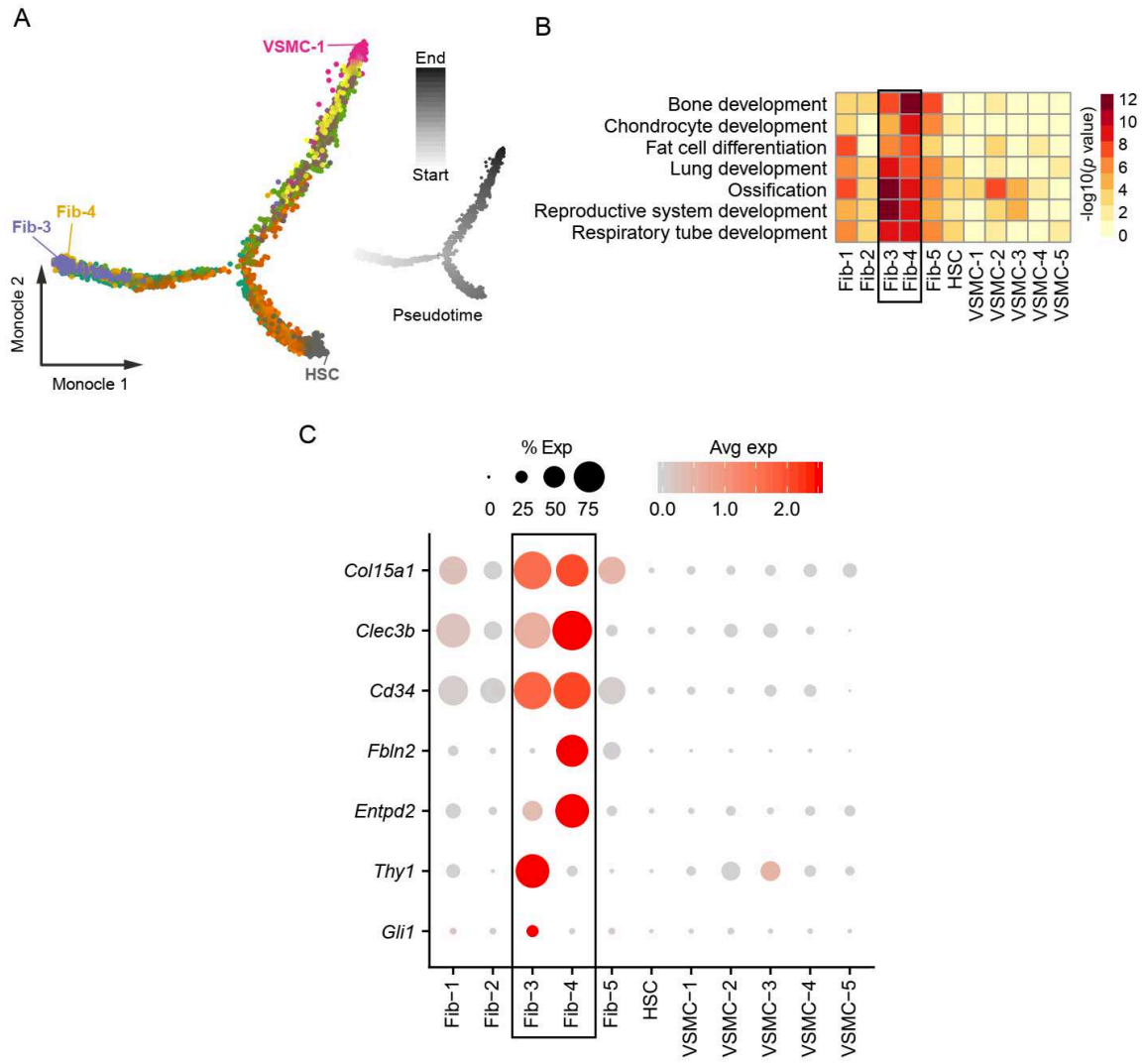


Figure 3

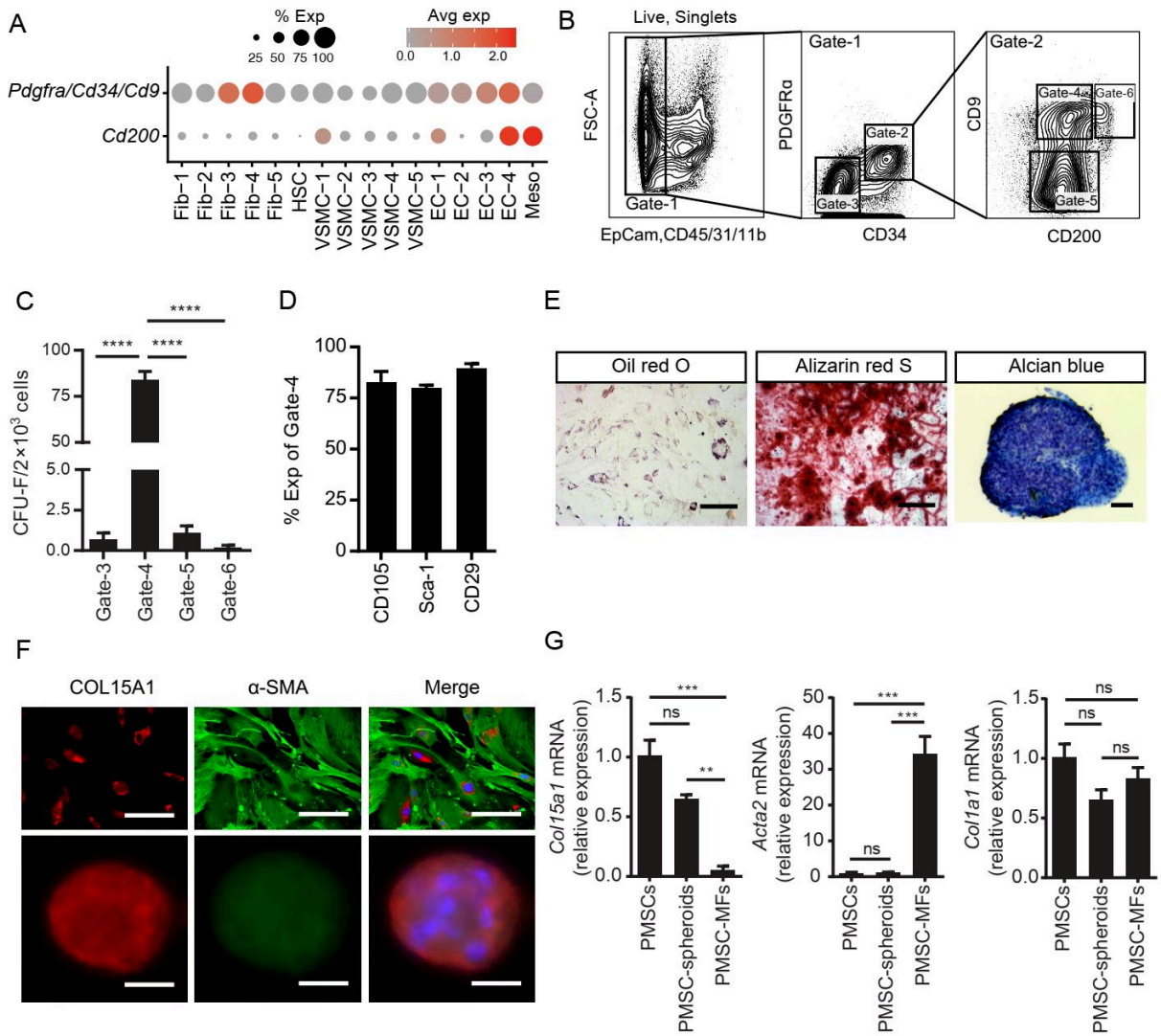


Figure 4

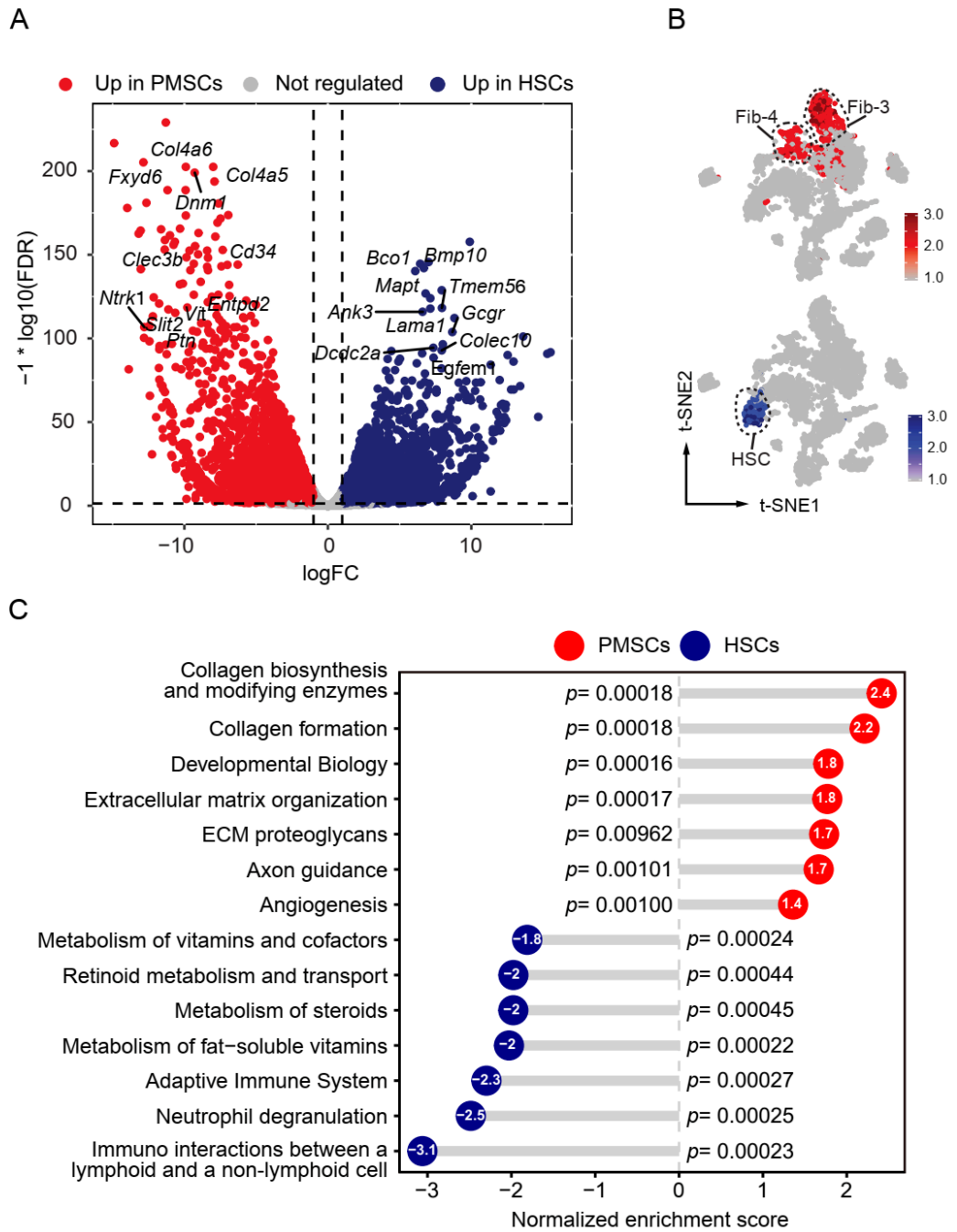


Figure 5

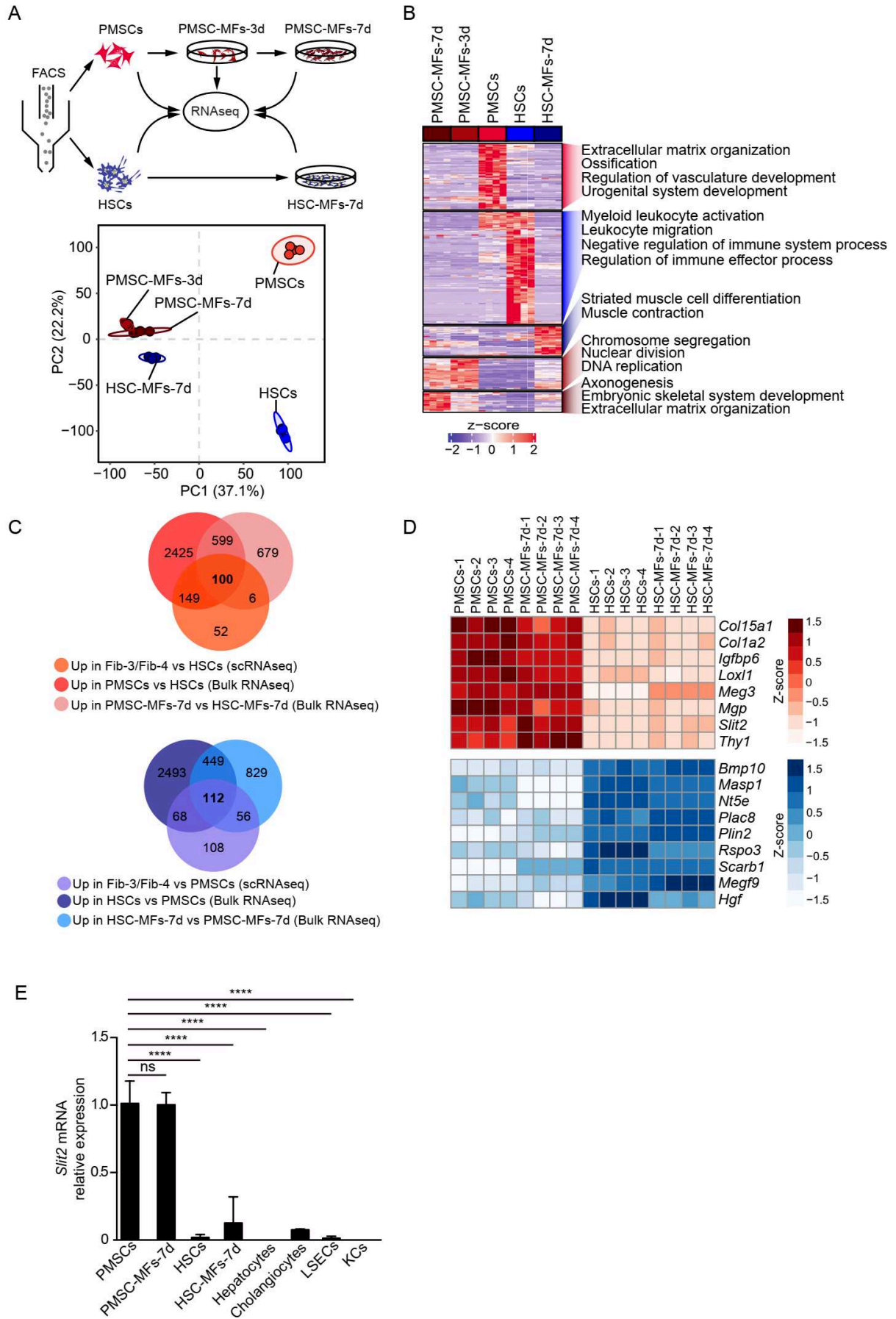
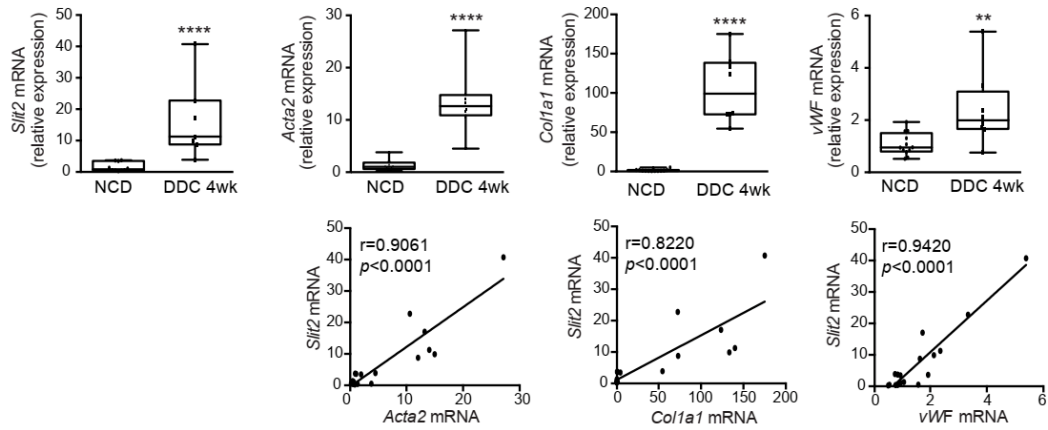
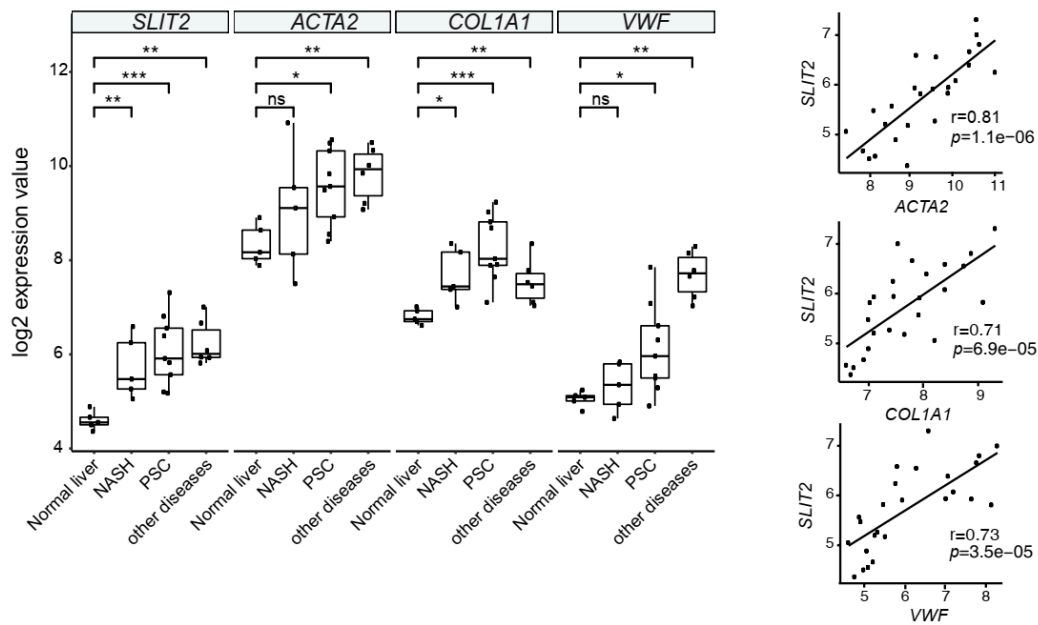


Figure 6

A



B



C

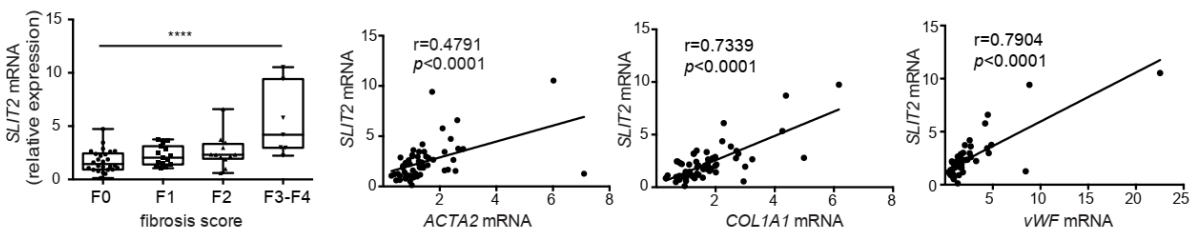
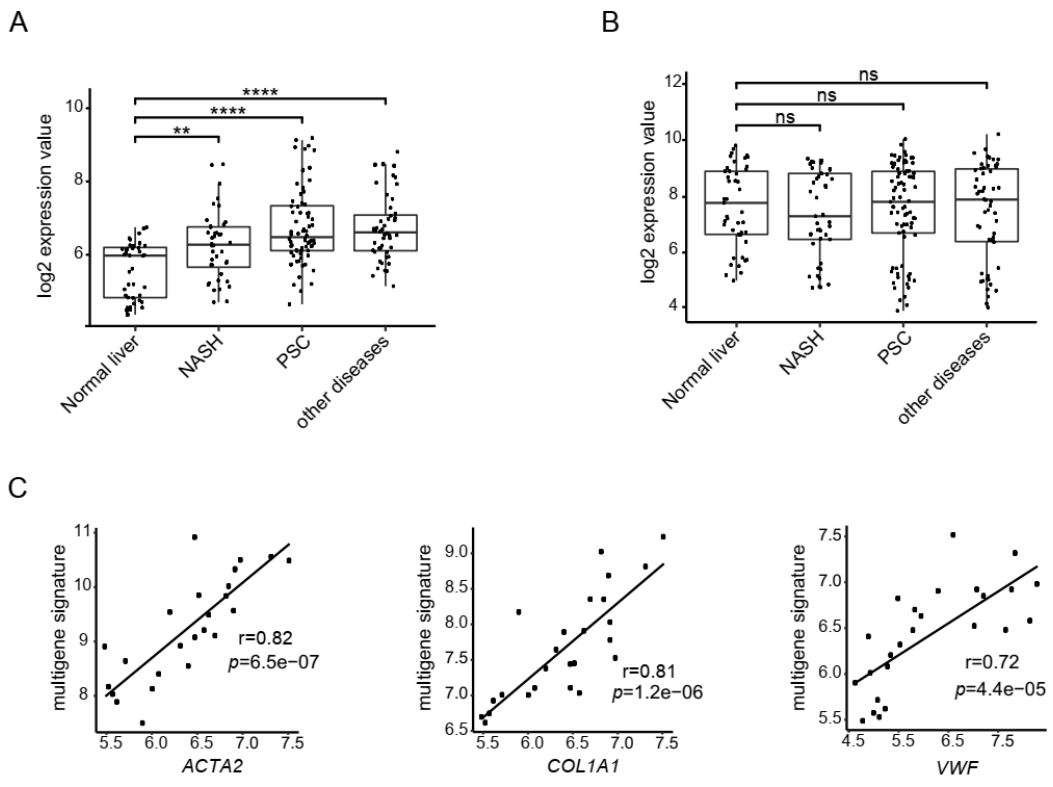


Figure 7



Single-cell transcriptomics enable uncovering portal mesenchymal stem cells as precursors of myofibroblasts in liver fibrosis. Lin Lei *et al.*

Supplementary material

Suppl. Table S1 Differentially expressed genes in each cluster compared to all others.

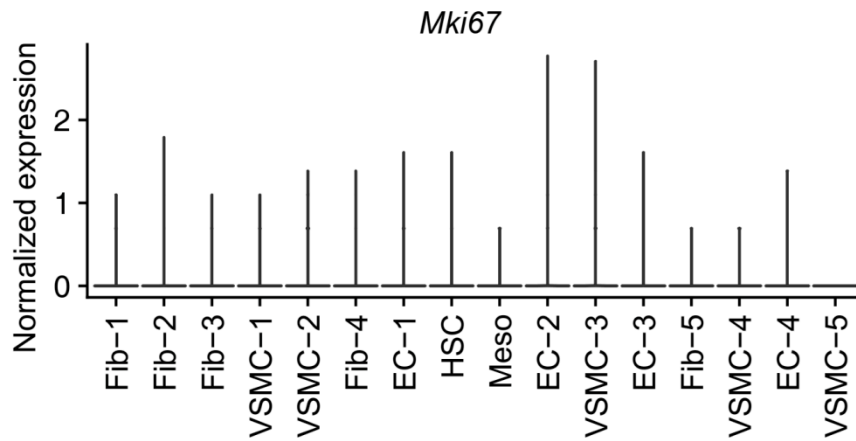
<https://filesender.renater.fr/?s=download&token=58a98724-9c79-4035-aeda-f9361eb38ab7>

Suppl. Table S2 Gene Ontology (GO) enrichment of differentially expressed genes in Fibroblast (Fib), Hepatic stellate cell (HSC), and Vascular smooth muscle cell (VSMC) clusters.

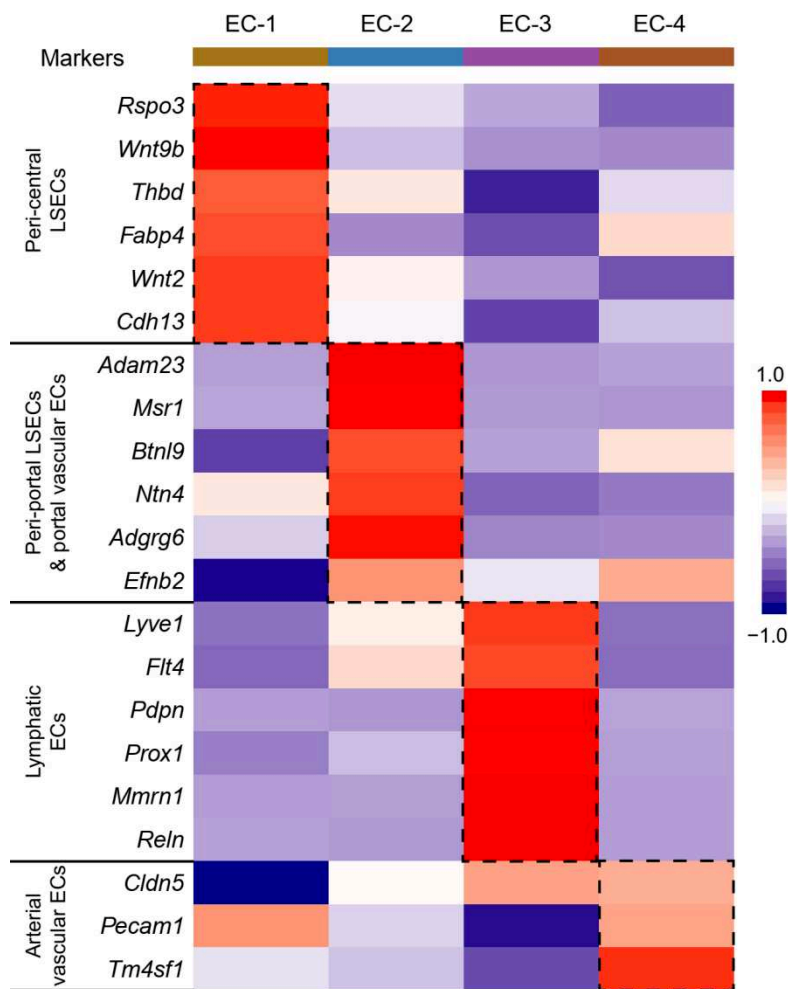
<https://filesender.renater.fr/?s=download&token=778b3e29-ddf2-4bcf-9dd9-4c8360aa550f>

Supplementary Table 3. Primers used for qPCR.

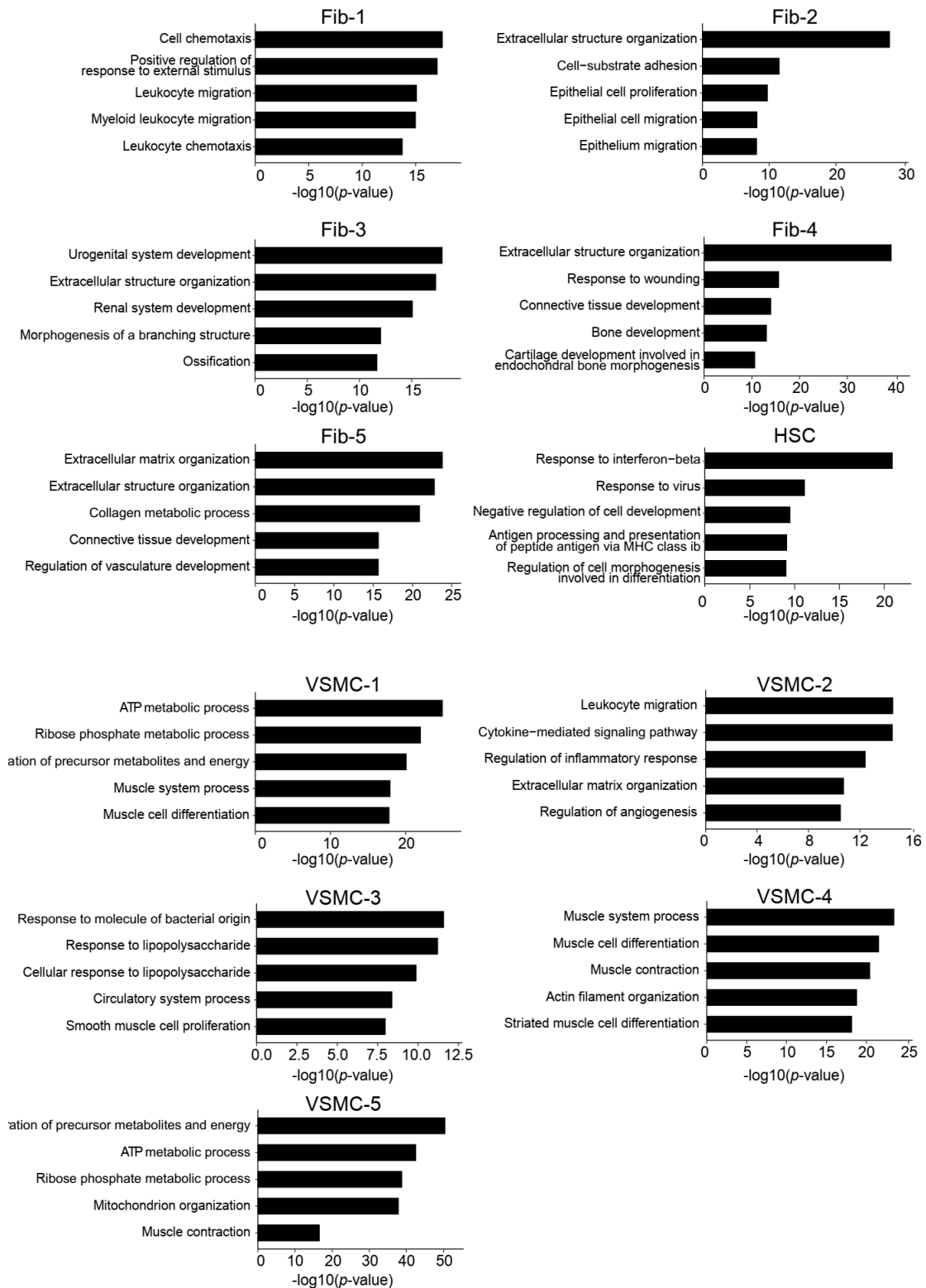
Gene	GenBank accession No	Forward primer	Reverse primer
Mouse			
<i>Acta2</i>	NM_007392.3	CTGTCAGGAACCCTGAGACGCT	TACTCCCTGATGTCTGGGAC
<i>Slit2</i>	NM_178804.5	ATCTGCCTGAGACCATCACA	CGTCTAAGCTTTTTGTATGGTGAG
<i>Col1a1</i>	NM_007742.4	GCTCCTTAGGGGCCAC	CCACGTCTCACCATTGGGG
<i>Col15a1</i>	NM_009928.3	AGATTTACGGTTCCATACA	CAACGTGTGATTCTTTAGGC
<i>vWf</i>	NM_011708.4	CTACCTAGAACGCGAGGCTG	CATCGATTCTGGCCGAAAG
<i>Hprt</i>	NM_013556.2	TCAAATCCCTGAAGTACTCAT	AGGACCTCTCGAAGTGT
<i>18S</i>	NR_003278.3	GAGCGAAAGCATTGCCAAG	GGCATCGTTTATGGTCGGAA
Human			
<i>ACTA2</i>	NM_001613.4	GACAATGGCTCTGGGCTCTGTAA	CTGTGCTTCGTCACCCACGTA
<i>SLIT2</i>	NM_004787.4	GTGTTCTGTCAGCTATGAC	TTCCATCATTGATTGTCTCCAC
<i>COL1A1</i>	NM_000088.4	GTGCGATGACGTGATCTGTGA	CGGTGGTTTCTTGGTCGGT
<i>vWF</i>	NM_000552.5	CTCCCACGCCTACATCGG	GCGGTGATCTTGCTGAAG
<i>HPRT</i>	NM_000194.3	TAATTGGTGGAGATGATCTCTCAAC	TGCCTGACCAAGGAAAGC



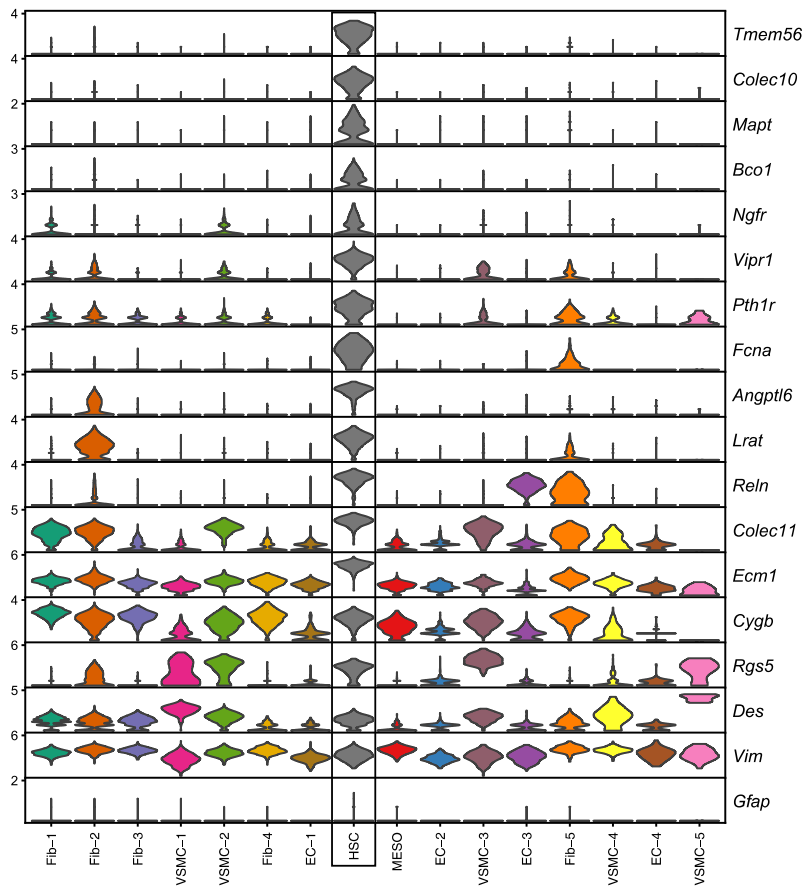
Suppl. Fig. S1 Violin plots showing the expression of the proliferation marker *Mki67* across all clusters.



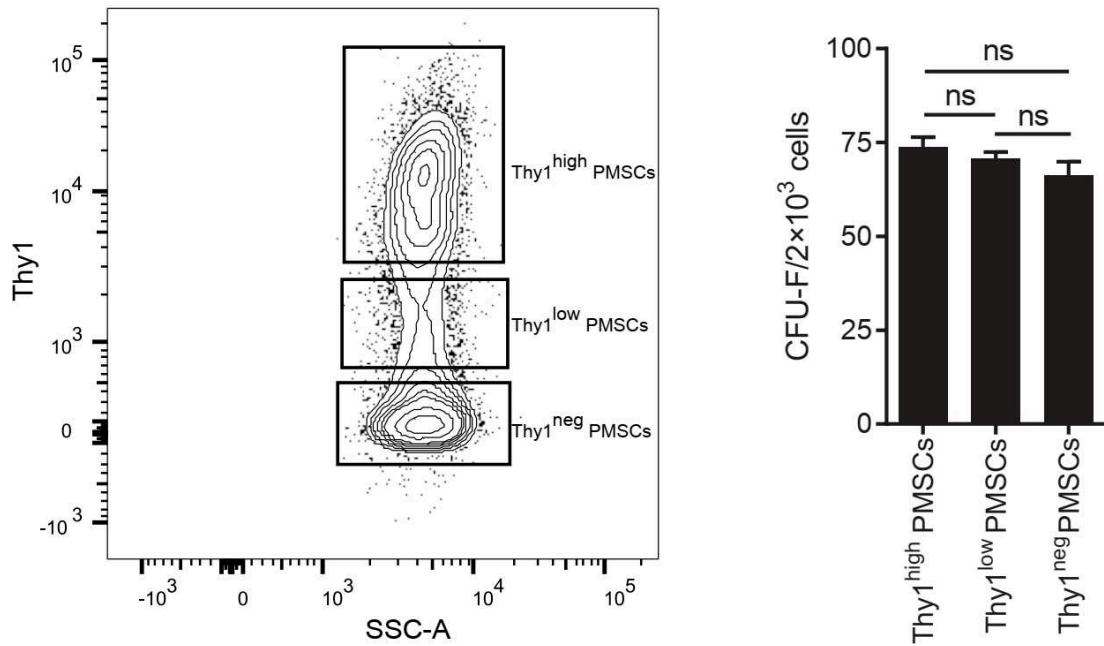
Suppl. Fig. S2 Heatmap depicting representative genes expressed in the endothelial cell (EC) clusters. Color-scale represents the average expression level across all cells within cluster. LSECs, liver sinusoidal endothelial cells.



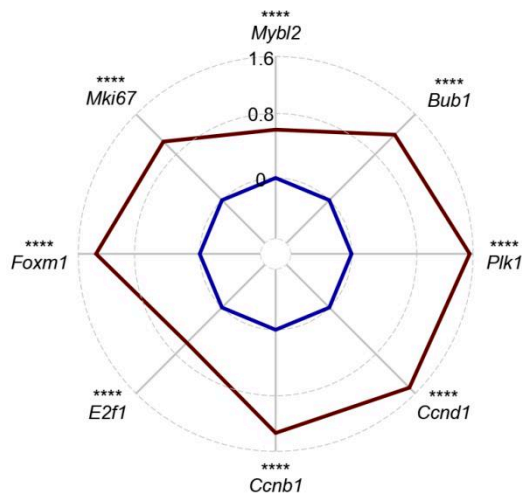
Suppl. Fig. S3 Gene ontology (GO) enrichment of genes significantly overexpressed in the different mesenchymal cell clusters according to scRNA-seq. See also Table S2.



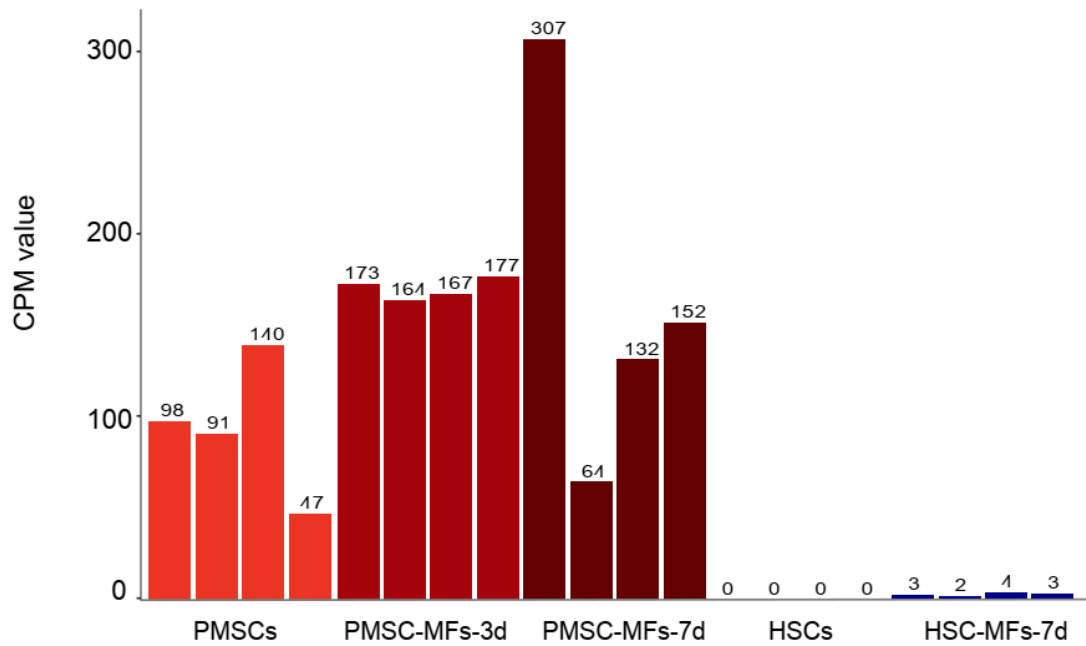
Suppl. Fig. S4 Violin plots showing gene expressions previously reported in hepatic stellate cells (HSCs) across all clusters.



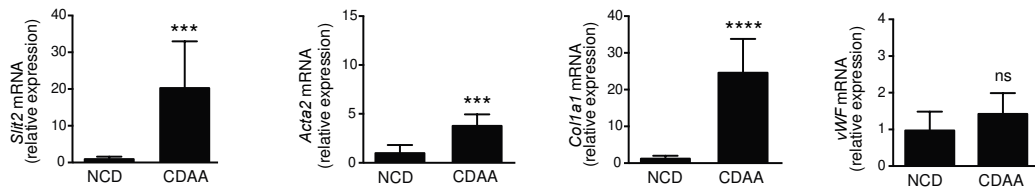
Suppl. Fig. S5 Clonogenicity of PMSCs with various expression of Thy1. Left panel: Representative flow cytogram of Thy1 expression on PMSCs. Right panel: CFU-F formed by Thy1^{neg}, Thy1^{low} and Thy1^{high} PMSCs. Data represent means \pm SEM (n=3). ns, non-significant; Statistical significance was evaluated by Student *t* test.



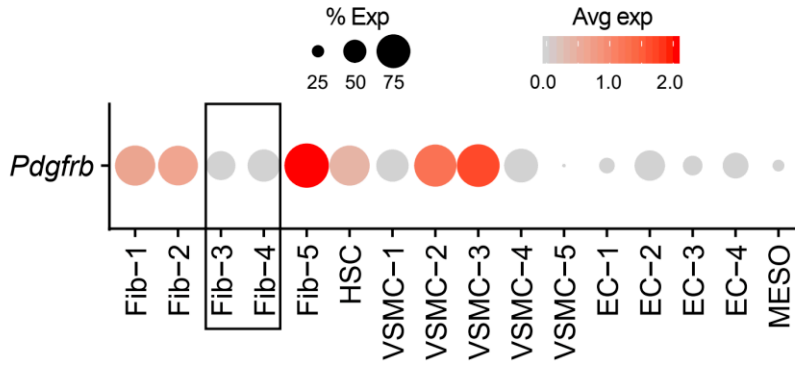
Suppl. Fig. S6 Proliferation-related gene expressions in PMSC- vs. HSC-derived myofibroblasts. Radar plot showing the log₂ fold-difference in the expression of cell proliferation related genes in PMSC-derived (red line) and HSC-derived (blue line) myofibroblasts after 7 days in culture, in bulk RNA-seq. *****p*<0.0001; Statistical significance was evaluated by Student *t* test.



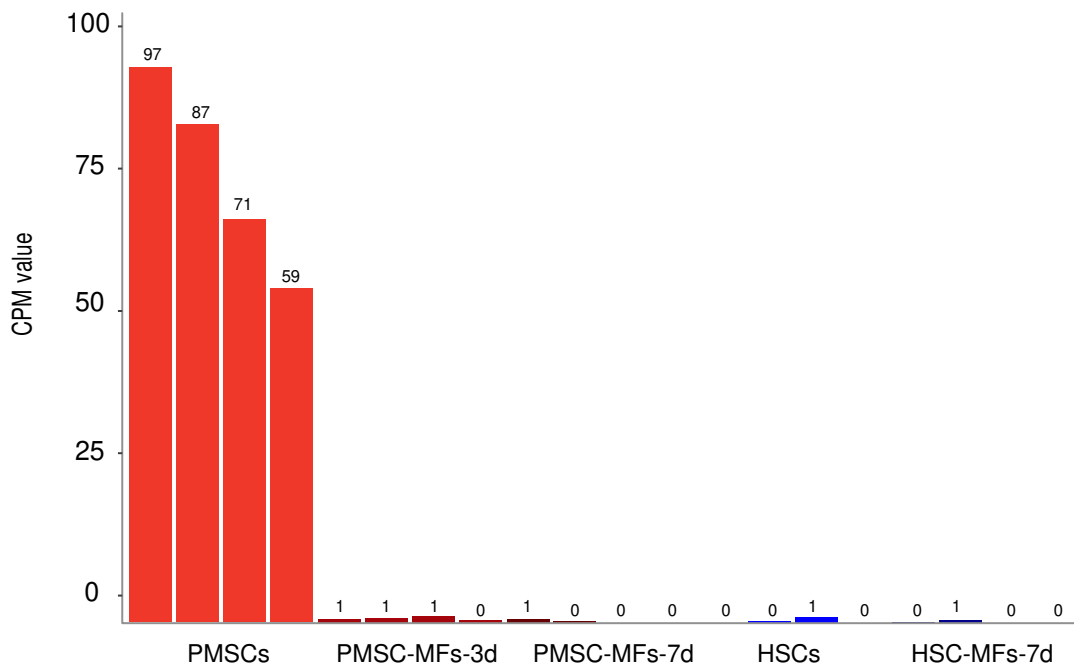
Suppl. Fig. S7 *Slit2* expression in the bulk RNA-seq analysis of PMSCs and HSCs, in quiescent or myofibroblastic states after 3 days (-MFs-3d) or 7 days (-MFs-7d) in culture. CPM, counts per million.



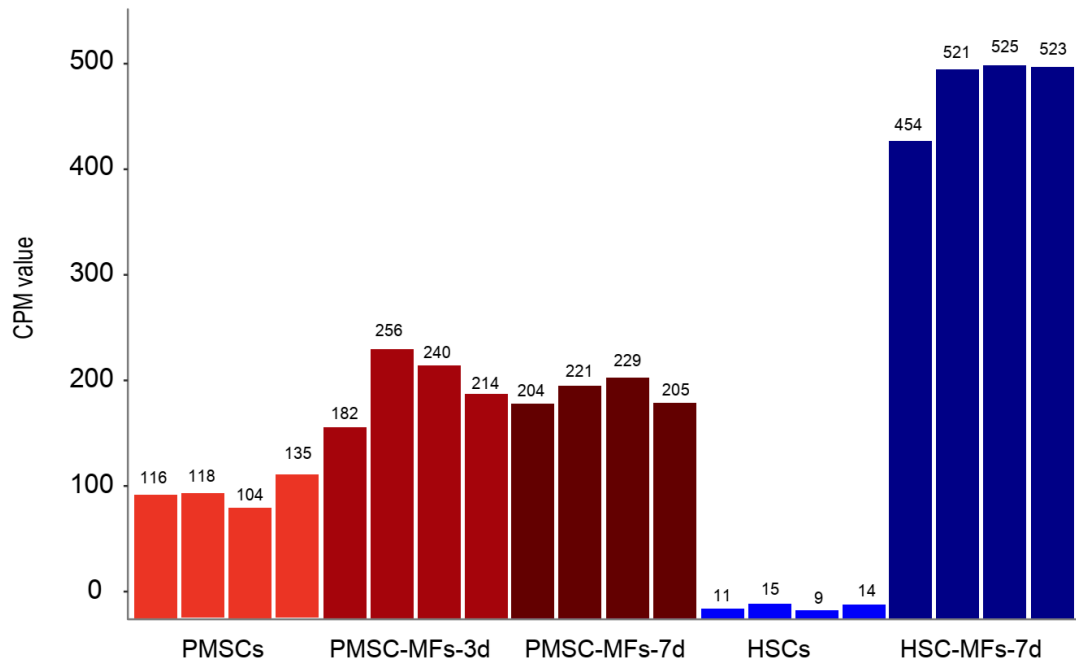
Suppl. Fig. S8 *Slit2* expression in a diet model of non-alcoholic steatohepatitis (NASH) with liver fibrosis. Hepatic expression of *Slit2*, *Acta2*, *Col1a1* and *vWF* was measured by RT-qPCR in liver tissue from normal control diet (NCD, n= 5) and choline deficient, defined amino acid (CDAA, n=17) diet-fed mice. Data represented means \pm SEM. *** p <0.001; **** p <0.0001; ns, non-significant; Statistical significance was evaluated by Student *t* test.



Suppl. Fig. S9 Dot plot showing the expression of *Pdgfrb* in all clusters. Individual dot size and color reflect the percentage of cells expressing the marker gene (% Exp) and its average expression (Avg exp) across all cells.



Suppl. Fig. S10 *Gli1* expression in the bulk RNA-seq analysis of PMSCs and HSCs, in quiescent or myofibroblastic states after 3 days (-MFs-3d) or 7 days (-MFs-7d) in culture. CPM, counts per million.



Suppl. Fig. S11 *Pcdh7* expression in the bulk RNA-seq analysis of PMSCs and HSCs, in quiescent or myofibroblastic states after 3 days (-MFs-3d) or 7 days (-MFs-7d) in culture. CPM, counts per million.

III) Discussion

The role of the mesenchymal compartment in liver homeostasis or disease is increasingly recognized, and the new emerging single-cell genomics has provided a powerful tool for unraveling the complexity of liver cells in health and disease with unprecedented resolution. However, the characterization of liver mesenchymal cell subpopulations, especially portal mesenchymal cells in liver tissue has remained limited. This situation might in part, reflect challenges in cell isolation, with portal mesenchymal cells representing a very small proportion of cells in previous single-cell RNA sequencing (scRNA-seq) atlas studies. In this study, we provide a detailed landscape of portal mesenchymal cells. To obtain the whole atlas of portal mesenchymal cells and avoid an overrepresentation of parenchymal cells, we utilized an approach that was different from the one used in previous scRNA-seq analyses of the liver (Strauss et al., 2017) (MacParland et al., 2018) (Halpern et al., 2018) (Xiong et al., 2019) (Su et al., 2020) (Aizarani et al., 2019). this allowed us to gain access to a broader view of portal mesenchymal cells. Our scRNA-seq analysis identified sixteen clusters, including non-mesenchymal cells, *i.e.*, ECs and mesothelial cells, as well as mesenchymal cells, *i.e.*, fibroblasts, VSMCs, and HSCs. Because of CD31 intracellular localization in LSECs (DeLeve et al., 2004; Poisson et al., 2017), and the high fluctuation of CD31 expression level in liver ECs (Strauss et al., 2017), we could not avoid the escape of ECs, to a negative selection of ECs we applied to our cell preparation by using FACS with CD31 staining. Several scRNA-seq studies have addressed previously unknown functional zonation of LSECs across the liver lobule (Aizarani et al., 2019; Halpern et al., 2018; MacParland et al., 2018; Su et al., 2020; Xiong et al., 2019). We identified four EC clusters in our dataset and confirmed them as peri-central LSECs, (peri)portal ECs, lymphatic ECs, and arterial ECs, respectively. Thus, our data recovered and provided further proof of preciously reported landmarks of endothelial cells zonation in mouse liver. Hepatic VSMCs have been reported as a contributor to portal hypertension in the fibrotic liver (Bomzon & Huang, 2001; Iwakiri, 2014; Shim et al., 2018; Zeng et al., 2018). However, there are few studies that ever addressed the characteristics of VSMCs in normal or diseased liver. In our dataset, VSMCs were clustered into five clusters, uniformly showing hallmarks of their vascular regional identity, which is consistent with that recently found in the

liver of a *Pdgfrb*-GFP mouse model by scRNA-seq (Dobie et al., 2019). Furthermore, VSMC clusters displayed distinct molecular and functional differences suggesting that VSMC heterogeneity exists in healthy mouse liver. Such heterogeneity is noteworthy as it may indicate the existence of specific subsets of cells with particular disease relevant properties. Sources of heterogeneity may include further developmental differences within the VSMC lineage (Sawada et al., 2017), differences in the cells' microenvironment (*i.e.*, Oxygen and nutrients concentration) and hepatic haemodynamic or stochastic factors. Analyses focused on individual genes are required to further investigate the mechanisms and functional consequences of VSMC heterogeneity in the vessels of healthy liver. With a high resolution of scRNA-seq, we also captured a cell cluster defined as mesothelial cells, which display a distinct molecular profile, without tangling with other fibroblast clusters. Mesothelial cells are recognized to form a single layer that covers the liver surface (Lua & Asahina, 2016). Our data showed the existence of mesothelial cells remote from the liver surface, consistent with their migration inward from the surface during liver development (Asahina et al., 2011). Intriguingly, Lua and colleagues reported that MSLN was exclusively expressed in mesothelial cells, but no MSLN expression was observed in the portal triad by immunohistochemistry in their study (Lua et al., 2016a). However, Iwaisako and colleagues identified MSLN as a marker of PFs by using the whole mouse genome microarray (Iwaisako et al., 2014). Perhaps some of the confusion about the localization of mesothelial cells may result from the different methods of detection with different scales and resolutions. In line with a previous study, using the scRNA-seq approach, Ramachandran and colleagues also found mesothelial cells in their dataset of human healthy and cirrhotic liver NPCs (Ramachandran et al., 2019). HSCs are also retrieved and recognized in our data, showing highly consistent gene expression with the published scRNA-seq studies (Dobie et al., 2019; Krenkel et al., 2019). As introduced in the previous section, HSCs are regarded as the main contributor to the myofibroblasts in liver fibrosis. However, the approach (cell fate tracing, immunohistochemistry, and FACS) to address this question heavily relies on specific markers. So far, *Lrat*, *Reln*, *Cygb* and *Gfap* have been considered as the most specific markers of HSCs in the liver (Cassiman et al., 2002; T. Knittel, D. Kobold, F. Piscaglia, et al., 1999; Lua et al., 2016b; Mederacke et al., 2013; Okina et al., 2020). Our data indicated that *Lrat* and *Reln* were not exclusively expressed by HSCs, but also considerably expressed in other fibroblast

and endothelial cell clusters even if expression levels were lower than in HSCs. In line with previous studies, we found that the classic HSC marker *Des* was expressed at variable level in all clusters, including not only HSCs, but also fibroblasts, VSMCs, mesothelial cells, and even endothelial cells and that *Gfap* expression was negligible in HSCs (Dobie et al., 2019; Mederacke et al., 2013). Additionally, we revealed additional markers of HSCs, exclusively expressed in HSCs, including *Colec10*, *Vipr1*, *Ank3*, *Mapt*, which may provide additional support to develop new strategies to investigate HSCs.

Importantly, consistent with a previous report in a *Pdgfrb*-GFP knockin reporter mouse that was used to label mesenchymal cells in the mouse liver (Dobie et al., 2019), we found fibroblasts clearly distinct from HSCs. Furthermore, we individualized five subpopulations of fibroblasts, revealing a certain degree of heterogeneity of portal fibroblasts in the liver. Notably, among these fibroblast clusters, Fib-3 and Fib-4 displayed the lowest levels of *Pdgfrb* expression and may have been overlooked, in the study of PDGFR β expressing liver mesenchymal cells (Dobie et al., 2019).

Fib3 and Fib4 exhibited at highest level functions related to differentiation and development compared to other mesenchymal clusters. In addition, these two clusters displayed the highest levels of expression of genes previously reported as markers of portal fibroblasts or myofibroblasts, *i.e.*, *Col15a1*, *Thy1*, *Entpd2*, *Fbln2* (Dranoff et al., 2002; Dudas et al., 2009a; Katsumata et al., 2017; T. Knittel, D. Kobold, B. Saile, et al., 1999; Lemoine et al., 2015; Nishio et al., 2019). Therefore, we postulated that Fib-3 and Fib-4 might provide of reservoir of mesenchymal progenitor cells in the adult liver. To address this hypothesis, a panel of surface markers (Lin-PDGFR α +CD34+CD9+CD200mid-low) was identified to purify these progenitors. Based on our scRNA-seq data, endothelial cells escaped CD31 negative selection to a certain extent. *Cd200* was highly expressed in EC clusters in our data set; also, CD200 was reported highly expressed in endothelial cells in different organs (Wakabayashi et al., 2018). To further eliminate endothelial cells and purify this subset of portal fibroblasts CD200, as a negative selection surface marker, was added to the FACS panel.

Fibroblasts that were hereby isolated possessed the capacity of tri-lineage differentiation and a high clonogenic ability, as well as the expression of MSC markers. Therefore, these fibroblasts were authenticated as portal mesenchymal stem cells (PMSCs). We demonstrated that PMSCs are able to differentiate into PMFs *in vitro* based on the expression of COL15A1, the marker of PMFs we previously identified (Lemoinne et al., 2015). Intriguingly, this phenotypic change was accompanied by an up-regulation of *Acta2* as expected, whereas *Coll5a1* was down-regulated and *Colla1* was not regulated, which was unexpected. The mechanisms underlying this phenotypic switch of PMSCs deserves to be further investigated in the future. Furthermore, we found PMSCs were retained in quiescence by culture in spheroids, on ultra-low attachment plates. These results may suggest that the loss of cell-cell interaction is not sufficient to promote the differentiation and activation of PMSC *in vitro*. Moreover, this PMSCs culture model provides a promising *in vitro* model that can be used to evaluate the effect of profibrogenic or antifibrogenic factors on liver fibrosis *in vitro* and test antifibrotic compounds.

By using RNA-seq to compare the transcriptomes of PMSCs and HSCs, we further demonstrated how distinct these two mesenchymal cell populations and derived myofibroblasts are from each other. In turn, the results obtained from bulk RNA-seq further strengthen our finding in scRNA-seq. The comparison of transcriptional profiles showed that in their quiescent state, PMSCs primarily ensure extracellular matrix organization and vasculature development. HSCs are mainly involved in immunity, and the metabolism of vitamin A. Our RNA-seq data showed that the GO terms associated with cell proliferation and DNA duplication were enriched in PMSC-MFs (3 days and 7 days cultured). In contrast, HSC-MFs exhibited low expression levels of these genes (*e.g.*, *Mybl2*, *Bub1*, *Plk1*, *Ccnd1*, *Ccnb1*, *E2f1*, *Foxm1* and *Mki67*) although cultured in the same conditions, indicating that PMSC-MFs displayed higher proliferation ability than HSC-MFs. These results are consistent with the observation during the culture experiments. Bartneck and colleagues reported that they did not observe HSC division using time-lapse microscopy (Bartneck et al., 2015). However, some studies reported primarily isolated HSCs displayed a strong proliferation property *in vitro* (Mannaerts et al., 2015). This discrepancy may result from the difference in methods these studies used to purify HSCs. A widely used method is based on density-gradient centrifugation (Scott L Friedman & Roll, 1987).

However, the contamination from other cells, probably PFs, will lead to confusion. Therefore, an add-on protocol for ultrapure HSCs isolation via subsequent flow cytometric sorting has been proposed (Mederacke et al., 2015).

We identified 100 genes in PMSCs and 112 genes in HSCs that maintained high differential expression after myofibroblastic differentiation based on scRNA-seq and bulk RNA-seq data. In translational efforts, we identified a PMSC gene signature that including *Coll15a1*, *Thy1*, *Loxl1*, *Meg3*, *Igfbp6*, *Colla2*, *Slit2* and *Mgp* that was very specific of PMSCs and PMSC-MFs, with virtually no or low expression in HSCs and HSC-MFs. Our results showed that PMSC gene signature was highly expressed in human fibrotic liver (NASH, PSC, other liver diseases) compared with normal human liver. We also designed a transcriptomic signature of HSCs, including *Megf9*, *Plin2*, *Plac8*, *Nt5E*, *Bmp10*, *Hgf*, *Masp1*, *Rspo3*, *Scarb*. However, our data showed that the expression of HSC gene signature did not vary in mouse or human liver diseases. This result may reflect the low rate of proliferation of HSCs in liver diseases, which is consistent with our bulk RNA-seq data, showing the low expression level of genes associated with cell proliferation and cell cycle in HSC-MFs and with previous morphological study of HSCs (Bartneck et al., 2015). Recently, a scRNA-seq study focused on HSC population revealed spatial zonation of HSCs across the hepatic lobule and generated gene signatures that partition HSCs into two lobule regions, namely portal vein-associated HSCs (PaHSCs) and central vein-associated HSCs (CaHSCs). It was shown in this study that CaHSCs, marked by *Adamtsl2* gene, but not PaHSCs, are the dominant pathogenic collagen-producing cells in a mouse model of centrilobular liver injury (CCl₄ fibrosis model). However, the marker of CaHSCs that was used, *Adamtsl2*, was highly expressed not only in the HSC cluster but also in several fibroblast clusters in our dataset. This discrepancy may result from the relative abundance of each cell population and the robustness of scRNA-seq in the two studies. Overall, although the discrepancy exists, these findings have implications for the understanding of liver fibrosis progression. Moreover, they could help to identify potential molecular targets for anti-fibrotic drug development.

Coll15a1 and *Thy1* are markers that have been recognized as markers of portal fibroblasts/myofibroblasts (Dezso et al., 2007; Dudas et al., 2009b; Dudas et al., 2007; Katsumata et al., 2017; Lemoinne et al., 2015). ScRNA-seq data showed that *Coll15a1* was expressed at the highest level in Fib-3 and Fib-4, but also expressed in Fib-1 and

Fib-5 even though at lower expression. *Thy1* was strictly expressed in Fib-3, whereas we showed that the sub-populations of *Thy1*⁺ and *Thy1*⁻ PMSCs were equally clonogenic, indicating the existence of *Thy1*- PMF precursors. Therefore, to evaluate the contribution of PMSC to the PMF repository more precisely and at full-scale, a gene signature of PMSCS was necessary. Checking the expression level of each gene in the PMSCs gene signature with Tabula Muris database (<https://tabula-muris.ds.czbiohub.org/>) (Tabula Muris et al., 2018). Except for *Thy1* that was expressed in a small part of natural killer cells in normal mouse liver, all other genes have no or very low expression in the natural killer cells, B cells, hepatocytes, Kupffer cells, LSECs, leukocytes, and cholangiocytes showing a high specificity of PMSC gene signature. *Loxl1* encodes LOXL1 that belongs the family of lysyl oxidases, involved in elastin crosslinking (Csiszar, 2001). Consist with this finding, portal fibroblasts are the source of elastic fibers, which are composed of a cross-linked elastin core surrounded by fibrillin-rich microfibrils (Wells, 2014). Furthermore, it has been reported that LOXL1 expression increased 34-fold in cirrhosis, and colocalized with α -SMA (W. Zhao et al., 2018). The long noncoding RNA maternally expressed gene 3 (MEG3) was shown as a guide RNA scaffold to recruit RNA-binding protein polypyrimidine tract-binding protein 1 (PTBP1) to facilitate small heterodimer partner (shp) mRNA degradation and cause cholestatic liver injury. In addition, the expression of MEG3 and PTBP1 increases in human fibrotic and cirrhotic livers (steatosis, fibrosis, and NASH) (L. Zhang et al., 2017). Interestingly, two other studies reported that MEG3 displayed inhibitory effects on HSC activation and liver fibrogenesis, and showed MEG3 down-regulation in human fibrotic liver and CCl₄ mouse liver (He et al., 2014; Yu et al., 2018). *Igfbp6* encodes insulin like growth factor binding protein 6 (IGFBP6). Recently, Martínez-Castillo and colleagues reported that the serum concentration of IGFBP-6 was downregulated in patients with chronic hepatitis C. Moreover, the authors reported that there was a negative regulation of IGFBP6 in F0, F1, and F2, but an upregulation in F3 and F4 when the patients were evaluated according to fibrosis stage. Thus, the authors speculated that IGFBP-6 participated in the regulation of ECM deposition and the senescence process, during chronic hepatitis C and showed that among IGFBPs, IGFBP-6 was the best coincident with fibrosis stage identification (Martinez-Castillo et al., 2020). Among genes of PMSC signature, *Slit2* is the unique gene that remains stably expressed across PMSC quiescent and myofibroblastic states, without being

induced in HSC-MFs. Therefore, we identified *Slit2* as a new marker of PMSCs and derived myofibroblasts. However, Chang and colleagues reported SLIT2 was secreted by HSCs and attributed to HSC activation via roundabout guidance receptor 1 (ROBO-1). We showed that *Slit2* expression was increased in the liver of DDC or CDAA fed mice, and in the liver of patients with NASH or PSC, based on Affymetrix data and RT-QPCR. Moreover, both in experimental and human liver fibrosis, we found a correlation between the expression of *SLIT2* and that of *vWF* and *COL1A1*, consistent with a contribution of PMSCs to angiogenesis as a driving force for fibrosis progression, and with the studies showing that Slit2 signaling promoted developmental and pathological ocular neovascularization (Rama et al., 2015), and tumor angiogenesis and lymphangiogenesis (B. Wang et al., 2003).

Of note, as mentioned in the introduction part, exogenous administration of MSCs is showing out a promising therapeutic potential, largely relying on MSC paracrine secretion of antiapoptotic, anti-scarring, proangiogenic, and immunomodulatory factors involved in tissue regeneration (Caplan & Correa, 2011). In this context, the role of PMSCs might show a two-sideic property during the progression of liver fibrosis. *e.g.*, proangiogenic and fibrogenic characteristics of PMSCs, as a recent study showed that portal angiogenesis would attenuate liver fibrogenesis (M. Xu et al., 2019). Because of the “stemness” features of PMSCs, the differentiation status of PMSCs might be determined or changed by their environmental factors in the progression of liver fibrosis, which should be further investigated.

PART III:
CONCLUSIONS AND
PERSPECTIVES

Conclusions and perspectives

A better knowledge of the landscape of portal mesenchymal cells should help to understand better the potential functional roles of portal mesenchymal cells in physiological and pathophysiological conditions. In this thesis work, we provide a detailed atlas of portal mesenchymal cells in normal murine liver for the first time. Our scRNA-seq analysis revealed three populations of liver mesenchymal cells, *i.e.*, fibroblasts, VSMCs and HSCs, with distinct marker genes. It will be interesting to further validate the spatial localization of these markers for each cluster by immunohistochemistry or *in situ* hybridization to reconstruct the portal mesenchymal populations and their general spatial distributions. The main aim of this present work is to focus on the heterogeneity of portal mesenchymal cells in normal liver. It is of particular interest to investigate the reprogramming of portal mesenchymal cells in liver fibrosis and decode the cellular and molecular basis of fibrosis progression from the portal tract in diseased liver by scRNA-seq.

Notably, on this basis of scRNA-seq data, we identified a population of portal mesenchymal cells that displayed “stemness” functions. We further defined PDGFR α , CD34 and CD9 positivity, combined with CD200 mid-low expression (intermediate between negative and high), as the minimal set of markers required to isolate a cell population qualifying for MSCs (PMSCs), *i.e.*, with high clonogenic potential and the ability to undergo trilineage differentiation (chondrogenic, osteogenic and adipogenic), and the ability to differentiate into COL15A1-expressing myofibroblasts in culture. Interestingly, we found a three-dimensional spheroid culture model of PMSCs that better mimics the *in vivo* microarchitecture than plastic. This PMSC culture model provides a promising *in vitro* model that can be used in compound testing for liver fibrosis or evaluating the effect of profibrogenic or antifibrogenic factors on liver fibrosis *in vitro*. Combined with the data of ligand-receptor interaction networks from scRNA-seq in the future work, this PMSC spheroid culture model could also be applied in determining the interaction of PMSCs and PMSC-MFs with other cell types, *e.g.*, HSCs, cholangiocytes, endothelial cells, and macrophages, by using co-culture in spheroids.

The setting up of the method to isolate PMSC population allowed us to further determine the transcriptional profiles of PMSCs and PMSC-MFs in comparison with HSCs and HSC-MFs. Combined with the analysis of scRNA-seq and bulk-RNA-seq, we identified *Slit2* and a multigene transcriptomic signature (*Coll15a1*, *Coll1a2*, *Igfbp6*, *Loxl1*, *Meg3*, *Mgp*, *Thy1*, *Slit2*) as markers of PMSCs and derived myofibroblasts. We showed that PMSCs expanded in correlation with fibrogenesis and angiogenesis in different murine and human liver diseases by using these markers. We also designed a transcriptomic signature of HSCs (*Megf9*, *Plin2*, *Plac8*, *Nt5E*, *Bmp10*, *Hgf*, *Masp1*, *Rspo3*, *Scarb1*) that did not vary in these disorders. In conclusion, PMSCs are a small population of myofibroblast precursors that largely expand with the progression of liver fibrosis, and represent a potential therapeutic target.

In future work, *Slit2*, the marker of PMSCs, is the functional candidate we are going to test, which has been previously involved both in angiogenesis (Rama et al., 2015) and in liver fibrosis (J. Chang et al., 2015). *In vitro* experiments will rely on *Slit2* silencing in plastic or ULA spheroid culture models. For *in vivo* depletion of *Slit2* in mouse models of fibrosis, we will use intravenous injection of an adenovirus encoding ROBO1-Fc (Rama et al., 2015). We also have access to a *Slit2*lox mouse line (Rama et al., 2015), in which we can inject a Cre-encoding adenovirus before the induction or during the course of liver fibrosis.

Future work should also focus on revealing the unknown roles and mechanisms of PMSCs in different types and stages of liver fibrosis, *e.g.*, fibrogenesis, angiogenesis, inflammatory, and regeneration. Moreover, further data analysis will be applied to the data of bulk RNA-seq, in comparison with freshly isolated PMSCs and PMSCs cultured on plastic at early (PMSC-MFs-3d) and late stages (PMSC-MFs-7d) to gain insight into the mechanisms regulating the differentiation of PMSCs into PMSC-MFs.

LIST OF FIGURES AND TABLES

Figure 1: The hepatic lobule, a functional unit of the liver.....	5
Figure 2: Natural evolution of liver fibrosis.....	6
Figure 3: Localization of HSCs in the liver.....	13
Figure 4: HSC specific markers.....	15
Figure 5: Localization of portal fibroblasts and hepatic stellate cells in normal liver.....	17
Figure 6: Potential functions of portal fibroblasts.....	25
Figure 7: The differentiation potential of mesenchymal stem cells.....	28
Figure 8: Zonation of HSCs and LSECs across the liver sinusoid.....	37
Figure 9: The role of profibrogenic cells in liver angiogenesis in a cirrhotic liver.....	42
Table 1: The Metavir scoring system and fibrosis stage.....	7
Table 2: Tissue-resident mesenchymal cells source of myofibroblasts in multiple organs.....	11
Table 3: Localization of the main makers of PFs in liver.....	23
Table 4: Surface marker expression profile of MSCs in human and mouse.....	27
Table 5: Liver endothelial cell zonation and landmark genes.....	39

REFERENCES

- Abdel Aziz, M. T., Atta, H. M., Mahfouz, S., Fouad, H. H., Roshdy, N. K., Ahmed, H. H., et al. (2007). Therapeutic potential of bone marrow-derived mesenchymal stem cells on experimental liver fibrosis. *Clin Biochem*, 40(12), 893-899
- Aggarwal, S., Pittenger, M. F. (2005). Human mesenchymal stem cells modulate allogeneic immune cell responses. *Blood*, 105(4), 1815-1822
- Aird, W. C. (2007a). Phenotypic heterogeneity of the endothelium: I. Structure, function, and mechanisms. *Circ Res*, 100(2), 158-173
- Aird, W. C. (2007b). Phenotypic heterogeneity of the endothelium: II. Representative vascular beds. *Circ Res*, 100(2), 174-190
- Aizarani, N., Saviano, A., Sagar, M., Maily, L., Durand, S., Herman, J. S., et al. (2019). A human liver cell atlas reveals heterogeneity and epithelial progenitors. *Nature*, 572(7768), 199-204
- Aleffi, S., Petrai, I., Bertolani, C., Parola, M., Colombatto, S., Novo, E., et al. (2005). Upregulation of proinflammatory and proangiogenic cytokines by leptin in human hepatic stellate cells. *Hepatology*, 42(6), 1339-1348
- Ali, S. R., Ranjbarvaziri, S., Talkhabi, M., Zhao, P., Subat, A., Hojjat, A., et al. (2014). Developmental heterogeneity of cardiac fibroblasts does not predict pathological proliferation and activation. *Circ Res*, 115(7), 625-635
- Andrzejewska, A., Lukomska, B., Janowski, M. (2019). Concise Review: Mesenchymal Stem Cells: From Roots to Boost. *Stem Cells*, 37(7), 855-864
- Ankoma-Sey, V., Wang, Y., Dai, Z. (2000). Hypoxic stimulation of vascular endothelial growth factor expression in activated rat hepatic stellate cells. *Hepatology*, 31(1), 141-148
- Arthur, A., Rychkov, G., Shi, S., Koblar, S. A., Gronthos, S. (2008). Adult human dental pulp stem cells differentiate toward functionally active neurons under appropriate environmental cues. *Stem Cells*, 26(7), 1787-1795
- Asahina, K., Zhou, B., Pu, W. T., Tsukamoto, H. (2011). Septum transversum-derived mesothelium gives rise to hepatic stellate cells and perivascular mesenchymal cells in developing mouse liver. *Hepatology*, 53(3), 983-995
- Baba, S., Fujii, H., Hirose, T., Yasuchika, K., Azuma, H., Hoppo, T., et al. (2004). Commitment of bone marrow cells to hepatic stellate cells in mouse. *J Hepatol*, 40(2), 255-260
- Baddoo, M., Hill, K., Wilkinson, R., Gaupp, D., Hughes, C., Kopen, G. C., et al. (2003). Characterization of mesenchymal stem cells isolated from murine bone marrow by negative selection. *J Cell Biochem*, 89(6), 1235-1249

- Bartneck, M., Warzecha, K. T., Tag, C. G., Sauer-Lehnen, S., Heymann, F., Trautwein, C., et al. (2015). Isolation and time lapse microscopy of highly pure hepatic stellate cells. *Anal Cell Pathol (Amst)*, 2015, 417023
- Baruteau, J., Nyabi, O., Najimi, M., Fauvart, M., Sokal, E. (2014). Adult human liver mesenchymal progenitor cells express phenylalanine hydroxylase. *J Pediatr Endocrinol Metab*, 27(9-10), 863-868
- Bataller, R., Brenner, D. A. (2005). Liver fibrosis. *J Clin Invest*, 115(2), 209-218
- Bera, T. K., Pastan, I. (2000). Mesothelin is not required for normal mouse development or reproduction. *Mol Cell Biol*, 20(8), 2902-2906
- Berardis, S., Dwisthi Sattwika, P., Najimi, M., Sokal, E. M. (2015). Use of mesenchymal stem cells to treat liver fibrosis: current situation and future prospects. *World J Gastroenterol*, 21(3), 742-758
- Bianco, P., Cao, X., Frenette, P. S., Mao, J. J., Robey, P. G., Simmons, P. J., et al. (2013). The meaning, the sense and the significance: translating the science of mesenchymal stem cells into medicine. *Nat Med*, 19(1), 35-42
- Birbrair, A., Zhang, T., Wang, Z. M., Messi, M. L., Mintz, A., Delbono, O. (2013). Type-1 pericytes participate in fibrous tissue deposition in aged skeletal muscle. *Am J Physiol Cell Physiol*, 305(11), C1098-1113
- Bomzon, A., Huang, Y. T. (2001). Vascular smooth muscle cell signaling in cirrhosis and portal hypertension. *Pharmacol Ther*, 89(3), 255-272
- Bosch, J., Abraldes, J. G., Fernandez, M., Garcia-Pagan, J. C. (2010). Hepatic endothelial dysfunction and abnormal angiogenesis: new targets in the treatment of portal hypertension. *J Hepatol*, 53(3), 558-567
- Boxall, S. A., Jones, E. (2012). Markers for characterization of bone marrow multipotential stromal cells. *Stem Cells Int*, 2012, 975871
- Campana, L., Iredale, J. P. (2017). Regression of Liver Fibrosis. *Semin Liver Dis*, 37(1), 1-10
- Cannito, S., Paternostro, C., Busletta, C., Bocca, C., Colombatto, S., Miglietta, A., et al. (2014). Hypoxia, hypoxia-inducible factors and fibrogenesis in chronic liver diseases. *Histol Histopathol*, 29(1), 33-44
- Caplan, A. I., Correa, D. (2011). The MSC: an injury drugstore. *Cell Stem Cell*, 9(1), 11-15
- Caplan, A. I., Dennis, J. E. (2006). Mesenchymal stem cells as trophic mediators. *J Cell Biochem*, 98(5), 1076-1084
- Carlson, S., Trial, J., Soeller, C., Entman, M. L. (2011). Cardiac mesenchymal stem cells contribute to scar formation after myocardial infarction. *Cardiovasc Res*, 91(1), 99-107

- Cassiman, D., Libbrecht, L., Desmet, V., Deneff, C., Roskams, T. (2002). Hepatic stellate cell/myofibroblast subpopulations in fibrotic human and rat livers. *Journal of hepatology*, 36(2), 200-209
- Chang, J., Lan, T., Li, C., Ji, X., Zheng, L., Gou, H., et al. (2015). Activation of Slit2-Robo1 signaling promotes liver fibrosis. *J Hepatol*, 63(6), 1413-1420
- Chang, K., Pastan, I. (1996). Molecular cloning of mesothelin, a differentiation antigen present on mesothelium, mesotheliomas, and ovarian cancers. *Proc Natl Acad Sci U S A*, 93(1), 136-140
- Chang, Y. J., Liu, J. W., Lin, P. C., Sun, L. Y., Peng, C. W., Luo, G. H., et al. (2009). Mesenchymal stem cells facilitate recovery from chemically induced liver damage and decrease liver fibrosis. *Life Sci*, 85(13-14), 517-525
- Chen, L., Tredget, E. E., Wu, P. Y., Wu, Y. (2008). Paracrine factors of mesenchymal stem cells recruit macrophages and endothelial lineage cells and enhance wound healing. *PLoS One*, 3(4), e1886
- Chen, S. W., Zhang, X. R., Wang, C. Z., Chen, W. Z., Xie, W. F., Chen, Y. X. (2008). RNA interference targeting the platelet-derived growth factor receptor beta subunit ameliorates experimental hepatic fibrosis in rats. *Liver Int*, 28(10), 1446-1457
- Chi, J. T., Chang, H. Y., Haraldsen, G., Jahnsen, F. L., Troyanskaya, O. G., Chang, D. S., et al. (2003). Endothelial cell diversity revealed by global expression profiling. *Proc Natl Acad Sci U S A*, 100(19), 10623-10628
- Cho, K. A., Ju, S. Y., Cho, S. J., Jung, Y. J., Woo, S. Y., Seoh, J. Y., et al. (2009). Mesenchymal stem cells showed the highest potential for the regeneration of injured liver tissue compared with other subpopulations of the bone marrow. *Cell Biol Int*, 33(7), 772-777
- Choi, S. S., Diehl, A. M. (2009). Epithelial-to-mesenchymal transitions in the liver. *Hepatology*, 50(6), 2007-2013
- Chu, A. S., Diaz, R., Hui, J. J., Yanger, K., Zong, Y., Alpini, G., et al. (2011). Lineage tracing demonstrates no evidence of cholangiocyte epithelial-to-mesenchymal transition in murine models of hepatic fibrosis. *Hepatology*, 53(5), 1685-1695
- Clouston, A. D., Powell, E. E., Walsh, M. J., Richardson, M. M., Demetris, A. J., Jonsson, J. R. (2005). Fibrosis correlates with a ductular reaction in hepatitis C: roles of impaired replication, progenitor cells and steatosis. *Hepatology*, 41(4), 809-818
- Clouzeau-Girard, H., Guyot, C., Combe, C., Moronville-Halley, V., Housset, C., Lamireau, T., et al. (2006). Effects of bile acids on biliary epithelial cell proliferation and portal fibroblast activation using rat liver slices. *Lab Invest*, 86(3), 275-285
- Constandinou, C., Henderson, N., Iredale, J. P. (2005). Modeling liver fibrosis in rodents. *Methods Mol Med*, 117, 237-250

Copland, I., Sharma, K., Lejeune, L., Eliopoulos, N., Stewart, D., Liu, P., et al. (2008). CD34 expression on murine marrow-derived mesenchymal stromal cells: impact on neovascularization. *Exp Hematol*, 36(1), 93-103

Corpechot, C., Barbu, V., Wendum, D., Kinnman, N., Rey, C., Poupon, R., et al. (2002). Hypoxia-induced VEGF and collagen I expressions are associated with angiogenesis and fibrogenesis in experimental cirrhosis. *Hepatology*, 35(5), 1010-1021

Corselli, M., Chen, C. W., Sun, B., Yap, S., Rubin, J. P., Peault, B. (2012). The tunica adventitia of human arteries and veins as a source of mesenchymal stem cells. *Stem Cells Dev*, 21(8), 1299-1308

Coulon, S., Heindryckx, F., Geerts, A., Van Steenkiste, C., Colle, I., Van Vlierberghe, H. (2011). Angiogenesis in chronic liver disease and its complications. *Liver Int*, 31(2), 146-162

Crisan, M., Chen, C. W., Corselli, M., Andriolo, G., Lazzari, L., Peault, B. (2009). Perivascular multipotent progenitor cells in human organs. *Ann N Y Acad Sci*, 1176, 118-123

Crisan, M., Corselli, M., Chen, W. C., Peault, B. (2012). Perivascular cells for regenerative medicine. *J Cell Mol Med*, 16(12), 2851-2860

Crisan, M., Yap, S., Casteilla, L., Chen, C. W., Corselli, M., Park, T. S., et al. (2008). A perivascular origin for mesenchymal stem cells in multiple human organs. *Cell Stem Cell*, 3(3), 301-313

Csiszar, K. (2001). Lysyl oxidases: a novel multifunctional amine oxidase family. *Prog Nucleic Acid Res Mol Biol*, 70, 1-32

da Silva Meirelles, L., Chagastelles, P. C., Nardi, N. B. (2006). Mesenchymal stem cells reside in virtually all post-natal organs and tissues. *J Cell Sci*, 119(Pt 11), 2204-2213

Degott, C., Zafrani, E. S., Callard, P., Balkau, B., Poupon, R. E., Poupon, R. (1999). Histopathological study of primary biliary cirrhosis and the effect of ursodeoxycholic acid treatment on histology progression. *Hepatology*, 29(4), 1007-1012

DeLeve, L. D. (2015). Liver sinusoidal endothelial cells in hepatic fibrosis. *Hepatology*, 61(5), 1740-1746

DeLeve, L. D., Wang, X., Hu, L., McCuskey, M. K., McCuskey, R. S. (2004). Rat liver sinusoidal endothelial cell phenotype is maintained by paracrine and autocrine regulation. *Am J Physiol Gastrointest Liver Physiol*, 287(4), G757-763

Devine, S. M., Cobbs, C., Jennings, M., Bartholomew, A., Hoffman, R. (2003). Mesenchymal stem cells distribute to a wide range of tissues following systemic infusion into nonhuman primates. *Blood*, 101(8), 2999-3001

Dezso, K., Jelnes, P., Laszlo, V., Baghy, K., Bodor, C., Paku, S., et al. (2007). Thy-1 is expressed in hepatic myofibroblasts and not oval cells in stem cell-mediated liver regeneration. *Am J Pathol*, 171(5), 1529-1537

di Bonzo, L. V., Ferrero, I., Cravanzola, C., Mareschi, K., Rustichell, D., Novo, E., et al. (2008). Human mesenchymal stem cells as a two-edged sword in hepatic regenerative medicine: engraftment and hepatocyte differentiation versus profibrogenic potential. *Gut*, 57(2), 223-231

Di Carlo, S. E., Peduto, L. (2018). The perivascular origin of pathological fibroblasts. *J Clin Invest*, 128(1), 54-63

Ding, B. S., Cao, Z., Lis, R., Nolan, D. J., Guo, P., Simons, M., et al. (2014). Divergent angiocrine signals from vascular niche balance liver regeneration and fibrosis. *Nature*, 505(7481), 97-102

Dobie, R., Wilson-Kanamori, J. R., Henderson, B. E. P., Smith, J. R., Matchett, K. P., Portman, J. R., et al. (2019). Single-Cell Transcriptomics Uncovers Zonation of Function in the Mesenchyme during Liver Fibrosis. *Cell Rep*, 29(7), 1832-1847 e1838

Dominici, M., Le Blanc, K., Mueller, I., Slaper-Cortenbach, I., Marini, F., Krause, D., et al. (2006). Minimal criteria for defining multipotent mesenchymal stromal cells. The International Society for Cellular Therapy position statement. *Cytotherapy*, 8(4), 315-317

Dranoff, J. A., Kruglov, E. A., Robson, S. C., Braun, N., Zimmermann, H., Seigny, J. (2002). The ecto-nucleoside triphosphate diphosphohydrolase NTPDase2/CD39L1 is expressed in a novel functional compartment within the liver. *Hepatology*, 36(5), 1135-1144

Dranoff, J. A., Wells, R. G. (2010). Portal fibroblasts: Underappreciated mediators of biliary fibrosis. *Hepatology*, 51(4), 1438-1444

Dudas, J., Mansuroglu, T., Batusic, D., Ramadori, G. (2009a). Thy-1 is expressed in myofibroblasts but not found in hepatic stellate cells following liver injury. *Histochemistry and cell biology*, 131(1), 115-127

Dudas, J., Mansuroglu, T., Batusic, D., Ramadori, G. (2009b). Thy-1 is expressed in myofibroblasts but not found in hepatic stellate cells following liver injury. *Histochem Cell Biol*, 131(1), 115-127

Dudas, J., Mansuroglu, T., Batusic, D., Saile, B., Ramadori, G. (2007). Thy-1 is an in vivo and in vitro marker of liver myofibroblasts. *Cell Tissue Res*, 329(3), 503-514

Dulauroy, S., Di Carlo, S. E., Langa, F., Eberl, G., Peduto, L. (2012). Lineage tracing and genetic ablation of ADAM12(+) perivascular cells identify a major source of profibrotic cells during acute tissue injury. *Nat Med*, 18(8), 1262-1270

El-Kehdy, H., Pourcher, G., Zhang, W., Hamidouche, Z., Goulinet-Mainot, S., Sokal, E., et al. (2016). Hepatocytic Differentiation Potential of Human Fetal Liver Mesenchymal Stem Cells: In Vitro and In Vivo Evaluation. *Stem Cells Int*, 2016, 6323486

El Agha, E., Herold, S., Al Alam, D., Quantius, J., MacKenzie, B., Carraro, G., et al. (2014). Fgf10-positive cells represent a progenitor cell population during lung development and postnatally. *Development*, 141(2), 296-306

- El Agha, E., Kramann, R., Schneider, R. K., Li, X., Seeger, W., Humphreys, B. D., et al. (2017). Mesenchymal Stem Cells in Fibrotic Disease. *Cell Stem Cell*, 21(2), 166-177
- El Mourabit, H., Loeuillard, E., Lemoine, S., Cadoret, A., Housset, C. (2016). Culture Model of Rat Portal Myofibroblasts. *Front Physiol*, 7, 120
- Elpek, G. O. (2015). Angiogenesis and liver fibrosis. *World J Hepatol*, 7(3), 377-391
- Fabian, S. L., Penchev, R. R., St-Jacques, B., Rao, A. N., Sipila, P., West, K. A., et al. (2012). Hedgehog-Gli pathway activation during kidney fibrosis. *Am J Pathol*, 180(4), 1441-1453
- Fabris, L., Strazzabosco, M. (2011). Epithelial-mesenchymal interactions in biliary diseases. *Semin Liver Dis*, 31(1), 11-32
- Fang, B., Shi, M., Liao, L., Yang, S., Liu, Y., Zhao, R. C. (2004). Systemic infusion of FLK1(+) mesenchymal stem cells ameliorate carbon tetrachloride-induced liver fibrosis in mice. *Transplantation*, 78(1), 83-88
- Feldbrugge, L., Jiang, Z. G., Csizmadia, E., Mitsuhashi, S., Tran, S., Yee, E. U., et al. (2018). Distinct roles of ecto-nucleoside triphosphate diphosphohydrolase-2 (NTPDase2) in liver regeneration and fibrosis. *Purinergic Signal*, 14(1), 37-46
- Fernandez, M., Semela, D., Bruix, J., Colle, I., Pinzani, M., Bosch, J. (2009). Angiogenesis in liver disease. *J Hepatol*, 50(3), 604-620
- Fickert, P., Stöger, U., Fuchsbichler, A., Moustafa, T., Marschall, H.-U., Weiglein, A. H., et al. (2007). A new xenobiotic-induced mouse model of sclerosing cholangitis and biliary fibrosis. *The American journal of pathology*, 171(2), 525-536
- Forbes, S. J., Russo, F. P., Rey, V., Burra, P., Ruge, M., Wright, N. A., et al. (2004). A significant proportion of myofibroblasts are of bone marrow origin in human liver fibrosis. *Gastroenterology*, 126(4), 955-963
- Friedenstein, A. J., Deriglasova, U. F., Kulagina, N. N., Panasuk, A. F., Rudakowa, S. F., Luria, E. A., et al. (1974). Precursors for fibroblasts in different populations of hematopoietic cells as detected by the in vitro colony assay method. *Exp Hematol*, 2(2), 83-92
- Friedman, S. L. (2003). Liver fibrosis -- from bench to bedside. *J Hepatol*, 38 Suppl 1, S38-53
- Friedman, S. L. (2008). Hepatic stellate cells: protean, multifunctional, and enigmatic cells of the liver. *Physiol Rev*, 88(1), 125-172
- Friedman, S. L. (2008). Hepatic stellate cells: protean, multifunctional, and enigmatic cells of the liver. *Physiological reviews*, 88(1), 125-172
- Friedman, S. L., Roll, F. J. (1987). Isolation and culture of hepatic lipocytes, Kupffer cells, and sinusoidal endothelial cells by density gradient centrifugation with Stractan. *Analytical biochemistry*, 161(1), 207-218

- Friedman, S. L., Sheppard, D., Duffield, J. S., Violette, S. (2013). Therapy for fibrotic diseases: nearing the starting line. *Sci Transl Med*, 5(167), 167sr161
- Geerts, A. (2001). History, heterogeneity, developmental biology, and functions of quiescent hepatic stellate cells. *Semin Liver Dis*, 21(3), 311-335
- Gnecchi, M., Zhang, Z., Ni, A., Dzau, V. J. (2008). Paracrine mechanisms in adult stem cell signaling and therapy. *Circ Res*, 103(11), 1204-1219
- Gouw, A. S., Clouston, A. D., Theise, N. D. (2011). Ductular reactions in human liver: diversity at the interface. *Hepatology*, 54(5), 1853-1863
- Govindasamy, V., Ronald, V. S., Abdullah, A. N., Nathan, K. R., Ab Aziz, Z. A., Abdullah, M., et al. (2011). Differentiation of dental pulp stem cells into islet-like aggregates. *J Dent Res*, 90(5), 646-652
- Gronthos, S., Simmons, P., Graves, S., Robey, P. G. (2001). Integrin-mediated interactions between human bone marrow stromal precursor cells and the extracellular matrix. *Bone*, 28(2), 174-181
- Group, F. M. C. S., Bedossa, P. (1994). Intraobserver and interobserver variations in liver biopsy interpretation in patients with chronic hepatitis C. *Hepatology*, 20(1), 15-20
- Gupta, V., Gupta, I., Park, J., Bram, Y., Schwartz, R. E. (2020). Hedgehog Signaling Demarcates a Niche of Fibrogenic Peribiliary Mesenchymal Cells. *Gastroenterology*
- Halpern, K. B., Shenhav, R., Massalha, H., Toth, B., Egozi, A., Massasa, E. E., et al. (2018). Paired-cell sequencing enables spatial gene expression mapping of liver endothelial cells. *Nat Biotechnol*, 36(10), 962-970
- Hamik, A., Wang, B., Jain, M. K. (2006). Transcriptional regulators of angiogenesis. *Arterioscler Thromb Vasc Biol*, 26(9), 1936-1947
- Hammoutene, A., Rautou, P. E. (2019). Role of liver sinusoidal endothelial cells in non-alcoholic fatty liver disease. *J Hepatol*, 70(6), 1278-1291
- Han, Y., Li, X., Zhang, Y., Han, Y., Chang, F., Ding, J. (2019). Mesenchymal Stem Cells for Regenerative Medicine. *Cells*, 8(8)
- He, Y., Wu, Y. T., Huang, C., Meng, X. M., Ma, T. T., Wu, B. M., et al. (2014). Inhibitory effects of long noncoding RNA MEG3 on hepatic stellate cells activation and liver fibrogenesis. *Biochim Biophys Acta*, 1842(11), 2204-2215
- Higashi, T., Friedman, S. L., Hoshida, Y. (2017). Hepatic stellate cells as key target in liver fibrosis. *Adv Drug Deliv Rev*, 121, 27-42
- Higashiyama, R., Moro, T., Nakao, S., Mikami, K., Fukumitsu, H., Ueda, Y., et al. (2009). Negligible contribution of bone marrow-derived cells to collagen production during hepatic fibrogenesis in mice. *Gastroenterology*, 137(4), 1459-1466 e1451

- Hui, C. C., Angers, S. (2011). Gli proteins in development and disease. *Annu Rev Cell Dev Biol*, 27, 513-537
- Humphreys, B. D., Lin, S.-L., Kobayashi, A., Hudson, T. E., Nowlin, B. T., Bonventre, J. V., et al. (2010). Fate tracing reveals the pericyte and not epithelial origin of myofibroblasts in kidney fibrosis. *The American journal of pathology*, 176(1), 85-97
- Hung, C., Linn, G., Chow, Y. H., Kobayashi, A., Mittelsteadt, K., Altemeier, W. A., et al. (2013). Role of lung pericytes and resident fibroblasts in the pathogenesis of pulmonary fibrosis. *Am J Respir Crit Care Med*, 188(7), 820-830
- Ieronimakis, N., Hays, A. L., Janebodin, K., Mahoney, W. M., Jr., Duffield, J. S., Majesky, M. W., et al. (2013). Coronary adventitial cells are linked to perivascular cardiac fibrosis via TGFbeta1 signaling in the mdx mouse model of Duchenne muscular dystrophy. *J Mol Cell Cardiol*, 63, 122-134
- Inoue, Y., Iriyama, A., Ueno, S., Takahashi, H., Kondo, M., Tamaki, Y., et al. (2007). Subretinal transplantation of bone marrow mesenchymal stem cells delays retinal degeneration in the RCS rat model of retinal degeneration. *Exp Eye Res*, 85(2), 234-241
- Islam, S., Kjallquist, U., Moliner, A., Zajac, P., Fan, J. B., Lonnerberg, P., et al. (2011). Characterization of the single-cell transcriptional landscape by highly multiplex RNA-seq. *Genome Res*, 21(7), 1160-1167
- Iwaisako, K., Jiang, C., Zhang, M., Cong, M., Moore-Morris, T. J., Park, T. J., et al. (2014). Origin of myofibroblasts in the fibrotic liver in mice. *Proc Natl Acad Sci U S A*, 111(32), E3297-3305
- Iwakiri, Y. (2014). Pathophysiology of portal hypertension. *Clin Liver Dis*, 18(2), 281-291
- Iwakiri, Y., Grisham, M., Shah, V. (2008). Vascular biology and pathobiology of the liver: Report of a single-topic symposium. *Hepatology*, 47(5), 1754-1763
- Iwakiri, Y., Shah, V., Rockey, D. C. (2014). Vascular pathobiology in chronic liver disease and cirrhosis - current status and future directions. *J Hepatol*, 61(4), 912-924
- Iwayama, T., Steele, C., Yao, L., Dozmorov, M. G., Karamichos, D., Wren, J. D., et al. (2015). PDGFRalpha signaling drives adipose tissue fibrosis by targeting progenitor cell plasticity. *Genes Dev*, 29(11), 1106-1119
- Javazon, E. H., Beggs, K. J., Flake, A. W. (2004). Mesenchymal stem cells: paradoxes of passaging. *Exp Hematol*, 32(5), 414-425
- Jhandier, M. N., Kruglov, E. A., Lavoie, E. G., Sevigny, J., Dranoff, J. A. (2005). Portal fibroblasts regulate the proliferation of bile duct epithelia via expression of NTPDase2. *J Biol Chem*, 280(24), 22986-22992

- Ji, J., Eggert, T., Budhu, A., Forgues, M., Takai, A., Dang, H., et al. (2015). Hepatic stellate cell and monocyte interaction contributes to poor prognosis in hepatocellular carcinoma. *Hepatology*, 62(2), 481-495
- Ji, R., Zhang, N., You, N., Li, Q., Liu, W., Jiang, N., et al. (2012). The differentiation of MSCs into functional hepatocyte-like cells in a liver biomatrix scaffold and their transplantation into liver-fibrotic mice. *Biomaterials*, 33(35), 8995-9008
- Jiang, X. X., Zhang, Y., Liu, B., Zhang, S. X., Wu, Y., Yu, X. D., et al. (2005). Human mesenchymal stem cells inhibit differentiation and function of monocyte-derived dendritic cells. *Blood*, 105(10), 4120-4126
- Joe, A. W., Yi, L., Natarajan, A., Le Grand, F., So, L., Wang, J., et al. (2010). Muscle injury activates resident fibro/adipogenic progenitors that facilitate myogenesis. *Nat Cell Biol*, 12(2), 153-163
- Ju, C., Colgan, S. P., Eltzschig, H. K. (2016). Hypoxia-inducible factors as molecular targets for liver diseases. *J Mol Med (Berl)*, 94(6), 613-627
- Jung, K. H., Shin, H. P., Lee, S., Lim, Y. J., Hwang, S. H., Han, H., et al. (2009). Effect of human umbilical cord blood-derived mesenchymal stem cells in a cirrhotic rat model. *Liver Int*, 29(6), 898-909
- Juza, R. M., Pauli, E. M. (2014). Clinical and surgical anatomy of the liver: a review for clinicians. *Clin Anat*, 27(5), 764-769
- Kantari-Mimoun, C., Castells, M., Klose, R., Meinecke, A. K., Lemberger, U. J., Rautou, P. E., et al. (2015). Resolution of liver fibrosis requires myeloid cell-driven sinusoidal angiogenesis. *Hepatology*, 61(6), 2042-2055
- Karin, D., Koyama, Y., Brenner, D., Kisseleva, T. (2016). The characteristics of activated portal fibroblasts/myofibroblasts in liver fibrosis. *Differentiation*, 92(3), 84-92
- Karp, J. M., Leng Teo, G. S. (2009). Mesenchymal stem cell homing: the devil is in the details. *Cell Stem Cell*, 4(3), 206-216
- Katsumata, L. W., Miyajima, A., Itoh, T. (2017). Portal fibroblasts marked by the surface antigen Thy1 contribute to fibrosis in mouse models of cholestatic liver injury. *Hepatol Commun*, 1(3), 198-214
- Kawada, N. (2015). Cytoglobin as a Marker of Hepatic Stellate Cell-derived Myofibroblasts. *Front Physiol*, 6, 329
- Khuu, D. N., Nyabi, O., Maerckx, C., Sokal, E., Najimi, M. (2013). Adult human liver mesenchymal stem/progenitor cells participate in mouse liver regeneration after hepatectomy. *Cell Transplant*, 22(8), 1369-1380
- Kim, J., Braun, T. (2015). Targeting the cellular origin of organ fibrosis. *Cell Stem Cell*, 16(1), 3-4

Kinnman, N., Francoz, C., Barbu, V., Wendum, D., Rey, C., Hulcrantz, R., et al. (2003). The myofibroblastic conversion of peribiliary fibrogenic cells distinct from hepatic stellate cells is stimulated by platelet-derived growth factor during liver fibrogenesis. *Lab Invest*, 83(2), 163-173

Kinnman, N., Housset, C. (2002). Peribiliary myofibroblasts in biliary type liver fibrosis. *Front Biosci*, 7, d496-503

Kisseleva, T. (2017). The origin of fibrogenic myofibroblasts in fibrotic liver. *Hepatology*, 65(3), 1039-1043

Kisseleva, T., Brenner, D. A. (2006). Hepatic stellate cells and the reversal of fibrosis. *J Gastroenterol Hepatol*, 21 Suppl 3, S84-87

Kisseleva, T., Uchinami, H., Feirt, N., Quintana-Bustamante, O., Segovia, J. C., Schwabe, R. F., et al. (2006). Bone marrow-derived fibrocytes participate in pathogenesis of liver fibrosis. *J Hepatol*, 45(3), 429-438

Kivirikko, S., Heinamaki, P., Rehn, M., Honkanen, N., Myers, J. C., Pihlajaniemi, T. (1994). Primary structure of the alpha 1 chain of human type XV collagen and exon-intron organization in the 3' region of the corresponding gene. *J Biol Chem*, 269(7), 4773-4779

Klimczak, A., Kozłowska, U. (2016). Mesenchymal Stromal Cells and Tissue-Specific Progenitor Cells: Their Role in Tissue Homeostasis. *Stem Cells Int*, 2016, 4285215

Knittel, T., Kobold, D., Piscaglia, F., Saile, B., Neubauer, K., Mehde, M., et al. (1999). Localization of liver myofibroblasts and hepatic stellate cells in normal and diseased rat livers: distinct roles of (myo-)fibroblast subpopulations in hepatic tissue repair. *Histochemistry and cell biology*, 112(5), 387-401

Knittel, T., Kobold, D., Saile, B., Grundmann, A., Neubauer, K., Piscaglia, F., et al. (1999). Rat liver myofibroblasts and hepatic stellate cells: different cell populations of the fibroblast lineage with fibrogenic potential. *Gastroenterology*, 117(5), 1205-1221

Knittel, T., Kobold, D., Saile, B., Grundmann, A., Neubauer, K., Piscaglia, F., et al. (1999). Rat liver myofibroblasts and hepatic stellate cells: different cell populations of the fibroblast lineage with fibrogenic potential. *Gastroenterology*, 117(5), 1205-1221

Kordes, C., Sawitza, I., Gotze, S., Herebian, D., Haussinger, D. (2014). Hepatic stellate cells contribute to progenitor cells and liver regeneration. *J Clin Invest*, 124(12), 5503-5515

Kordes, C., Sawitza, I., Müller-Marbach, A., Ale-Agha, N., Keitel, V., Klonowski-Stumpe, H., et al. (2007). CD133+ hepatic stellate cells are progenitor cells. *Biochem Biophys Res Commun*, 352(2), 410-417

Koyama, Y., Wang, P., Liang, S., Iwaisako, K., Liu, X., Xu, J., et al. (2017). Mesothelin/mucin 16 signaling in activated portal fibroblasts regulates cholestatic liver fibrosis. *J Clin Invest*, 127(4), 1254-1270

Kramann, R., Schneider, R. K., DiRocco, D. P., Machado, F., Fleig, S., Bondzie, P. A., et al. (2015). Perivascular Gli1+ progenitors are key contributors to injury-induced organ fibrosis. *Cell Stem Cell*, 16(1), 51-66

Krampera, M., Glennie, S., Dyson, J., Scott, D., Laylor, R., Simpson, E., et al. (2003). Bone marrow mesenchymal stem cells inhibit the response of naive and memory antigen-specific T cells to their cognate peptide. *Blood*, 101(9), 3722-3729

Krempein, K., Grotkopp, D., Hall, K., Bache, A., Gillan, A., Rippe, R. A., et al. (1999). Far Upstream Regulatory Elements Enhance Position-Independent and Uterus-Specific Expression of the Murine $\alpha 1$ (1) Collagen Promoter in Transgenic Mice. *Gene Expression The Journal of Liver Research*, 8(3), 151-163

Krenkel, O., Hundertmark, J., Ritz, T. P., Weiskirchen, R., Tacke, F. (2019). Single Cell RNA Sequencing Identifies Subsets of Hepatic Stellate Cells and Myofibroblasts in Liver Fibrosis. *Cells*, 8(5)

Kruglov, E. A., Jain, D., Dranoff, J. A. (2002). Isolation of primary rat liver fibroblasts. *J Investig Med*, 50(3), 179-184

Kukla, M. (2013). Angiogenesis: a phenomenon which aggravates chronic liver disease progression. *Hepatol Int*, 7(1), 4-12

Kuo, T. K., Hung, S. P., Chuang, C. H., Chen, C. T., Shih, Y. R., Fang, S. C., et al. (2008). Stem cell therapy for liver disease: parameters governing the success of using bone marrow mesenchymal stem cells. *Gastroenterology*, 134(7), 2111-2121, 2121 e2111-2113

LaGory, E. L., Giaccia, A. J. (2016). The ever-expanding role of HIF in tumour and stromal biology. *Nat Cell Biol*, 18(4), 356-365

LeBleu, V. S., Taduri, G., O'Connell, J., Teng, Y., Cooke, V. G., Woda, C., et al. (2013). Origin and function of myofibroblasts in kidney fibrosis. *Nat Med*, 19(8), 1047-1053

Lee, J. S., Semela, D., Iredale, J., Shah, V. H. (2007). Sinusoidal remodeling and angiogenesis: a new function for the liver-specific pericyte? *Hepatology*, 45(3), 817-825

Lee, K. D., Kuo, T. K., Whang-Peng, J., Chung, Y. F., Lin, C. T., Chou, S. H., et al. (2004). In vitro hepatic differentiation of human mesenchymal stem cells. *Hepatology*, 40(6), 1275-1284

Lemoine, S., Cadoret, A., El Mourabit, H., Thabut, D., Housset, C. (2013). Origins and functions of liver myofibroblasts. *Biochim Biophys Acta*, 1832(7), 948-954

Lemoine, S., Cadoret, A., Rautou, P. E., El Mourabit, H., Ratziu, V., Corpechot, C., et al. (2015). Portal myofibroblasts promote vascular remodeling underlying cirrhosis formation through the release of microparticles. *Hepatology*, 61(3), 1041-1055

Lemoine, S., Thabut, D., Housset, C. (2016). Portal myofibroblasts connect angiogenesis and fibrosis in liver. *Cell Tissue Res*, 365(3), 583-589

Lemos, D. R., Babaeijandaghi, F., Low, M., Chang, C. K., Lee, S. T., Fiore, D., et al. (2015). Nilotinib reduces muscle fibrosis in chronic muscle injury by promoting TNF-mediated apoptosis of fibro/adipogenic progenitors. *Nat Med*, 21(7), 786-794

Lepreux, S., Desmouliere, A. (2015). Human liver myofibroblasts during development and diseases with a focus on portal (myo)fibroblasts. *Front Physiol*, 6, 173

Li, C., Kong, Y., Wang, H., Wang, S., Yu, H., Liu, X., et al. (2009). Homing of bone marrow mesenchymal stem cells mediated by sphingosine 1-phosphate contributes to liver fibrosis. *J Hepatol*, 50(6), 1174-1183

Li, H., Zhu, L., Chen, H., Li, T., Han, Q., Wang, S., et al. (2018). Generation of Functional Hepatocytes from Human Adipose-Derived MYC(+) KLF4(+) GMNN(+) Stem Cells Analyzed by Single-Cell RNA-Seq Profiling. *Stem Cells Transl Med*, 7(11), 792-805

Li, Q., Zhou, X., Shi, Y., Li, J., Zheng, L., Cui, L., et al. (2013). In vivo tracking and comparison of the therapeutic effects of MSCs and HSCs for liver injury. *PLoS One*, 8(4), e62363

Liedtke, C., Luedde, T., Sauerbruch, T., Scholten, D., Streetz, K., Tacke, F., et al. (2013). Experimental liver fibrosis research: update on animal models, legal issues and translational aspects. *Fibrogenesis Tissue Repair*, 6(1), 19

Lilly, M. A., Kulkulka, N. A., Firmiss, P. R., Ross, M. J., Flum, A. S., Santos, G. B., et al. (2015). The Murine Bladder Supports a Population of Stromal Sca-1+/CD34+/lin-Mesenchymal Stem Cells. *PLoS One*, 10(11), e0141437

Lin, S. L., Kisseleva, T., Brenner, D. A., Duffield, J. S. (2008). Pericytes and perivascular fibroblasts are the primary source of collagen-producing cells in obstructive fibrosis of the kidney. *Am J Pathol*, 173(6), 1617-1627

Liu, X., Xu, J., Rosenthal, S., Zhang, L. J., McCubbin, R., Meshgin, N., et al. (2020). Identification of Lineage-Specific Transcription Factors That Prevent Activation of Hepatic Stellate Cells and Promote Fibrosis Resolution. *Gastroenterology*

Loeuillard, E., El Mourabit, H., Lei, L., Lemoine, S., Housset, C., Cadoret, A. (2018). Endoplasmic reticulum stress induces inverse regulations of major functions in portal myofibroblasts during liver fibrosis progression. *Biochim Biophys Acta Mol Basis Dis*, 1864(12), 3688-3696

Lua, I., Asahina, K. (2016). The Role of Mesothelial Cells in Liver Development, Injury, and Regeneration. *Gut Liver*, 10(2), 166-176

Lua, I., Li, Y., Pappoe, L. S., Asahina, K. (2015). Myofibroblastic Conversion and Regeneration of Mesothelial Cells in Peritoneal and Liver Fibrosis. *Am J Pathol*, 185(12), 3258-3273

Lua, I., Li, Y., Zagory, J. A., Wang, K. S., French, S. W., Sevigny, J., et al. (2016a). Characterization of hepatic stellate cells, portal fibroblasts, and mesothelial cells in normal and fibrotic livers. *J Hepatol*, 64(5), 1137-1146

Lua, I., Li, Y., Zagory, J. A., Wang, K. S., French, S. W., Seigny, J., et al. (2016b). Characterization of hepatic stellate cells, portal fibroblasts, and mesothelial cells in normal and fibrotic livers. *Journal of hepatology*, 64(5), 1137-1146

Luedde, T., Kaplowitz, N., Schwabe, R. F. (2014). Cell death and cell death responses in liver disease: mechanisms and clinical relevance. *Gastroenterology*, 147(4), 765-783 e764

MacParland, S. A., Liu, J. C., Ma, X. Z., Innes, B. T., Bartczak, A. M., Gage, B. K., et al. (2018). Single cell RNA sequencing of human liver reveals distinct intrahepatic macrophage populations. *Nat Commun*, 9(1), 4383

Mannaerts, I., Leite, S. B., Verhulst, S., Claerhout, S., Eysackers, N., Thoen, L. F., et al. (2015). The Hippo pathway effector YAP controls mouse hepatic stellate cell activation. *J Hepatol*, 63(3), 679-688

Marcellin, P., Kutala, B. K. (2018). Liver diseases: A major, neglected global public health problem requiring urgent actions and large-scale screening. *Liver Int*, 38 Suppl 1, 2-6

Marrone, G., Russo, L., Rosado, E., Hide, D., Garcia-Cardena, G., Garcia-Pagan, J. C., et al. (2013). The transcription factor KLF2 mediates hepatic endothelial protection and paracrine endothelial-stellate cell deactivation induced by statins. *J Hepatol*, 58(1), 98-103

Martinez-Castillo, M., Rosique-Oramas, D., Medina-Avila, Z., Perez-Hernandez, J. L., Higuera-De la Tijera, F., Santana-Vargas, D., et al. (2020). Differential production of insulin-like growth factor-binding proteins in liver fibrosis progression. *Mol Cell Biochem*, 469(1-2), 65-75

Mattar, P., Bieback, K. (2015). Comparing the Immunomodulatory Properties of Bone Marrow, Adipose Tissue, and Birth-Associated Tissue Mesenchymal Stromal Cells. *Front Immunol*, 6, 560

Mauad, T. H., Van Nieuwkerk, C. M., Dingemans, K. P., Smit, J. J., Schinkel, A. H., Notenboom, R. G., et al. (1994). Mice with homozygous disruption of the *mdr2* P-glycoprotein gene a novel animal model for studies of nonsuppurative inflammatory cholangitis and hepatocarcinogenesis. *The American journal of pathology*, 145(5), 1237

Mederacke, I., Dapito, D. H., Affo, S., Uchinami, H., Schwabe, R. F. (2015). High-yield and high-purity isolation of hepatic stellate cells from normal and fibrotic mouse livers. *Nat Protoc*, 10(2), 305-315

Mederacke, I., Hsu, C. C., Troeger, J. S., Huebener, P., Mu, X., Dapito, D. H., et al. (2013). Fate tracing reveals hepatic stellate cells as dominant contributors to liver fibrosis independent of its aetiology. *Nat Commun*, 4, 2823

Medina, J., Arroyo, A. G., Sanchez-Madrid, F., Moreno-Otero, R. (2004). Angiogenesis in chronic inflammatory liver disease. *Hepatology*, 39(5), 1185-1195

Meirelles Lda, S., Fontes, A. M., Covas, D. T., Caplan, A. I. (2009). Mechanisms involved in the therapeutic properties of mesenchymal stem cells. *Cytokine Growth Factor Rev*, 20(5-6), 419-427

Mejias, M., Garcia-Pras, E., Tiani, C., Miquel, R., Bosch, J., Fernandez, M. (2009). Beneficial effects of sorafenib on splanchnic, intrahepatic, and portocollateral circulations in portal hypertensive and cirrhotic rats. *Hepatology*, 49(4), 1245-1256

Moore-Morris, T., Guimaraes-Camboa, N., Banerjee, I., Zambon, A. C., Kisseleva, T., Velayoudon, A., et al. (2014). Resident fibroblast lineages mediate pressure overload-induced cardiac fibrosis. *J Clin Invest*, 124(7), 2921-2934

Morita, S. Y., Tsuda, T., Horikami, M., Teraoka, R., Kitagawa, S., Terada, T. (2013). Bile salt-stimulated phospholipid efflux mediated by ABCB4 localized in nonraft membranes. *J Lipid Res*, 54(5), 1221-1230

Muhanna, N., Doron, S., Wald, O., Horani, A., Eid, A., Pappo, O., et al. (2008). Activation of hepatic stellate cells after phagocytosis of lymphocytes: A novel pathway of fibrogenesis. *Hepatology*, 48(3), 963-977

Muragaki, Y., Abe, N., Ninomiya, Y., Olsen, B. R., Ooshima, A. (1994). The human alpha 1(XV) collagen chain contains a large amino-terminal non-triple helical domain with a tandem repeat structure and homology to alpha 1(XVIII) collagen. *J Biol Chem*, 269(6), 4042-4046

Murfee, W. L., Skalak, T. C., Peirce, S. M. (2005). Differential arterial/venous expression of NG2 proteoglycan in perivascular cells along microvessels: identifying a venule-specific phenotype. *Microcirculation*, 12(2), 151-160

Myers, J. C., Kivirikko, S., Gordon, M. K., Dion, A. S., Pihlajaniemi, T. (1992). Identification of a previously unknown human collagen chain, alpha 1(XV), characterized by extensive interruptions in the triple-helical region. *Proc Natl Acad Sci U S A*, 89(21), 10144-10148

Nasir, G. A., Mohsin, S., Khan, M., Shams, S., Ali, G., Khan, S. N., et al. (2013). Mesenchymal stem cells and Interleukin-6 attenuate liver fibrosis in mice. *J Transl Med*, 11, 78

Nath, B., Szabo, G. (2012). Hypoxia and hypoxia inducible factors: diverse roles in liver diseases. *Hepatology*, 55(2), 622-633

Neuss, S., Schneider, R. K., Tietze, L., Knuchel, R., Jahnen-Dechent, W. (2010). Secretion of fibrinolytic enzymes facilitates human mesenchymal stem cell invasion into fibrin clots. *Cells Tissues Organs*, 191(1), 36-46

Newman, R. E., Yoo, D., LeRoux, M. A., Danilkovitch-Miagkova, A. (2009). Treatment of inflammatory diseases with mesenchymal stem cells. *Inflamm Allergy Drug Targets*, 8(2), 110-123

Nishio, T., Hu, R., Koyama, Y., Liang, S., Rosenthal, S. B., Yamamoto, G., et al. (2019). Activated hepatic stellate cells and portal fibroblasts contribute to cholestatic liver fibrosis in MDR2 knockout mice. *J Hepatol*, 71(3), 573-585

- Nobili, V., Carpino, G., Alisi, A., Franchitto, A., Alpini, G., De Vito, R., et al. (2012). Hepatic progenitor cells activation, fibrosis, and adipokines production in pediatric nonalcoholic fatty liver disease. *Hepatology*, 56(6), 2142-2153
- Nolan, D. J., Ginsberg, M., Israely, E., Palikuqi, B., Poulos, M. G., James, D., et al. (2013). Molecular signatures of tissue-specific microvascular endothelial cell heterogeneity in organ maintenance and regeneration. *Dev Cell*, 26(2), 204-219
- Nombela-Arrieta, C., Ritz, J., Silberstein, L. E. (2011). The elusive nature and function of mesenchymal stem cells. *Nat Rev Mol Cell Biol*, 12(2), 126-131
- Novo, E., Cannito, S., Zamara, E., Valfre di Bonzo, L., Caligiuri, A., Cravanzola, C., et al. (2007). Proangiogenic cytokines as hypoxia-dependent factors stimulating migration of human hepatic stellate cells. *Am J Pathol*, 170(6), 1942-1953
- Novo, E., di Bonzo, L. V., Cannito, S., Colombatto, S., Parola, M. (2009). Hepatic myofibroblasts: a heterogeneous population of multifunctional cells in liver fibrogenesis. *Int J Biochem Cell Biol*, 41(11), 2089-2093
- Okina, Y., Sato-Matsubara, M., Matsubara, T., Daikoku, A., Longato, L., Rombouts, K., et al. (2020). TGF-beta-driven reduction of cytoglobin leads to oxidative DNA damage in stellate cells during non-alcoholic steatohepatitis. *Journal of hepatology*
- Olaso, E., Salado, C., Egilegor, E., Gutierrez, V., Santisteban, A., Sancho-Bru, P., et al. (2003). Proangiogenic role of tumor-activated hepatic stellate cells in experimental melanoma metastasis. *Hepatology*, 37(3), 674-685
- Osterreicher, C. H., Penz-Osterreicher, M., Grivennikov, S. I., Guma, M., Koltsova, E. K., Datz, C., et al. (2011). Fibroblast-specific protein 1 identifies an inflammatory subpopulation of macrophages in the liver. *Proc Natl Acad Sci U S A*, 108(1), 308-313
- Pan, T. C., Sasaki, T., Zhang, R. Z., Fassler, R., Timpl, R., Chu, M. L. (1993). Structure and expression of fibulin-2, a novel extracellular matrix protein with multiple EGF-like repeats and consensus motifs for calcium binding. *J Cell Biol*, 123(5), 1269-1277
- Parekkadan, B., van Poll, D., Megeed, Z., Kobayashi, N., Tilles, A. W., Berthiaume, F., et al. (2007). Immunomodulation of activated hepatic stellate cells by mesenchymal stem cells. *Biochem Biophys Res Commun*, 363(2), 247-252
- Parekkadan, B., van Poll, D., Suganuma, K., Carter, E. A., Berthiaume, F., Tilles, A. W., et al. (2007). Mesenchymal stem cell-derived molecules reverse fulminant hepatic failure. *PLoS One*, 2(9), e941
- Park, S., Kim, J. W., Kim, J. H., Lim, C. W., Kim, B. (2015). Differential Roles of Angiogenesis in the Induction of Fibrogenesis and the Resolution of Fibrosis in Liver. *Biol Pharm Bull*, 38(7), 980-985
- Pastan, I., Hassan, R. (2014). Discovery of mesothelin and exploiting it as a target for immunotherapy. *Cancer Res*, 74(11), 2907-2912

Patel, S. A., Sherman, L., Munoz, J., Rameshwar, P. (2008). Immunological properties of mesenchymal stem cells and clinical implications. *Arch Immunol Ther Exp (Warsz)*, 56(1), 1-8

Paternostro, C., David, E., Novo, E., Parola, M. (2010). Hypoxia, angiogenesis and liver fibrogenesis in the progression of chronic liver diseases. *World J Gastroenterol*, 16(3), 281-288

Patsenker, E., Popov, Y., Stickel, F., Schneider, V., Ledermann, M., Sagesser, H., et al. (2009). Pharmacological inhibition of integrin α v β 3 aggravates experimental liver fibrosis and suppresses hepatic angiogenesis. *Hepatology*, 50(5), 1501-1511

Peister, A., Mellad, J. A., Larson, B. L., Hall, B. M., Gibson, L. F., Prockop, D. J. (2004). Adult stem cells from bone marrow (MSCs) isolated from different strains of inbred mice vary in surface epitopes, rates of proliferation, and differentiation potential. *Blood*, 103(5), 1662-1668

Pelekanos, R. A., Li, J., Gongora, M., Chandrakanthan, V., Scown, J., Suhaimi, N., et al. (2012). Comprehensive transcriptome and immunophenotype analysis of renal and cardiac MSC-like populations supports strong congruence with bone marrow MSC despite maintenance of distinct identities. *Stem Cell Res*, 8(1), 58-73

Pellicoro, A., Ramachandran, P., Iredale, J. P., Fallowfield, J. A. (2014). Liver fibrosis and repair: immune regulation of wound healing in a solid organ. *Nat Rev Immunol*, 14(3), 181-194

Phadnis, S. M., Joglekar, M. V., Dalvi, M. P., Muthyala, S., Nair, P. D., Ghaskadbi, S. M., et al. (2011). Human bone marrow-derived mesenchymal cells differentiate and mature into endocrine pancreatic lineage in vivo. *Cytotherapy*, 13(3), 279-293

Piscaglia, F., Dudas, J., Knittel, T., Di Rocco, P., Kobold, D., Saile, B., et al. (2009). Expression of ECM proteins fibulin-1 and -2 in acute and chronic liver disease and in cultured rat liver cells. *Cell Tissue Res*, 337(3), 449-462

Poisson, J., Lemoine, S., Boulanger, C., Durand, F., Moreau, R., Valla, D., et al. (2017). Liver sinusoidal endothelial cells: Physiology and role in liver diseases. *Journal of hepatology*, 66(1), 212-227

Rabani, V., Shahsavani, M., Gharavi, M., Piryaei, A., Azhdari, Z., Baharvand, H. (2010). Mesenchymal stem cell infusion therapy in a carbon tetrachloride-induced liver fibrosis model affects matrix metalloproteinase expression. *Cell Biol Int*, 34(6), 601-605

Rama, N., Dubrac, A., Mathivet, T., Ni Charthaigh, R. A., Genet, G., Cristofaro, B., et al. (2015). Slit2 signaling through Robo1 and Robo2 is required for retinal neovascularization. *Nat Med*, 21(5), 483-491

Ramachandran, P., Dobie, R., Wilson-Kanamori, J. R., Dora, E. F., Henderson, B. E. P., Luu, N. T., et al. (2019). Resolving the fibrotic niche of human liver cirrhosis at single-cell level. *Nature*, 575(7783), 512-518

Ramachandran, P., Matchett, K. P., Dobie, R., Wilson-Kanamori, J. R., Henderson, N. C. (2020). Single-cell technologies in hepatology: new insights into liver biology and disease pathogenesis. *Nat Rev Gastroenterol Hepatol*

Ramakrishnan, S., Anand, V., Roy, S. (2014). Vascular endothelial growth factor signaling in hypoxia and inflammation. *J Neuroimmune Pharmacol*, 9(2), 142-160

Rinkevich, Y., Mori, T., Sahoo, D., Xu, P. X., Bermingham, J. R., Jr., Weissman, I. L. (2012). Identification and prospective isolation of a mesothelial precursor lineage giving rise to smooth muscle cells and fibroblasts for mammalian internal organs, and their vasculature. *Nat Cell Biol*, 14(12), 1251-1260

Rosmorduc, O., Housset, C. (2010). Hypoxia: a link between fibrogenesis, angiogenesis, and carcinogenesis in liver disease. *Semin Liver Dis*, 30(3), 258-270

Rosmorduc, O., Wendum, D., Corpechot, C., Galy, B., Sebbagh, N., Raleigh, J., et al. (1999). Hepatocellular hypoxia-induced vascular endothelial growth factor expression and angiogenesis in experimental biliary cirrhosis. *Am J Pathol*, 155(4), 1065-1073

Russo, F. P., Alison, M. R., Bigger, B. W., Amofah, E., Florou, A., Amin, F., et al. (2006). The bone marrow functionally contributes to liver fibrosis. *Gastroenterology*, 130(6), 1807-1821

Sawada, H., Rateri, D. L., Moorleggen, J. J., Majesky, M. W., Daugherty, A. (2017). Smooth Muscle Cells Derived From Second Heart Field and Cardiac Neural Crest Reside in Spatially Distinct Domains in the Media of the Ascending Aorta-Brief Report. *Arterioscler Thromb Vasc Biol*, 37(9), 1722-1726

Schepers, K., Pietras, E. M., Reynaud, D., Flach, J., Binnewies, M., Garg, T., et al. (2013). Myeloproliferative neoplasia remodels the endosteal bone marrow niche into a self-reinforcing leukemic niche. *Cell Stem Cell*, 13(3), 285-299

Scholten, D., Osterreicher, C. H., Scholten, A., Iwaisako, K., Gu, G., Brenner, D. A., et al. (2010). Genetic labeling does not detect epithelial-to-mesenchymal transition of cholangiocytes in liver fibrosis in mice. *Gastroenterology*, 139(3), 987-998

Seki, E., Schwabe, R. F. (2015). Hepatic inflammation and fibrosis: functional links and key pathways. *Hepatology*, 61(3), 1066-1079

Semela, D., Das, A., Langer, D., Kang, N., Leof, E., Shah, V. (2008). Platelet-derived growth factor signaling through ephrin-b2 regulates hepatic vascular structure and function. *Gastroenterology*, 135(2), 671-679

Shi, Y., Hu, G., Su, J., Li, W., Chen, Q., Shou, P., et al. (2010). Mesenchymal stem cells: a new strategy for immunosuppression and tissue repair. *Cell Res*, 20(5), 510-518

Shim, K. Y., Eom, Y. W., Kim, M. Y., Kang, S. H., Baik, S. K. (2018). Role of the renin-angiotensin system in hepatic fibrosis and portal hypertension. *Korean J Intern Med*, 33(3), 453-461

Shin, D. H., Dier, U., Melendez, J. A., Hempel, N. (2015). Regulation of MMP-1 expression in response to hypoxia is dependent on the intracellular redox status of metastatic bladder cancer cells. *Biochim Biophys Acta*, 1852(12), 2593-2602

Sims, D. E. (1986). The pericyte--a review. *Tissue Cell*, 18(2), 153-174

Strauss, O., Phillips, A., Ruggiero, K., Bartlett, A., Dunbar, P. R. (2017). Immunofluorescence identifies distinct subsets of endothelial cells in the human liver. *Sci Rep*, 7, 44356

Su, T., Yang, Y., Lai, S., Jeong, J., Jung, Y., McConnell, M., et al. (2020). Single-cell transcriptomics reveals zone-specific alterations of liver sinusoidal endothelial cells in cirrhosis. *bioRxiv*

Tabula Muris, C., Overall, c., Logistical, c., Organ, c., processing, Library, p., et al. (2018). Single-cell transcriptomics of 20 mouse organs creates a Tabula Muris. *Nature*, 562(7727), 367-372

Takase, H. M., Itoh, T., Ino, S., Wang, T., Koji, T., Akira, S., et al. (2013). FGF7 is a functional niche signal required for stimulation of adult liver progenitor cells that support liver regeneration. *Genes Dev*, 27(2), 169-181

Tang, F., Barbacioru, C., Wang, Y., Nordman, E., Lee, C., Xu, N., et al. (2009). mRNA-Seq whole-transcriptome analysis of a single cell. *Nat Methods*, 6(5), 377-382

Tanimoto, H., Terai, S., Taro, T., Murata, Y., Fujisawa, K., Yamamoto, N., et al. (2013). Improvement of liver fibrosis by infusion of cultured cells derived from human bone marrow. *Cell Tissue Res*, 354(3), 717-728

Tateaki, Y., Ogawa, T., Kawada, N., Kohashi, T., Arihiro, K., Tateno, C., et al. (2004). Typing of hepatic nonparenchymal cells using fibulin-2 and cytoglobin/STAP as liver fibrogenesis-related markers. *Histochem Cell Biol*, 122(1), 41-49

Thabut, D., Routray, C., Lomberk, G., Shergill, U., Glaser, K., Huebert, R., et al. (2011). Complementary vascular and matrix regulatory pathways underlie the beneficial mechanism of action of sorafenib in liver fibrosis. *Hepatology*, 54(2), 573-585

Tsuda, T., Wang, H., Timpl, R., Chu, M. L. (2001). Fibulin-2 expression marks transformed mesenchymal cells in developing cardiac valves, aortic arch vessels, and coronary vessels. *Dev Dyn*, 222(1), 89-100

Tzaribachev, N., Vaegler, M., Schaefer, J., Reize, P., Rudert, M., Handgretinger, R., et al. (2008). Mesenchymal stromal cells: a novel treatment option for steroid-induced avascular osteonecrosis. *Isr Med Assoc J*, 10(3), 232-234

Ubil, E., Duan, J., Pillai, I. C., Rosa-Garrido, M., Wu, Y., Bargiacchi, F., et al. (2014). Mesenchymal-endothelial transition contributes to cardiac neovascularization. *Nature*, 514(7524), 585-590

- Uccelli, A., Moretta, L., Pistoia, V. (2008). Mesenchymal stem cells in health and disease. *Nat Rev Immunol*, 8(9), 726-736
- Valfre di Bonzo, L., Novo, E., Cannito, S., Busletta, C., Paternostro, C., Povero, D., et al. (2009). Angiogenesis and liver fibrogenesis. *Histol Histopathol*, 24(10), 1323-1341
- van Poll, D., Parekkadan, B., Cho, C. H., Berthiaume, F., Nahmias, Y., Tilles, A. W., et al. (2008). Mesenchymal stem cell-derived molecules directly modulate hepatocellular death and regeneration in vitro and in vivo. *Hepatology*, 47(5), 1634-1643
- Wakabayashi, T., Naito, H., Suehiro, J. I., Lin, Y., Kawaji, H., Iba, T., et al. (2018). CD157 Marks Tissue-Resident Endothelial Stem Cells with Homeostatic and Regenerative Properties. *Cell Stem Cell*, 22(3), 384-397 e386
- Walter, T. J., Cast, A. E., Huppert, K. A., Huppert, S. S. (2014). Epithelial VEGF signaling is required in the mouse liver for proper sinusoid endothelial cell identity and hepatocyte zonation in vivo. *Am J Physiol Gastrointest Liver Physiol*, 306(10), G849-862
- Wang, B., Xiao, Y., Ding, B. B., Zhang, N., Yuan, X., Gui, L., et al. (2003). Induction of tumor angiogenesis by Slit-Robo signaling and inhibition of cancer growth by blocking Robo activity. *Cancer Cell*, 4(1), 19-29
- Wang, Y., Lian, F., Li, J., Fan, W., Xu, H., Yang, X., et al. (2012). Adipose derived mesenchymal stem cells transplantation via portal vein improves microcirculation and ameliorates liver fibrosis induced by CCl₄ in rats. *J Transl Med*, 10, 133
- Wang, Y. Q., Luk, J. M., Ikeda, K., Man, K., Chu, A. C., Kaneda, K., et al. (2004). Regulatory role of vHL/HIF-1 α in hypoxia-induced VEGF production in hepatic stellate cells. *Biochem Biophys Res Commun*, 317(2), 358-362
- Wells, R. G. (2014). The portal fibroblast: not just a poor man's stellate cell. *Gastroenterology*, 147(1), 41-47
- Wells, R. G., Kruglov, E., Dranoff, J. A. (2004). Autocrine release of TGF- β by portal fibroblasts regulates cell growth. *FEBS Lett*, 559(1-3), 107-110
- Wen, J. W., Olsen, A. L., Perepelyuk, M., Wells, R. G. (2012). Isolation of rat portal fibroblasts by in situ liver perfusion. *J Vis Exp*(64)
- Witek, R. P., Yang, L., Liu, R., Jung, Y., Omenetti, A., Syn, W. K., et al. (2009). Liver cell-derived microparticles activate hedgehog signaling and alter gene expression in hepatic endothelial cells. *Gastroenterology*, 136(1), 320-330 e322
- Xiong, X., Kuang, H., Ansari, S., Liu, T., Gong, J., Wang, S., et al. (2019). Landscape of Intercellular Crosstalk in Healthy and NASH Liver Revealed by Single-Cell Secretome Gene Analysis. *Mol Cell*, 75(3), 644-660 e645
- Xu, J., Kisseleva, T. (2015). Bone marrow-derived fibrocytes contribute to liver fibrosis. *Exp Biol Med (Maywood)*, 240(6), 691-700

Xu, J., Liu, X., Koyama, Y., Wang, P., Lan, T., Kim, I. G., et al. (2014). The types of hepatic myofibroblasts contributing to liver fibrosis of different etiologies. *Front Pharmacol*, 5, 167

Xu, M., Xu, H. H., Lin, Y., Sun, X., Wang, L. J., Fang, Z. P., et al. (2019). LECT2, a Ligand for Tie1, Plays a Crucial Role in Liver Fibrogenesis. *Cell*, 178(6), 1478-1492 e1420

Xu, W., Zhang, X., Qian, H., Zhu, W., Sun, X., Hu, J., et al. (2004). Mesenchymal stem cells from adult human bone marrow differentiate into a cardiomyocyte phenotype in vitro. *Exp Biol Med (Maywood)*, 229(7), 623-631

Yoshiji, H., Kuriyama, S., Yoshii, J., Ikenaka, Y., Noguchi, R., Hicklin, D. J., et al. (2003). Vascular endothelial growth factor and receptor interaction is a prerequisite for murine hepatic fibrogenesis. *Gut*, 52(9), 1347-1354

Yu, F., Geng, W., Dong, P., Huang, Z., Zheng, J. (2018). LncRNA-MEG3 inhibits activation of hepatic stellate cells through SMO protein and miR-212. *Cell Death Dis*, 9(10), 1014

Zadorozhna, M., Di Gioia, S., Conese, M., Mangieri, D. (2020). Neovascularization is a key feature of liver fibrosis progression: anti-angiogenesis as an innovative way of liver fibrosis treatment. *Mol Biol Rep*, 47(3), 2279-2288

Zeng, X., Huang, P., Chen, M., Liu, S., Wu, N., Wang, F., et al. (2018). TMEM16A regulates portal vein smooth muscle cell proliferation in portal hypertension. *Exp Ther Med*, 15(1), 1062-1068

Zhang, D. Y., Goossens, N., Guo, J., Tsai, M. C., Chou, H. I., Altunkaynak, C., et al. (2016). A hepatic stellate cell gene expression signature associated with outcomes in hepatitis C cirrhosis and hepatocellular carcinoma after curative resection. *Gut*, 65(10), 1754-1764

Zhang, L., Yang, Z., Trottier, J., Barbier, O., Wang, L. (2017). Long noncoding RNA MEG3 induces cholestatic liver injury by interaction with PTBP1 to facilitate shp mRNA decay. *Hepatology*, 65(2), 604-615

Zhang, Z., Zhang, F., Lu, Y., Zheng, S. (2015). Update on implications and mechanisms of angiogenesis in liver fibrosis. *Hepatol Res*, 45(2), 162-178

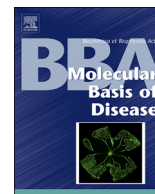
Zhao, D. C., Lei, J. X., Chen, R., Yu, W. H., Zhang, X. M., Li, S. N., et al. (2005). Bone marrow-derived mesenchymal stem cells protect against experimental liver fibrosis in rats. *World J Gastroenterol*, 11(22), 3431-3440

Zhao, H., Feng, J., Seidel, K., Shi, S., Klein, O., Sharpe, P., et al. (2014). Secretion of shh by a neurovascular bundle niche supports mesenchymal stem cell homeostasis in the adult mouse incisor. *Cell Stem Cell*, 14(2), 160-173

Zhao, W., Yang, A., Chen, W., Wang, P., Liu, T., Cong, M., et al. (2018). Inhibition of lysyl oxidase-like 1 (LOXL1) expression arrests liver fibrosis progression in cirrhosis by reducing elastin crosslinking. *Biochim Biophys Acta Mol Basis Dis*, 1864(4 Pt A), 1129-1137

ANNEXES

Loeuillard, E., El Mourabit, H., Lei, L., Lemoinne, S., Housset, C., & Cadoret, A. (2018). Endoplasmic reticulum stress induces inverse regulations of major functions in portal myofibroblasts during liver fibrosis progression. *Biochimica et Biophysica Acta (BBA)-Molecular Basis of Disease*, 1864(12), 3688-3696.



Endoplasmic reticulum stress induces inverse regulations of major functions in portal myofibroblasts during liver fibrosis progression



Emilien Loeuillard^{a,1}, Haquima El Mourabit^a, Lin Lei^a, Sara Lemoine^{a,b}, Chantal Housset^{a,b,*}, Axelle Cadoret^a

^a Sorbonne Université, INSERM, Saint-Antoine Research Center (CRSA), Institute of Cardiometabolism and Nutrition (ICAN), Paris, France

^b Assistance Publique-Hôpitaux de Paris, Hôpital Saint-Antoine, Hepatology Department, Reference Center for Inflammatory Biliary Diseases and Autoimmune Hepatitis, Paris, France

ARTICLE INFO

Keywords:

Liver fibrosis
Angiogenesis
Bile duct ligation
PKR-like endoplasmic reticulum kinase (PERK)
Unfolded protein response (UPR)

ABSTRACT

Portal myofibroblasts (PMF) form a sub-population of highly proliferative and proangiogenic liver myofibroblasts that derive from portal mesenchymal progenitors. Endoplasmic reticulum (ER) stress was previously shown to modulate fibrogenesis, notably in the liver. Our aim was to determine if ER stress occurred in PMF and affected their functions. PMF were obtained after their expansion *in vivo* from bile duct-ligated (BDL) rats and referred to as BDL PMF. Compared to standard PMF obtained from normal rats, BDL PMF were more myofibroblastic, as assessed by higher alpha-smooth muscle actin expression and collagen 1 production. Their proangiogenic properties were also higher, whereas their proliferative and migratory capacities were lower. CHOP expression was detected in the liver of BDL rats, at the leading edge of portal fibrosis where PMF accumulate. BDL PMF displayed ER dilatation and an overexpression of the PERK pathway downstream targets, *Chop*, *Gadd34* and *Trb3*, in comparison with standard PMF. *In vitro*, the induction of ER stress by tunicamycin in standard PMF, caused a decrease in their proliferative and migratory activity, and an increase in their proangiogenic activity, without affecting their myofibroblastic differentiation. Conversely, the treatment of BDL PMF with the PERK inhibitor GSK2656157 reduced ER stress, which caused a decrease in their angiogenic properties, and restored their proliferative and migratory capacity. In conclusion, PMF develop ER stress as they expand with the progression of fibrosis, which further increases their proangiogenic activity, but also inhibits their proliferation and migration. This phenotypic switch may restrict PMF expansion while they support angiogenesis.

1. Introduction

Myofibroblasts are matrix-producing cells that arise in fibrotic diseases. They have different possible origins and serve a wide range of functions related to wound healing. Alpha-smooth muscle actin (α -SMA) is their most commonly used marker [1]. In the liver, hepatic stellate cells (HSC) are the major but not exclusive source of myofibroblasts [2]. Portal myofibroblasts (PMF) form a distinct population of

liver myofibroblasts that derive from portal mesenchymal cells [3–7]. While PMF contribute to the progression of liver fibrosis in all types of liver diseases [8], they are the major population of myofibroblasts that accumulate at early stages of cholestatic liver injury [3,4,6,9,10]. We previously showed that PMF were highly proliferative, as opposed to HSC-derived myofibroblasts [11]. We also showed that they were key cells in angiogenesis, a mechanism which drives the progression of liver fibrosis from portal tracts into the parenchyma [8,12].

Abbreviations: α -SMA, alpha-smooth muscle actin; ATF6, activating transcription factor 6; BDL, bile duct ligation; BSA, bovine serum albumin; CHOP, CCAAT-enhancer-binding protein homologous protein; CM, conditioned medium; COL1a1, collagen, type 1, alpha 1; DMSO, dimethyl sulfoxide; ER, endoplasmic reticulum; FBS, fetal bovine serum; FGF2, fibroblast growth factor-2; GADD34, growth arrest and DNA damage-inducible protein 34; HPRT, hypoxanthine phosphoribosyl transferase; HSC, hepatic stellate cell; IRE1, inositol-requiring enzyme 1; MCP-1, monocyte chemoattractant protein-1; NAFLD, non-alcoholic fatty liver disease; PDGF-BB, platelet-derived growth factor-BB; PERK, PKR-like endoplasmic reticulum kinase; PMF, portal myofibroblast; RT-qPCR, Reverse transcription-quantitative polymerase chain reaction; TM, tunicamycin; UPR, unfolded protein response; VEGF, vascular endothelial growth factor; vWF, von Willebrand factor

* Corresponding author at: Faculté de Médecine Sorbonne Université, Site Saint-Antoine, 27 rue Chaligny, 75571 Paris cedex 12, France.

E-mail addresses: loeuillard.emilien@mayo.edu (E. Loeuillard), haquima.el-mourabit@inserm.fr (H. El Mourabit), lin.lei@inserm.fr (L. Lei), chantal.housset@inserm.fr (C. Housset), axelle.cadoret@inserm.fr (A. Cadoret).

¹ Present address: Division of Gastroenterology and Hepatology, Mayo Clinic, Rochester, Minnesota 55905, USA.

<https://doi.org/10.1016/j.bbadis.2018.10.008>

Received 22 June 2018; Received in revised form 27 September 2018; Accepted 2 October 2018

Available online 04 October 2018

0925-4439/ © 2018 Elsevier B.V. All rights reserved.

Mounting evidence indicates that endoplasmic reticulum (ER) stress is associated with the development and progression of fibrotic diseases [13–16]. Under stress conditions, the ER initiates the unfolded protein response (UPR) to restore homeostasis. The UPR is mediated by three ER transmembrane sensors: the inositol-requiring enzyme 1 (IRE1), the activating transcription factor 6 (ATF6) and the PERK-like endoplasmic reticulum kinase (PERK). Each pathway culminates to promote the expression of genes required to reestablish ER homeostasis, through i) translational attenuation of global protein synthesis and ii) protein degradation. The PERK pathway plays a major role in reducing translation rates via the phosphorylation of eIF2 α . Phosphorylated eIF2 α also promotes the preferential translation of the transcription factor ATF4, which in turn induces the up-regulation of CCAAT-enhancer-binding protein homologous protein (CHOP) and growth arrest and DNA damage-inducible protein 34 (GADD34) genes. Ultimately, this response allows to counteract stress or direct cell fate towards apoptosis. When UPR fails to adapt, ER stress triggers a pathological response.

Previous work provided evidence to indicate that ER stress can occur in HSC and thereby promote liver fibrosis. Thus, it was shown in mouse models of liver fibrosis caused by ethanol or carbon tetrachloride, that ER stress developed in HSC and triggered their fibrogenic activity [15,17]. Blockade of the IRE1 pathway decreased HSC fibrogenic activity [17], whereas the chemical induction of ER stress, by tunicamycin (TM) or thapsigargin in HSC, caused an up-regulation of fibrogenic genes [15,18]. On the other hand, ER stress could also promote HSC apoptosis and thereby contribute to the resolution of fibrosis. Thus, cannabidiol was shown to cause the death of myofibroblastic HSC by a mechanism of ER stress-induced apoptosis [19]. It has also been possible to trigger ER stress-induced apoptosis and thereby reduce collagen synthesis, by overexpressing the matricellular protein CCN1 in HSC [20].

As compared with HSC-derived myofibroblasts, PMF display a number of distinct phenotypic features [8,21]. They also accumulate with a different spatial and temporal pattern during the progression of liver fibrosis [6,7]. While the mechanisms regulating the phenotypic changes of HSC during fibrogenesis have been largely unraveled [2], those underlying the phenotypic changes of PMF are still poorly known. In the present study, we investigated PMF phenotype following their expansion *in vivo*, with particular attention to ER stress. We determined if PMF developed ER stress as they accumulated in the fibrotic liver and if this impacted their functions.

2. Materials and methods

2.1. Animals

Male Sprague Dawley rats weighing 200–250 g were purchased from Janvier Labs, Le Genest-Saint-Isle, France. Bile duct ligation (BDL) and sham operation were performed as previously described [4]. All procedures were approved by the Charles Darwin Ethical Committee for Animal Studies (Approval N°01163 01), and by the Institutional Animal Care and Use Department (DSV, Paris, Agreement N°75-12-01).

2.2. Cell models

PMF were obtained from normal or 2-week BDL rats, following an established protocol [11] and were referred to as standard and BDL PMF, respectively. Standard and BDL PMF were first compared in primary culture (P0). Subsequently, standard PMF were equally used at P0 or after one passage (P1), as their phenotype at P0 and P1 was previously shown to be the same [11]. When indicated, PMF were incubated with 1 μ mol/L of TM (Merck, Fontenay sous Bois, France) to induce ER stress or with 1 μ mol/L of the PERK inhibitor GSK2656157 (Merck, Darmstadt, Germany), for 24 h. Control cells were incubated with vehicle, *i.e.* dimethyl sulfoxide (DMSO, 1/1000). Conditioned

media (CM) were obtained from PMF incubated with serum-free or 10% fetal bovine serum (FBS)-containing medium, for 24 h.

2.3. (Immuno)staining

Paraffin-embedded formalin-fixed 4- μ m-thick liver tissue sections were subjected to Sirius red staining or immunostaining, using anti- α -SMA (#M0851; Dako, Les Ulis, France), anti-von Willebrand factor (vWF) (#GTx60934; Clinisciences, Nanterre, France) or anti-CHOP (#ab11419; Abcam, Paris, France), as primary antibodies, horseradish peroxidase-conjugated antibodies (Vector laboratories, Peterborough, UK), as secondary antibodies and 3-amino-9-ethylcarbazole (Vector laboratories) as a substrate. Tissue sections were counterstained with Mayer's hematoxylin. For immunofluorescence, cell preparations were fixed in 4% paraformaldehyde and incubated with primary antibodies against Calreticulin (#sc11398; Santa Cruz Biotechnology, Dallas, TX, USA) or α -SMA (#M0851; Dako). Nuclear staining was performed using Draq5 (Ozyme, Saint-Quentin-en-Yvelines, France). Cells were examined with a SP2 confocal microscope (Leica, Bannockburn, IL, USA).

2.4. Transmission electron microscopy

Cells were fixed with 2% glutaraldehyde in 0.1 mol/L sodium cacodylate buffer (pH 7.4) for 30 min at 4 °C and post-fixed with 1% osmium tetroxide in the same buffer for 30 min at 4 °C. Samples were then dehydrated and embedded in epoxy resin. Ultra-thin (60 nm) sections were contrast-enhanced using uranyl acetate and lead citrate and examined using a JEOL 1010 electron microscope with a MegaView III camera.

2.5. Reverse transcription-quantitative polymerase chain reaction (RT-qPCR)

The cDNA obtained from total RNA was subjected to quantitative real-time PCR using the Sybr Green Master Mix (Roche Diagnostics, Meylan, France) on a Lightcycler 96 device (Roche Diagnostics). Primer sequences are provided in Supplementary Table 1. Target gene mRNA levels are reported relative to a calibrator according to the $2^{-\Delta\Delta CT}$ method, using hypoxanthine phosphoribosyl transferase (HPRT) as a reference gene, the expression of which was stable in ER stress condition.

2.6. Immunoblotting

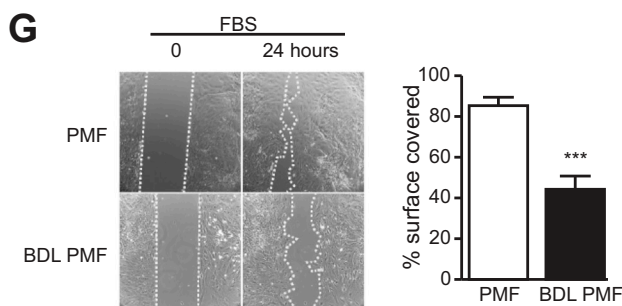
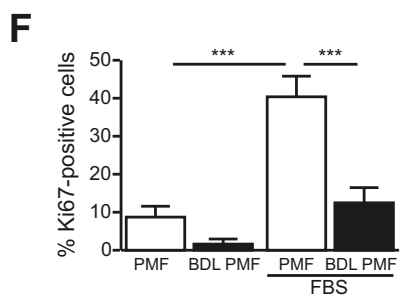
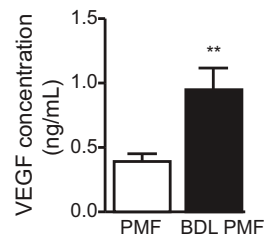
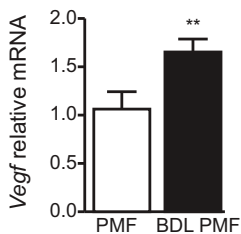
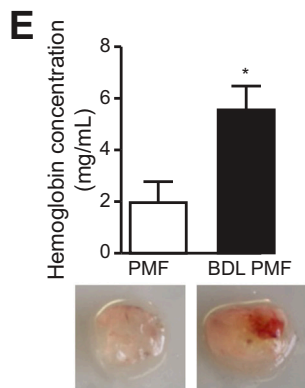
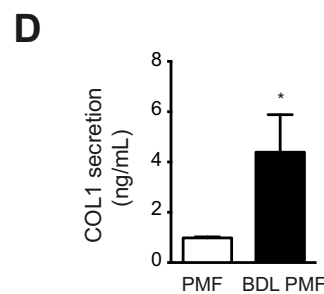
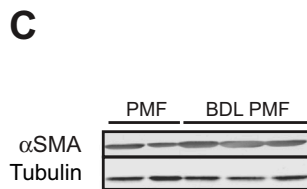
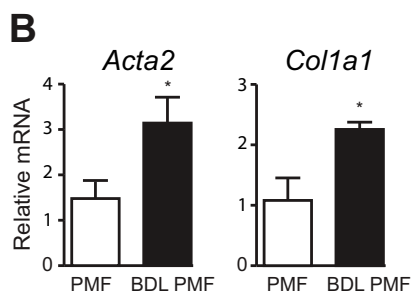
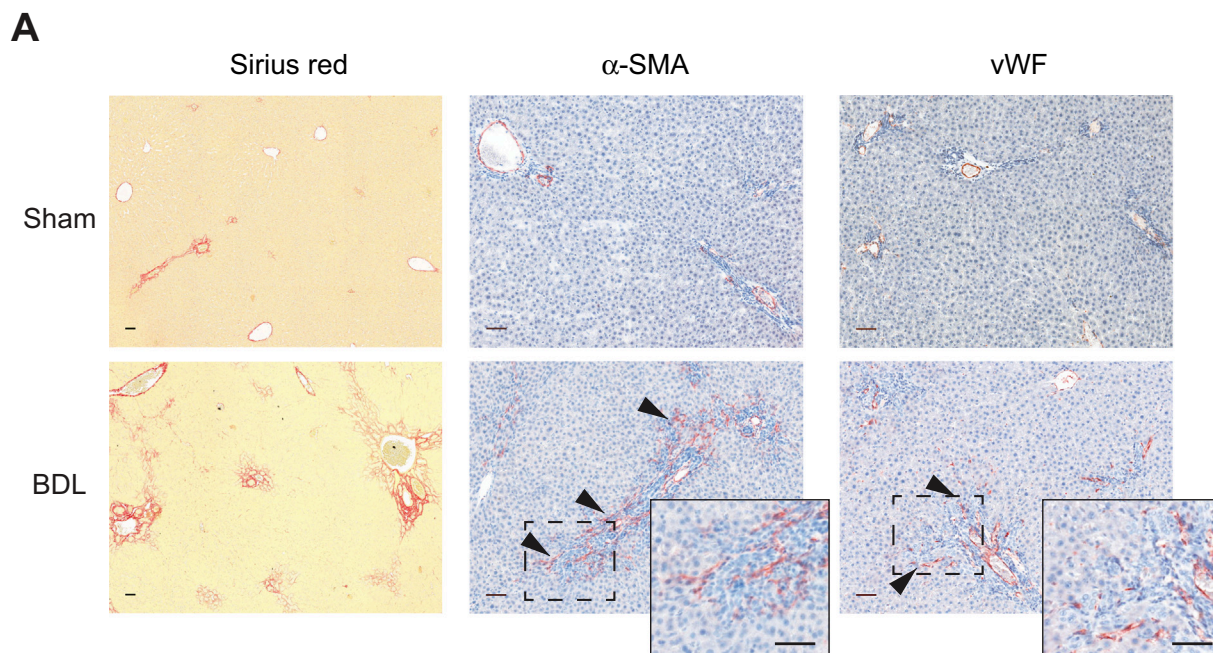
Cells were harvested in RIPA buffer with protease and phosphatase inhibitors. Proteins (30 μ g) were resolved by SDS-PAGE and transferred to nitrocellulose membranes. The following antibodies were used as primary antibodies: anti- α -SMA (#M0851; Dako), anti-GADD34 (#sc8327; Santa Cruz Biotechnology), anti-LC3I/II (#PM036; MBL International, Woburn, MA, USA), anti- α -tubulin (#T8203; Merck), anti- β -actin (#3700; Cell signaling, Danvers, MA, USA) and anti-GAPDH (#GTx627408; Clinisciences).

2.7. ELISA

ELISA was performed according to the manufacturer's instructions to measure the concentrations of collagen 1 (COL1) (#SEA571Ra, Euromedex, Souffelweyersheim, France) and vascular endothelial growth factor (VEGF) (#RRV00, R&D Systems, Minneapolis, MN, USA), in the supernatant of PMF incubated with 10% FBS-containing medium or serum-free medium, respectively, for 24 h. All samples were run in duplicate.

2.8. Cell proliferation

The proliferation of standard PMF at P1 was analyzed by two



(caption on next page)

Fig. 1. Phenotype of portal myofibroblasts (PMF) following *in vivo* expansion. (A) Liver tissue sections from bile duct-ligated (BDL) and sham-operated rats, on post-operative week 2, were subjected to Sirius red staining (original magnification $\times 10$), alpha-smooth muscle actin (α -SMA) and von Willebrand factor (vWF) immunostaining (original magnification $\times 20$); arrowheads point to stained cells at the leading or lateral edge of portal fibrosis. Insets: higher magnification of the boxed areas. Bar scale: 50 μ m. (B–G) Standard PMF (PMF) and BDL PMF derived from normal and BDL rats, respectively, were subjected to the following comparative analyses: B) RT-qPCR of *Acta2* and *Col1a1* mRNA; C) Immunoblot of α -SMA; D) ELISA of secreted collagen 1 (COL1); E) Assessment of proangiogenic activity by hemoglobin concentration in Matrigel plug assay (left panel showing representative explanted Matrigel plugs), RT-qPCR of *Vegf* mRNA (middle panel), ELISA of secreted VEGF (right panel); F) Fetal bovine serum (FBS)-induced proliferation, assessed by the percentage of Ki67-positive cells; G) FBS-induced migration, assessed by wound healing assay. Left panel showing representative phase-contrast pictures at time 0 and 24 h after insert removal; right panel showing the percentage of area covered by PMF after 24 h. Quantitative data represent means \pm SD of 5–18 cell preparations; *P < 0.05, ** P < 0.01, ***P < 0.001.

methods. Real-time cell proliferation was assessed using xCELLigence RTCA-DP System (Roche Diagnostics). By measuring electrical impedance, this device provides means to quantify cell number, viability and morphology. Cell-sensor impedance is expressed as an arbitrary unit called Cell Index. Cells were seeded in triplicate at 5000 cells/well in the E-Plate 96 (Roche Diagnostics) and allowed to grow for 24 h. After 24 h of serum deprivation, cells were incubated in DMEM with or without 10% FBS or with 50 ng/mL of fibroblast growth factor-2 (FGF2) or 100 ng/mL of monocyte chemoattractant protein-1 (MCP-1) in the presence of 0.5% FBS. Data were analyzed using RTCA Software 1.2 and expressed as means \pm SD of cell index at 24 h normalized to the cell index before stimulation.

Cell proliferation was also measured using the Click-it EdU microplate assay (Life Technologies, Paisley, UK). Briefly, cells were seeded in microplate (5000 cells/well) and after 24 h of serum deprivation, they were incubated in DMEM with or without 10% FBS in the presence of EdU for 24 h. EdU labeling was detected by fluorescence following the manufacturer's instructions.

Both aforementioned methods require cell counting before seeding, which was not possible for BDL PMF directly obtained by outgrowth at P0. Therefore, the proliferation of BDL PMF and of standard PMF to which they were compared, was assessed by Ki67 immunostaining. Cells were fixed in 4% paraformaldehyde for 15 min, then blocked and permeabilized with 2% bovine serum albumin (BSA)-0.1% Triton X100, for 1 h. Cells were then incubated with the Alexa Fluor 488-conjugated Ki67 antibody (#11882; Cell Signaling) overnight at 4 °C and nuclear staining was performed using DAPI. Ki67-positive cells were counted in five random fields at magnification $\times 20$ using ImageJ software and reported to the total number of cells.

2.9. Cell migration

Wound-healing was performed, using a culture insert made of two reservoirs separated by a 500- μ m-thick wall. An equal number of cells (25000) were plated in the two reservoirs. At confluence, cells were treated as indicated in the presence of 2 μ g/mL mitomycin-C to prevent further proliferation. The insert was removed and images were acquired between time 0 and 24 h. The area of wound coverage was calculated using the cell image analysis software ImageJ and normalized for the 0-h time point area.

Cell migration was also assessed using the xCELLigence RTCA-DP system and CIM-plates 16 (Roche Diagnostics). After 24 h of serum deprivation, cells were treated with TM (1 μ mol/L) for 24 h. Cells were seeded in the upper chamber of the CIM-plate in serum-free medium, whereas DMEM with or without FBS or with 50 ng/mL of platelet-derived growth factor-BB (PDGF-BB) was added to the lower chamber. The impedance value of each well was monitored during 24 h and data analysis was performed, using the RTCA software. Data are expressed as the rate of migration (slope) during the first 9 h.

2.10. Matrigel-plug assay

Matrigel preparations were obtained by mixing 400 μ L of growth factor-reduced Matrigel (BD Biosciences, Bedford, MA, USA) with 5 IU of heparin and 100 μ L of standard PMF or BDL PMF conditioned medium and injected subcutaneously into wild-type C57BL/6J mice

(Janvier Labs). Seven days after injection, the plugs were removed for macroscopic analysis and the hemoglobin concentration was measured using Drabkin's reagent (Sigma-Aldrich). Briefly, gel plugs were homogenized in RIPA buffer and centrifugated (8000 rpm at 4 °C, for 10 min). The supernatant was mixed with Drabkin's reagent and absorbance at 540 nm was measured. The hemoglobin concentration was calculated using a standard curve, according to the manufacturer's instructions.

2.11. Statistical analysis

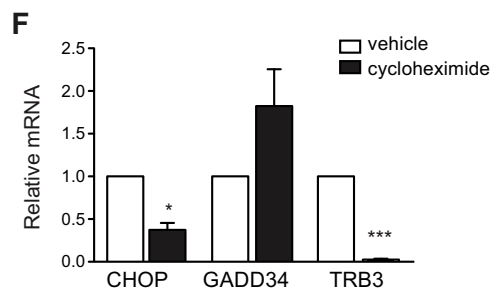
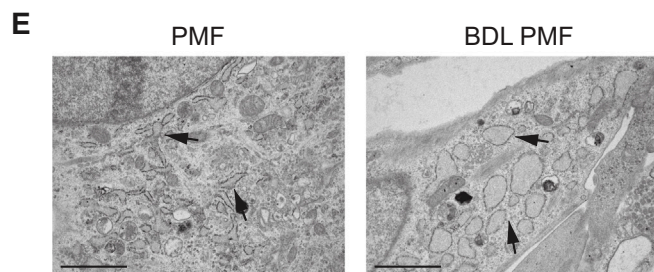
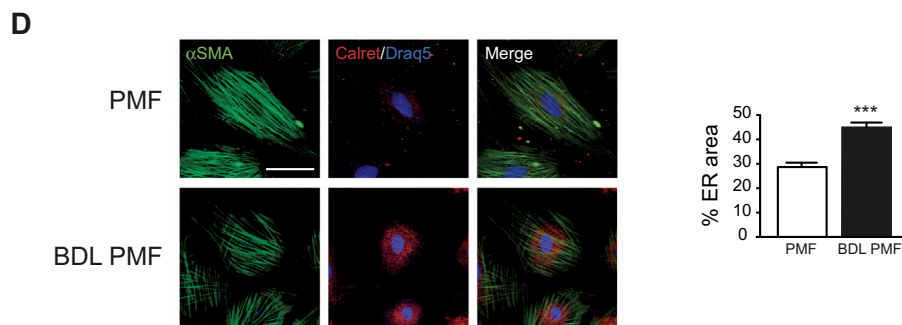
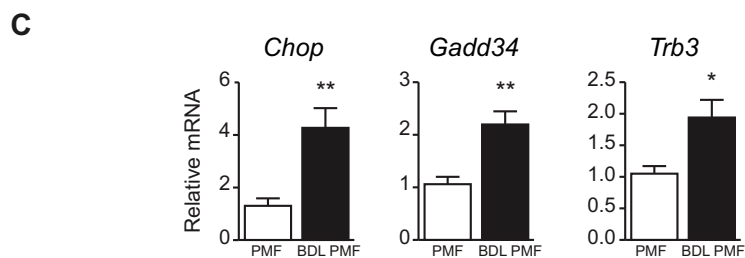
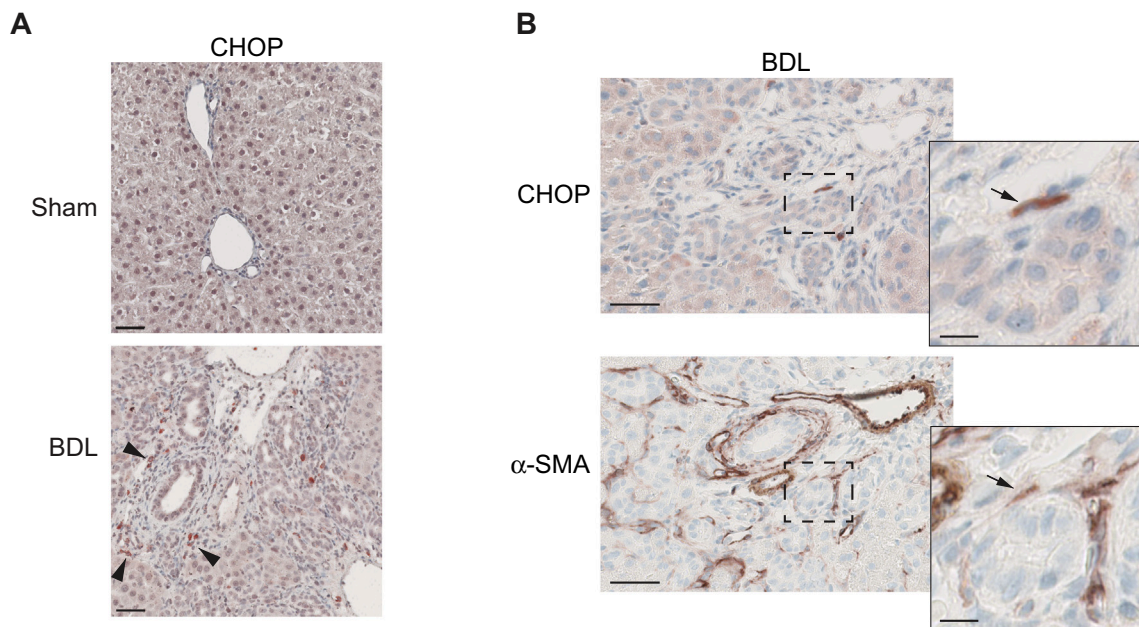
GraphPad Prism Software was used to perform statistical analysis. The Student *t*-test was used for comparisons. A P value of < 0.05 was considered significant.

3. Results

3.1. PMF expanding *in vivo* develop ER stress

PMF arise from the proliferation and myofibroblastic differentiation of portal mesenchymal progenitors in response to liver injury. They promote fibrosis and angiogenesis. In the BDL rat model, PMF accumulate around proliferating bile ducts [4]. Two weeks after BDL in rats of the present study, bile duct structures were surrounded by α -SMA-stained PMF that had migrated at the leading edge of fibrosis together with newly formed vessels (Fig. 1A). PMF that we refer to as BDL PMF, were obtained out of bile duct isolates from these BDL rats. Compared to standard PMF that emerged in culture from normal bile ducts, BDL PMF that arose *in vivo*, expressed *Acta2*/ α -SMA and *Col1a1* at higher levels and secreted larger amounts of collagen 1 (COL1) (Fig. 1, B–D), indicating that they were at a more advanced stage of myofibroblastic differentiation than standard PMF. BDL PMF were also more pro-angiogenic than standard PMF, as shown by Matrigel plug assay (Fig. 1E, left panel). To a large extent, this could be explained by a higher synthesis and secretion of VEGF (Fig. 1E, middle and right panels). By contrast, however, the proliferative and migratory capacity was lower in BDL PMF than in standard PMF, as shown in response to serum (Fig. 1, F and G). We concluded from these results that some of the fundamental functions of myofibroblasts, undergo opposite regulations in PMF following their expansion *in vivo*.

Next, we addressed the question as whether ER stress occurs and impacts phenotypic features in PMF. In the liver of BDL rats, the ER stress marker CHOP was detected by immunostaining in periductular cells consistent with PMF as shown by α -SMA staining, at the leading edge of portal fibrosis (Fig. 2, A and B). This suggested that PMF that emerged *in vivo* during BDL-induced fibrogenesis, developed ER stress, which was confirmed by the investigation of ER stress pathways in BDL PMF. Downstream targets of the PERK pathway, *i.e.* *Chop*, *Gadd34* and *Trb3*, were all overexpressed in BDL compared to standard PMF (Fig. 2C). The other two pathways of UPR, *i.e.* IRE1 and ATF6, were not activated (Supplementary Fig. S1A), suggesting a specific induction of the PERK pathway in PMF, following their expansion *in vivo*. We found no accumulation of LC3II, the conjugated form of LC3, in BDL PMF (Supplementary Fig. S1B), indicating no link with autophagy. Morphologically, the ER in BDL PMF was enlarged and dilated, as shown by calreticulin immunostaining and transmission electron microscopy



(caption on next page)

Fig. 2. Endoplasmic reticulum (ER) stress in PMF following *in vivo* expansion. (A, B) Liver tissue sections from BDL and sham-operated rats on post-operative week 2 were subjected to immunohistochemistry, showing that in BDL rats, CHOP staining is detected in periductular cells A) accumulating at the leading edge of portal fibrosis (arrowheads); B) expressing α -SMA, as shown on serial tissue sections (arrows). Original magnification $\times 20$; bar scale: 50 μ m. Insets: higher magnification of the boxed areas; bar scale: 10 μ m. (C–F) Standard PMF (PMF) and BDL PMF derived from normal and BDL rats, respectively, were subjected to the following analyses: C) RT-qPCR of *Chop*, *Gadd34* and *Trb3* mRNA; D) Co-immunostaining for α -SMA and calreticulin. Representative images (original magnification $\times 40$; bar scale: 50 μ m) are shown (left panel); ER size relative to the total cell surface, quantified by Image J (right panel); E) Transmission electron microscopy. Arrows point to ER (original magnification $\times 10000$; bar scale: 0.1 μ m); (F) RT-qPCR of *Chop*, *Gadd34* and *Trb3* mRNA in BDL PMF treated with 1 μ g/mL cycloheximide or vehicle (DMSO) for 18 h. Quantitative data represent means \pm SD of 3–13 cell preparations; *P < 0.05, ** P < 0.01, *** P < 0.001.

(Fig. 2, D and E). The overproduction of extracellular matrix components in BDL PMF compared to standard PMF likely explained these morphological features, so that protein overload could be the cause of ER stress in BDL PMF. To test this hypothesis, we treated BDL PMF with cycloheximide, a potent inhibitor of protein synthesis, which indeed reduced the expression of *Chop* and *Trb3* in these cells (Fig. 2F). This was not the case for *Gadd34* expression, which even showed a trend towards increased expression, consistent with previous data indicating that the reduction of protein synthesis by itself, is able to increase GADD34 expression [22]. Collectively, our results indicated that ER stress occurred in PMF that accumulated *in vivo* during liver fibrogenesis, likely as a result of increased secretory activity.

3.2. ER stress regulates PMF functions

To establish a potential link between ER stress and the phenotype of BDL PMF that expanded *in vivo*, we treated standard PMF obtained from normal rat liver with TM, a classical ER stress inducer. As anticipated, the treatment of PMF with TM caused a significant increase in the expression of the ER stress targets, *Chop*, *Gadd34* and *Trb3* (Fig. 3A). No change in α -SMA or *Col1a1* expression nor in COL1 secretion was observed in PMF following TM treatment (Fig. 3, B–D), indicating that ER stress had no impact on the process of myofibroblastic differentiation in these cells. We then examined the effect of TM on serum-induced proliferation and migration of PMF. TM treatment fully abolished the proliferative response (Fig. 3E) and significantly decreased the migratory response (Fig. 3F) of PMF to serum. The proliferative response of PMF to FGF2 and MCP-1 and their migratory response to PDGF-BB were also inhibited as a result of TM treatment (Supplementary Fig. S2). On the contrary, VEGF synthesis and secretion increased in PMF, following TM treatment, and *in vivo*, their proangiogenic capacity was increased, as shown by Matrigel plug assay (Fig. 3G).

3.3. PERK mediates the regulation of PMF functions by ER stress

Next, we sought to determine if PERK, the UPR pathway induced by ER stress in PMF, exerted regulatory functions in these cells. We inhibited the PERK pathway in BDL PMF using the specific inhibitor GSK2656157 [23]. The treatment of BDL PMF with 1 μ mol/L GSK2656157 reduced the expression of *Chop*, *Gadd34* and *Trb3*, the downstream targets of the PERK pathway (Fig. 4A). Such inhibition of the PERK pathway had no effect on the expression of *Acta2* or *Col1* (Fig. 4B) nor on the secretion of COL1 (Fig. 4C), confirming that ER stress had little influence on the myofibroblastic differentiation of PMF. GSK-treated BDL PMF displayed an increased proliferation rate (Fig. 4D) and migratory capacity (Fig. 4E), compared with vehicle-treated cells. By contrast, GSK treatment decreased the expression and secretion of VEGF by BDL PMF, as well as their proangiogenic activity (Fig. 4F). Together, these results indicated that the PERK pathway was induced in PMF following their expansion *in vivo* and regulated their phenotype. Whereas the proliferation and migration of PMF were down-regulated by the PERK pathway, their pro-angiogenic function was stimulated by this same pathway.

4. Discussion

In the present study, we showed that PMF develop ER stress as they expand *in vivo* during the progression of fibrosis. In its turn, ER stress, most notably the PERK pathway, further increases the proangiogenic activity of these cells, but also paradoxically inhibits their proliferation and migration.

PMF issued from the liver of BDL rats, exhibited an overexpression of the PERK downstream targets *Chop*, *Gadd34* and *Trb3*, from which we inferred that PMF developed ER stress as they accumulated *in vivo*. Of particular interest, *in situ*, CHOP was detected at the leading edge of fibrosis, where PMF accumulate [4] and where angiogenesis is the most active [24]. PMF synthesize and secrete large amounts of extracellular matrix components, which we hypothesized might trigger UPR. In keeping with this hypothesis, the global inhibition of protein synthesis by means of cycloheximide in BDL PMF, reduced ER stress. However, we cannot exclude that the pathological microenvironment, e.g. inflammation or hypoxia, previously shown to induce ER stress in hepatocytes, also participated in the induction of ER stress in PMF.

We found that ER stress did not contribute to the myofibroblastic phenotype of PMF. Neither the induction of ER stress by TM in standard PMF issued from normal rats nor the inhibition of the PERK pathway in *in vivo*-differentiated PMF derived from BDL rats, caused any change in the expression of α -SMA or the production of collagen. This is in contrast with what was previously observed in HSC, in which TM treatment stimulated the differentiation into myofibroblasts [15]. It was shown that ER stress stimulated the myofibroblastic differentiation of HSC by a mechanism involving the IRE1/XBP1 pathway and the activation of autophagy [17,18]. We found no activation of the IRE1 branch of UPR nor evidence of autophagy in BDL PMF, which had accumulated two weeks after the BDL trigger. However, we cannot exclude that such mechanisms took place at earlier stage of PMF differentiation following BDL-induced liver injury.

We also found that ER stress negatively regulated the proliferation and migration of PMF. Among the potential pathways mediating the anti-proliferative effect of ER stress, *Trb3*, the expression of which was increased in BDL PMF, was previously described as a negative regulator of Akt. This was shown in carcinoma cells, in which the down-regulation of *Trb3* expression caused a hyperphosphorylation of Akt and an increase in proliferation [25]. In TM-treated fibroblasts, it was also shown that PERK inhibited cyclin D1 translation, which resulted in cell-cycle arrest [26]. After they had proliferated *in vivo*, BDL PMF showed a switch towards decreased proliferative capacity, without any evidence of cellular senescence or apoptosis (not shown), even if CHOP is not only a negative regulator of cell growth but also a promoter of apoptosis [27]. Apoptosis was shown to occur as a result of TM- or cannabidiol-induced ER stress in myofibroblastic HSC [19,28]. It was also shown that ER stress contributed to the apoptosis of HSC, that takes place during the resolution of fibrosis [28]. HSC-derived myofibroblasts are intrinsically much more prone than PMF to undergo apoptosis [29], which may explain a different susceptibility to ER stress-induced apoptosis. It was suggested in a recent study that ER stress might actually cause apoptosis also in PMF, although direct evidence is currently lacking [30].

Previous work indicates that the three branches of the UPR stimulated the expression of VEGF [31,32]. In keeping with these lines, we

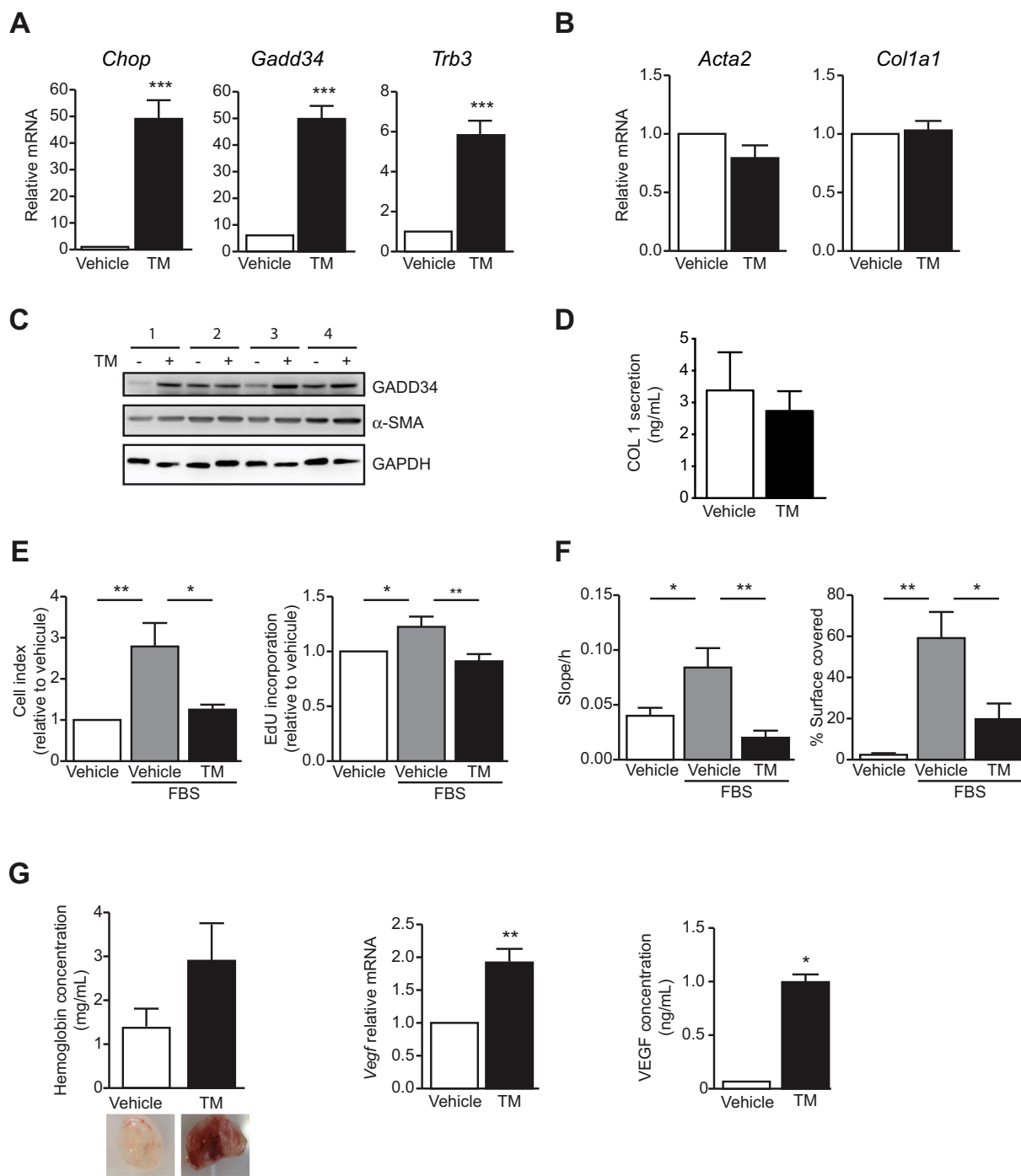


Fig. 3. Effect of tunicamycin-induced ER stress on PMF functions. Standard PMF derived from normal rats were incubated with 1 μ mol/L of tunicamycin (TM) or vehicle (DMSO) in culture and subjected to the following comparative analyses: (A) RT-qPCR of *Chop*, *Gadd34* and *Trb3* mRNA; (B) RT-qPCR of *Acta2* and *Col1a1* mRNA; (C) Immunoblot of GADD34 and α -SMA (numbers stand for replicates); (D) ELISA of secreted collagen 1 (COL1); (E) FBS-induced proliferation, assessed by the xCELLigence System (left panel) and by EdU incorporation (right panel). Data are expressed relative to the value of vehicle-treated PMF incubated without FBS; (F) FBS-induced migration, assessed by the xCELLigence System (left panel) and by wound healing assay (right panel); (G) Proangiogenic activity assessed by hemoglobin concentration in Matrigel plug assay (left panel showing representative explanted Matrigel plugs), RT-qPCR of *Vegf* mRNA (middle panel), ELISA of secreted VEGF. Quantitative data are reported as means \pm SD of 4–16 cell preparations; *P < 0.05, ** P < 0.01, ***P < 0.005.

found that PMF undergoing ER stress displayed increased synthesis and secretion of VEGF and a high pro-angiogenic activity. We previously demonstrated that PMF signaled to endothelial cells through VEGF-laden microparticles and acted as mural cells for newly formed vessels, whereby they promoted the vascular remodeling that leads to cirrhosis [8]. By triggering the formation of scar vessels, which provide a backbone for the deposition of extracellular matrix, PMF thus appear to

be critical in the progression of fibrosis towards cirrhosis. Therefore, by increasing the pro-angiogenic activity of PMF, ER stress could also foster liver fibrosis. To address this possibility, we tested the PERK inhibitor GSK2656157 *in vivo*. In BDL rats treated with this inhibitor, we found no significant effect on fibrosis or angiogenesis (Supplementary Fig. S3), although we cannot exclude insufficient local bioavailability of the drug. Targeting PERK could also interfere with ER stress occurring

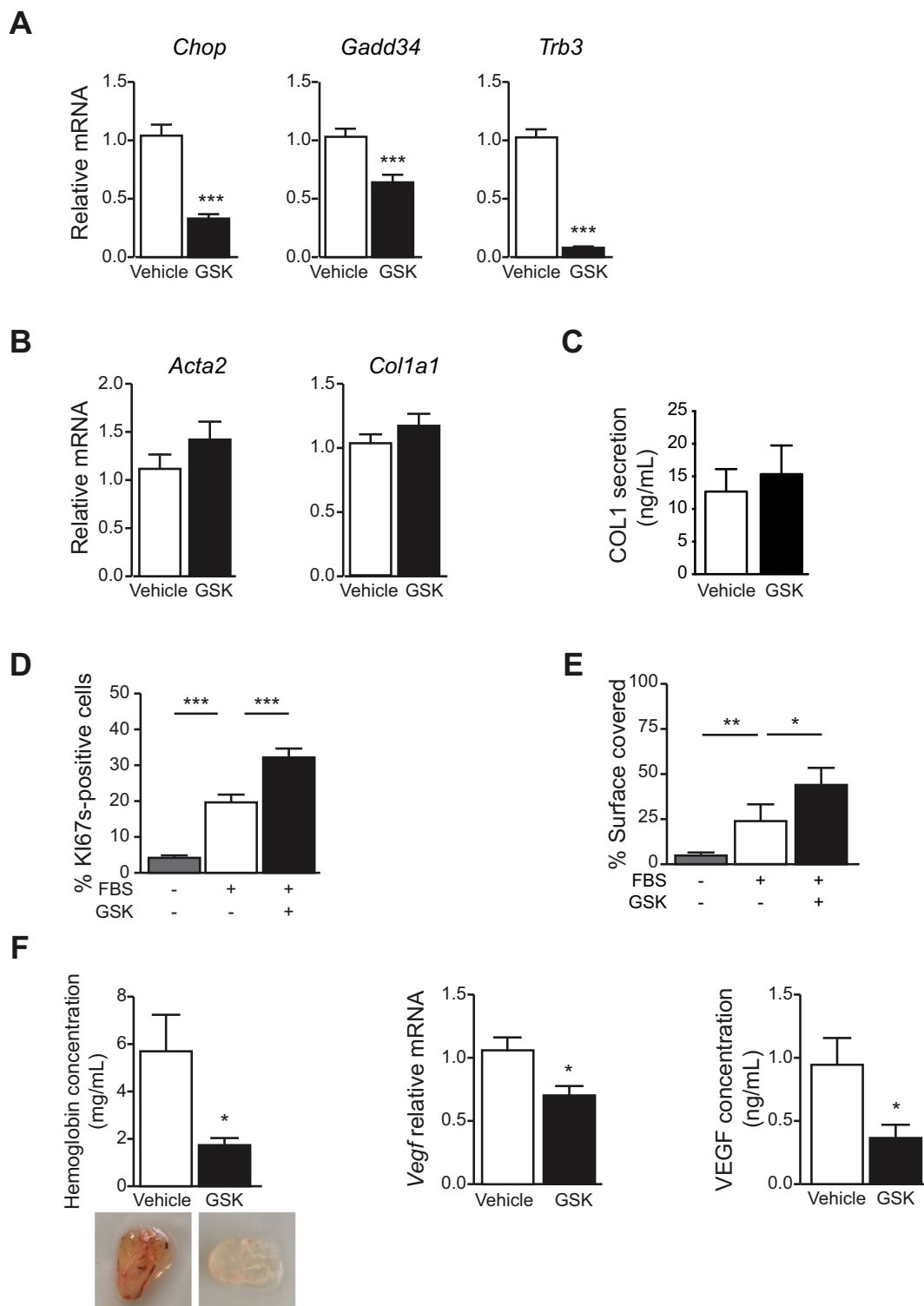


Fig. 4. Effect of PERK inhibition on the functions of *in vivo*-expanded PMF. BDL PMF derived from BDL rats were treated with 1 μ mol/L GSK265157 (GSK) or vehicle (DMSO) and subjected to the comparative analyses of (A) *Chop*, *Gadd34* and *Trb3* mRNA, (B) *Acta2* and *Col1a1* mRNA, by RT-qPCR, (C) secreted collagen 1 by ELISA (COL1); (D) FBS-induced proliferation, assessed by the percentage of Ki67-positive cells; (E) FBS-induced migration, assessed by wound healing assay; (F) Proangiogenic activity, assessed by hemoglobin concentration in Matrigel plug assay (left panel showing representative explanted Matrigel plugs), RT-qPCR of *Vegf* mRNA (middle panel), ELISA of secreted VEGF. Quantitative data are reported as means \pm SD of 5–14 cell preparations; *P < 0.05, ** P < 0.01, ***P < 0.005.

outside the liver after BDL, such as in the intestine [33]. In any event, PERK does not appear as a prime target to inhibit in liver fibrosis.

To conclude, during fibrogenesis, myofibroblasts and their precursors undergo phenotypic changes, that are often described as a unidirectional process called “activation”. The current findings indicate

that this view is incorrect and that different functions of myofibroblasts can be regulated in opposite directions. After they initially expand in the injured liver as a result of active proliferation and migration, PMF become highly pro-angiogenic but less proliferative and migratory. This phenotypic switch is induced at least partly by ER stress and may

provide a mechanism that restricts the expansion of PMF as they stabilize newly formed vessels at the leading edge of fibrosis.

Supplementary data to this article can be found online at <https://doi.org/10.1016/j.bbadis.2018.10.008>.

Transparency document

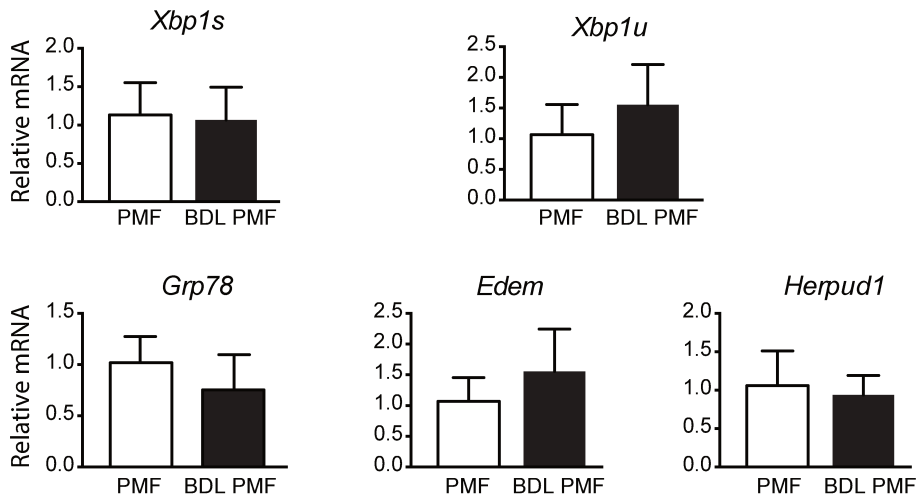
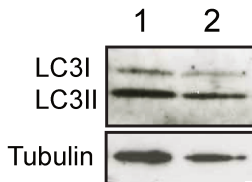
The Transparency document associated with this article can be found, in online version.

Acknowledgements

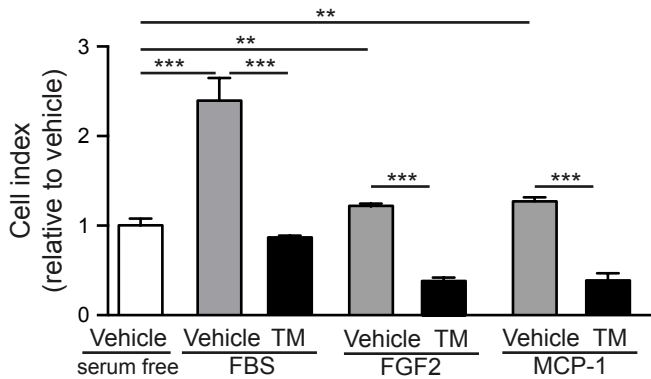
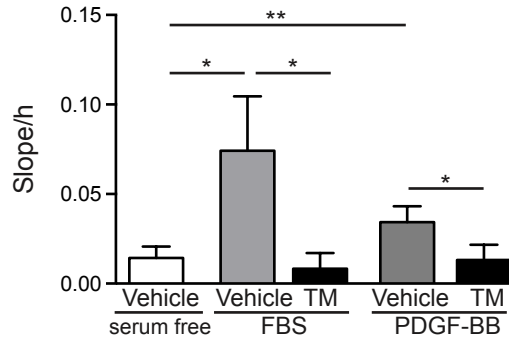
The authors thank Romain Morichon and Fatiha Merabte, UMS LUMIC, for cell microscopy and histomorphology, Marie-Christine Verpont, UMR_S 1155, for electron microscopy and the PHEA team for animal care. We acknowledge Jeffrey Axten (GlaxoSmithKline, PA, USA) for providing the PERK inhibitor for *in vivo* experiments. This work was supported by funding from the Microbiome Foundation, Paris, France.

References

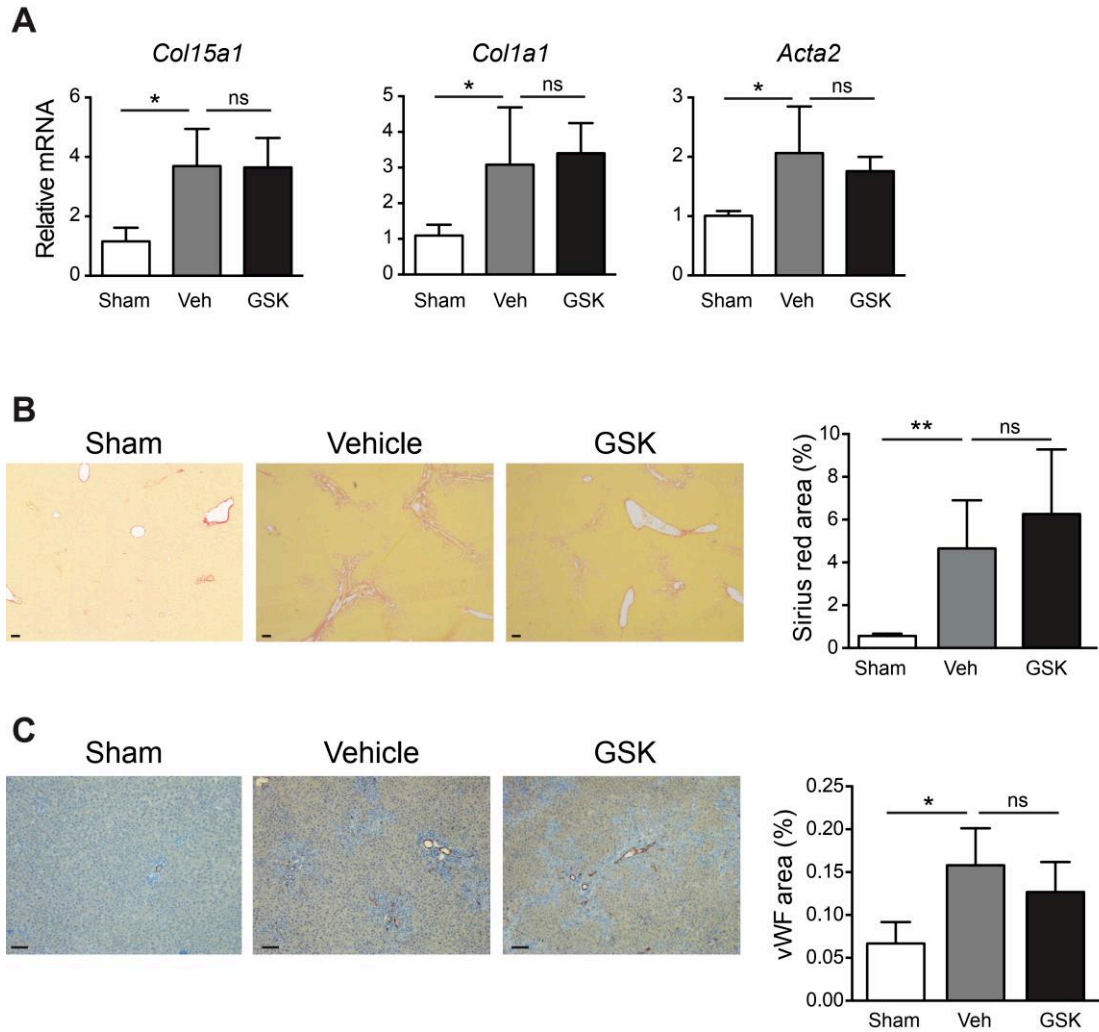
- [1] B. Hinz, S.H. Phan, V.J. Thannickal, M. Prunotto, A. Desmouliere, J. Varga, O. De Wever, M. Mareel, G. Gabbiani, Recent developments in myofibroblast biology: paradigms for connective tissue remodeling, *Am. J. Pathol.* 180 (2012) 1340–1355.
- [2] S.L. Friedman, Hepatic stellate cells: protean, multifunctional, and enigmatic cells of the liver, *Physiol. Rev.* 88 (2008) 125–172.
- [3] N. Kinnman, C. Francoz, V. Barbu, D. Wendum, C. Rey, R. Hultcrantz, R. Poupon, C. Housset, The myofibroblastic conversion of peribiliary fibrogenic cells distinct from hepatic stellate cells is stimulated by platelet-derived growth factor during liver fibrogenesis, *Lab. Invest.* 83 (2003) 163–173.
- [4] M. Beaussier, D. Wendum, E. Schiffer, S. Dumont, C. Rey, A. Lienhart, C. Housset, Prominent contribution of portal mesenchymal cells to liver fibrosis in ischemic and obstructive cholestatic injuries, *Lab. Invest.* 87 (2007) 292–303.
- [5] Z. Li, J.A. Dranoff, E.P. Chan, M. Uemura, J. Sevigny, R.G. Wells, Transforming growth factor-beta and substrate stiffness regulate portal fibroblast activation in culture, *Hepatology* 46 (2007) 1246–1256.
- [6] K. Iwaisako, C. Jiang, M. Zhang, M. Cong, T.J. Moore-Morris, T.J. Park, X. Liu, J. Xu, P. Wang, Y.H. Paik, F. Meng, M. Asagiri, L.A. Murray, A.F. Hofmann, T. Iida, C.K. Glass, D.A. Brenner, T. Kisseleva, Origin of myofibroblasts in the fibrotic liver in mice, *Proc. Natl. Acad. Sci. U. S. A.* 111 (2014) E3297–E3305.
- [7] I. Lua, Y. Li, J.A. Zagory, K.S. Wang, S.W. French, J. Sevigny, K. Asahina, Characterization of hepatic stellate cells, portal fibroblasts, and mesothelial cells in normal and fibrotic livers, *J. Hepatol.* 64 (2016) 1137–1146.
- [8] S. Lemoine, A. Cadoret, P.E. Rautou, H. El Mourabit, V. Ratzu, C. Corpechot, C. Rey, N. Bosselut, V. Barbu, D. Wendum, G. Feldmann, C. Boulanger, C. Henegar, C. Housset, D. Thabut, Portal myofibroblasts promote vascular remodeling underlying cirrhosis formation through the release of microparticles, *Hepatology* 61 (2015) 1041–1055.
- [9] B. Tuchweber, A. Desmouliere, M.L. Bochaton-Piallat, L. Rubbia-Brandt, G. Gabbiani, Proliferation and phenotypic modulation of portal fibroblasts in the early stages of cholestatic fibrosis in the rat, *Lab. Invest.* 74 (1996) 265–278.
- [10] J.A. Dranoff, R.G. Wells, Portal fibroblasts: underappreciated mediators of biliary fibrosis, *Hepatology* 51 (2010) 1438–1444.
- [11] H. El Mourabit, E. Loeuillard, S. Lemoine, A. Cadoret, C. Housset, Culture model of rat portal myofibroblasts, *Front. Physiol.* 7 (2016) 120.
- [12] S. Lemoine, D. Thabut, C. Housset, Portal myofibroblasts connect angiogenesis and fibrosis in liver, *Cell Tissue Res.* 365 (2016) 583–589.
- [13] L. Dara, C. Ji, N. Kaplowitz, The contribution of endoplasmic reticulum stress to liver diseases, *Hepatology* 53 (2011) 1752–1763.
- [14] P. Puri, F. Mirshahi, O. Cheung, R. Natarajan, J.W. Maher, J.M. Kellum, A.J. Sanyal, Activation and dysregulation of the unfolded protein response in nonalcoholic fatty liver disease, *Gastroenterology* 134 (2008) 568–576.
- [15] J.H. Koo, H.J. Lee, W. Kim, S.G. Kim, Endoplasmic reticulum stress in hepatic stellate cells promotes liver fibrosis via PERK-mediated degradation of HNRNP1A1 and up-regulation of SMAD2, *Gastroenterology* 150 (2016) 181–193 (e188).
- [16] N. Tamaki, E. Hatano, K. Taura, M. Tada, Y. Kodama, T. Nitta, K. Iwaisako, S. Seo, A. Nakajima, I. Ikai, S. Uemoto, CHOP deficiency attenuates cholestasis-induced liver fibrosis by reduction of hepatocyte injury, *Am. J. Physiol. Gastrointest. Liver Physiol.* 294 (2008) G498–G505.
- [17] V. Hernandez-Gea, M. Hilscher, R. Rozenfeld, M.P. Lim, N. Nieto, S. Werner, L.A. Devi, S.L. Friedman, Endoplasmic reticulum stress induces fibrogenic activity in hepatic stellate cells through autophagy, *J. Hepatol.* 59 (2013) 98–104.
- [18] R.S. Kim, D. Hasegawa, N. Goossens, T. Tsuchida, V. Athwal, X. Sun, C.L. Robinson, D. Bhattacharya, H.I. Chou, D.Y. Zhang, B.C. Fuchs, Y. Lee, Y. Hoshida, S.L. Friedman, The XBP1 arm of the unfolded protein response induces Fibrogenic activity in hepatic stellate cells through autophagy, *Sci. Rep.* 6 (2016) 39342.
- [19] M.P. Lim, L.A. Devi, R. Rozenfeld, Cannabidiol causes activated hepatic stellate cell death through a mechanism of endoplasmic reticulum stress-induced apoptosis, *Cell Death Dis.* 2 (2011) e170.
- [20] E. Borkham-Kamphorst, B.T. Steffen, E. Van de Leur, U. Haas, L. Tihaa, S.L. Friedman, R. Weiskirchen, CCN1/CYR61 overexpression in hepatic stellate cells induces ER stress-related apoptosis, *Cell. Signal.* 28 (2016) 34–42.
- [21] N. Bosselut, C. Housset, P. Marcelo, C. Rey, T. Burmester, J. Vinh, M. Vaubourdolle, A. Cadoret, B. Baudin, Distinct proteomic features of two fibrogenic liver cell populations: hepatic stellate cells and portal myofibroblasts, *Proteomics* 10 (2010) 1017–1028.
- [22] A. Dalet, R.J. Arguello, A. Combes, L. Spinelli, S. Jaeger, M. Fallet, T.P. Vu Manh, A. Mendes, J. Perego, M. Reverendo, V. Camosseto, M. Dalod, T. Weil, M.A. Santos, E. Gatti, P. Pierre, Protein synthesis inhibition and GADD34 control IFN-beta heterogeneous expression in response to dsRNA, *EMBO J.* 36 (2017) 761–782.
- [23] C. Atkins, Q. Liu, E. Minthorn, S.Y. Zhang, D.J. Figueroa, K. Moss, T.B. Stanley, B. Sanders, A. Goetz, N. Gaul, A.E. Choudhry, H. Alsaïd, B.M. Jucker, J.M. Axten, R. Kumar, Characterization of a novel PERK kinase inhibitor with antitumor and antiangiogenic activity, *Cancer Res.* 73 (2013) 1993–2002.
- [24] E. Novo, S. Cannito, E. Zamara, L. Valfre di Bonzo, A. Caligiuri, C. Cravanzola, A. Compagnone, S. Colombatto, F. Marra, M. Pinzani, M. Parola, Proangiogenic cytokines as hypoxia-dependent factors stimulating migration of human hepatic stellate cells, *Am. J. Pathol.* 170 (2007) 1942–1953.
- [25] H. Mujic, A. Nagelkerke, K.M. Rouschop, S. Chung, N. Chaudary, P.N. Span, B. Clarke, M. Milosevic, J. Sykes, R.P. Hill, M. Koritzinsky, B.G. Wouters, Hypoxic activation of the PERK/eIF2alpha arm of the unfolded protein response promotes metastasis through induction of LAMP3, *Clin. Cancer Res.* 19 (2013) 6126–6137.
- [26] J.W. Brewer, L.M. Hendershot, C.J. Sherr, J.A. Diehl, Mammalian unfolded protein response inhibits cyclin D1 translation and cell-cycle progression, *Proc. Natl. Acad. Sci. U. S. A.* 96 (1999) 8505–8510.
- [27] H. Malhi, R.J. Kaufman, Endoplasmic reticulum stress in liver disease, *J. Hepatol.* 54 (2011) 795–809.
- [28] S. De Minicis, C. Candelaresi, L. Agostinelli, S. Taffetani, S. Saccomanno, C. Rychlicki, L. Trozzi, M. Marzoni, A. Benedetti, G. Svegliati-Baroni, Endoplasmic reticulum stress induces hepatic stellate cell apoptosis and contributes to fibrosis resolution, *Liver Int.* 32 (2012) 1574–1584.
- [29] T. Knittel, D. Kobold, B. Saile, A. Grundmann, K. Neubauer, F. Piscaglia, G. Ramadori, Rat liver myofibroblasts and hepatic stellate cells: different cell populations of the fibroblast lineage with fibrogenic potential, *Gastroenterology* 117 (1999) 1205–1221.
- [30] E. Borkham-Kamphorst, B.T. Steffen, E. van de Leur, U. Haas, R. Weiskirchen, Portal myofibroblasts are sensitive to CCN-mediated endoplasmic reticulum stress-related apoptosis with potential to attenuate biliary fibrogenesis, *Cell. Signal.* 51 (2018) 72–85.
- [31] S.F. Abcouwer, P.L. Marjon, R.K. Loper, D.L. Vander Jagt, Response of VEGF expression to amino acid deprivation and inducers of endoplasmic reticulum stress, *Invest. Ophthalmol. Vis. Sci.* 43 (2002) 2791–2798.
- [32] R. Ghosh, K.L. Lipson, K.E. Sargent, A.M. Mercurio, J.S. Hunt, D. Ron, F. Urano, Transcriptional regulation of VEGF-A by the unfolded protein response pathway, *PLoS One* 5 (2010) e9575.
- [33] R. Liu, X. Li, Z. Huang, D. Zhao, B.S. Ganesh, G. Lai, W.M. Pandak, P.B. Hylemon, J.S. Bajaj, A.J. Sanyal, H. Zhou, C/EBP homologous protein-induced loss of intestinal epithelial stemness contributes to bile duct ligation-induced cholestatic liver injury in mice, *Hepatology* 67 (2018) 1441–1457.

A**B**

Supplementary Figure S1. Analysis of ER stress effectors and autophagy in BDL PMF. (A) PMFs obtained from normal or BDL rats were compared for *Xbp1s*, *Xbp1u* (IRE1 pathway), *Grp78*, *Edem* and *Herpud1* (ATF6 pathway) mRNA by RT-qPCR. Data represent means \pm SD of 8-15 cell preparations. (B) The expression of LC3I/II proteins was analyzed in PMF derived from normal (1) and BDL rats (2) by western blot.

A**B**

Supplementary Figure S2. Analysis of proliferation and migration of TM-treated PMF in response to different stimuli. PMF treated with 1 μ mol/L TM or vehicle (DMSO) were compared for (A) The proliferation in response to 10% FBS, 50 ng/mL FGF2 or 100 ng/mL MCP-1, assessed by the xCELLigence System; Data are expressed relative to the value of vehicle-treated PMF in serum-free medium; and (B) the FBS- or PDGF-BB-induced migration, assessed by the xCELLigence System. Data represent means \pm SD of 3 cell preparations, *P<0.05, ** P<0.01, ***P<0.005.



Supplementary Figure S3. Effect of the PERK inhibition on liver fibrosis in BDL rats. BDL rats were treated with vehicle or GSK 2656157 (an ethanesulfonate salt monohydrate received from GlaxoSmithKline, 75mg/kg by gavage twice/day) from D7 to D21. Liver tissue samples from these animals and sham-operated rats were analyzed for (A) RT-qPCR of *Col15a1*, *Col1a1* and *Acta2* mRNA, (B) Sirius red staining (original magnification x10) and (C) vWF immunostaining (magnification x20); bar scale: 50 μ m. Quantitative data represent means \pm SD of 4-5 rats. * P <0.05, ** P <0.01, ns: not significant.

Supplementary Table 1. Primers used for quantitative real-time PCR.

Gene	GenBank	Forward primer	Reverse primer
<i>Acta2</i>	NM_031004.2	GGGACGACATGGAAAAGATCTG	GGTTGGCCTTAGGGTTCAGC
<i>Col1a1</i>	NM_053304.1	TGAGCCAGCAGATTGAGAACA	GGGTCGATCCAGTACTCTCCG
<i>Col15a1</i>	NM_001100535.1	GCCCCCTACTTCATCCTCTC	CAGTACGGACCTCCAGGGTA
<i>Chop</i>	NM_001109986.1	AAGGTTTTTGGATTCTTCTCTTCGTT	GCAGGAGGTCTGTCTCAGAT
<i>Gadd34</i>	AH011730.2	CCTTGATGTGGAAGCCCAAAGTT	TCCACTTTCTTGCTCTCTAAGGCCAT
<i>Trb3</i>	NM_144755.2	CCCGGCTGGGGCCCTATATCC	CGCTGGCGGGATACACCTTGC
<i>Xbp1u</i>	NM_001004210.2	CACTCAGACTACGTGCGCCTC	TGCCAAAAGGATATCAGACTCA
<i>Xbp1s</i>	NM_001271731.1	TCCAAGGGGAATGGAGTAAGGCT	CCTGCACCTGCTGCGGACT
<i>Grp78</i>	M14050.1	GCGAGGATTGAAATTGAGTCCTTCT	GAGCGGAACAGGTCCATGTTCA
<i>Edem</i>	NM_001305279.1	CCTCTACCAGGCGACCAAGAATC	GCGTGGCATATCCACATTTGACT
<i>Herpud1</i>	NM_053523.1	GAACCTTCCTCCCTCTGGAT	CCTTGAAAGTCTGCTGGAC
<i>Vegf</i>	NM_031836.2	TGTTGACTGCTGTGGACTT	GACTTCGGCCTCTCTAAGAA
vWf	NM_053889.1	CCTTGTGAAGTGGCTCGTCT	GCAAGTGCAGTTGACCAGG
<i>Hprt</i>	AH005530.2	AGGACCTCTCGAAGTGT	ATCCCTGAAGTGCTCATTATA

Abstract

Previous work has demonstrated that portal myofibroblasts (PMFs) significantly contributed to liver fibrogenesis and modulated angiogenesis in liver fibrosis. The main aim of this thesis was to elucidate the landscape of portal mesenchymal cells, with a particular focus on a portal mesenchymal stem cell niche. We characterized the murine normal liver portal mesenchymal cell landscape. Importantly, we revealed a portal mesenchymal cell population with the features of mesenchymal stem cells (MSCs), designated portal mesenchymal stem cells (PMSCs) that possessed the ability to give rise to PMFs *in vitro*. Furthermore, we identified *Slit2* as a new marker of PMSCs based on scRNA-seq and bulk RNA-seq analysis. *In vivo*, we observed PMSC expansion (measured by the expression of *Slit2*) in liver from both animal fibrosis models (DDC and CDAA) and patients with chronic liver disease (NASH, PSC and other liver disease). Notably, we defined the specific gene signatures for PMSCs and hepatic stellate cells (HSCs), respectively. By using these markers, we provide further evidence indicating that PMSCs expand in correlation with fibrogenesis and angiogenesis in different murine and human liver diseases, whereas the HSCs gene signatures did not vary. In conclusion, our work collectively offers insights into the components and functions of the mammalian liver portal mesenchymal cell populations, and in particular, identify and characterize PMSCs and their derived myofibroblasts, opening up the possibility for the development of novel targeted drugs or biomarkers of clinical significance with increased precision.

Keywords: liver fibrosis, single-cell sequencing, portal mesenchymal stem cells, hepatic stellate cells, angiogenesis, myofibroblasts.

Résumé

Les travaux antérieurs ont permis de montrer que les myofibroblastes portaux (PMFs) contribuaient de manière significative à la fibrogenèse et à l'angiogénèse dans la fibrose hépatique. L'objectif principal de cette thèse était de cartographier les cellules mésenchymateuses portales, et plus particulièrement la niche des cellules souches mésenchymateuses portales. Nous avons caractérisé la variété des cellules mésenchymateuses portales du foie de souris en conditions normales. Résultat important, nous avons identifié une population de cellules mésenchymateuses portales ayant les caractéristiques de cellules souches mésenchymateuses (MSCs), désignées cellules souches mésenchymateuses portales (PMSCs), qui ont la capacité de se transformer en PMFs *in vitro*. Nous avons identifié *Slit2* comme un marqueur des PMSCs par les analyses de scRNA-seq et bulk RNA-seq. *In vivo*, nous avons mis en évidence l'expansion de PMSCs (évaluée par l'expression de *Slit2*) dans le foie de modèles murins de fibrose hépatique (DDC et CDAA) et de patients ayant une maladie chronique du foie (NASH, CSP et autres maladies du foie). Nous avons identifié des signatures transcriptomiques spécifiques des PMSCs d'une part et des cellules étoilées du foie (CEF), de l'autre. Les résultats obtenus par l'utilisation de ces marqueurs, renforcent nos conclusions selon lesquelles les PMSCs s'accumulent de façon corrélée avec la fibrogenèse et l'angiogénèse dans différentes pathologies du foie murines et humaines, tandis que la signature des CEFs ne varie pas. En conclusion, nos travaux apportent des éléments à la connaissance des populations de cellules mésenchymateuses portales du foie de mammifères. Ils ont permis d'identifier et caractériser les PMSCs ainsi que les myofibroblastes qui en dérivent, ouvrant de nouvelles perspectives dans le domaine des thérapies ciblées et des biomarqueurs pour la pratique clinique.

Mots clés: fibrose hépatique, séquençage unicellulaire, cellules souches mésenchymateuses portales, cellules étoilées du foie, angiogénèse, myofibroblastes.